Mathematical Modeling of Reductive Transformation Kinetics of Branched Degradation Pathways of Groundwater Contaminants

Ankit Gupta

Thesis submitted to the faculty of the Virginia Polytechnic Institute and State University in partial fulfillment of the requirements for the degree of

Master of Science

In

Environmental Engineering

Mark A. Widdowson, Chair

Amy J. Pruden

Madeline E. Schreiber

September 8, 2011

Blacksburg, Virginia

Keywords: Reductive Transformation, Branched Pathways, Biodegradation, TNT, Sorption

Mathematical Modeling of Reductive Transformation Kinetics of Branched Degradation Pathways of Groundwater Contaminants

Ankit Gupta

Abstract

Groundwater contaminants such as chlorinated ethenes, chlorinated ethanes and nitroaromatic explosive compounds (e.g. 2,4,6-Trinitrotoluene (TNT)) degrade in the subsurface primarily by microbially catalyzed reductive transformation reactions. From a regulatory point of view, the capability to simulate the kinetics of these reductive transformation reactions coupled with other attenuation processes in the subsurface (e.g., sorption, advection, and dispersion) is required for site-specific solute transport models. A kinetic model based on Michaelis-Menten type equations (Widdowson 2004) has been successfully validated for the linear reductive dechlorination pathway of chlorinated ethenes, and implemented in solute transport codes such as SEAM3D (Waddill and Widdowson 2000). However, TNT degrades through more complex branched pathways, and kinetic models are lacking in the current literature.

This research study was undertaken with the objective of extending the kinetic model developed for the linear reductive pathway of chlorinated ethenes to branched pathways. The proposed extended kinetic model was validated with experimental concentration-time data of TNT and its metabolites from two prior published laboratory studies (Daun et al. 2000; Hwang et al. 2000), both in the presence and absence of sorption. The model-predicted concentrations with time of TNT and its degradation intermediates and end-products correlated well with the experimental data. The model is further compatible with and can be easily incorporated into solute transport codes (e.g., SEAM3D), and used to evaluate the fate and transport of TNT and other similar contaminants in the subsurface.

Acknowledgements

I would like to thank my advisor, Dr. Mark A. Widdowson, for his continued support and guidance in my research work and over the whole two year duration of my masters program here at VirginiaTech. It is often said, that graduate degree advisors play an important role in how their graduate students shape up professionally, and I personally believe that saying to be definitely true. Dr. Widdowson has been both, a great advisor and a great mentor for me at all times. His advice and guidance has immensely helped me nurture myself professionally. I admire him deeply and will respect him always.

I would also like to thank my committee members, Dr. Amy J. Pruden and Dr. Madeline E. Schreiber. Their kind and encouraging words as well as continuous support and guidance made this whole journey a very pleasant experience even at the toughest of times.

Next I would like to thank my colleagues Mike Mobile and Nicole Fahrenfeld for their patience and making themselves available for me whenever I had any questions or doubts regarding subject matter. I learnt a lot from my discussions with them and those discussions were very helpful in my research.

I would also like to thank all my colleagues at the EWR department at Virginia Tech. I made some really good friends and met some really cool people here, and could not have chosen a better department to pursue my graduate studies in. Being an international student, and not having any family in US, they provided me emotional support when I needed it, and made me feel at home here.

Lastly, I would like to thank my parents and my sister, who are responsible for who I am today and have supported me in every possible way imaginable right from the moment I decided to be born on this planet Earth. I owe everything I have accomplished or will accomplish to them.

Table of Contents

List of Figures

List of Tables

Chapter 1

Introduction

1.0 Introduction

Biodegradation is the primary process responsible for the natural attenuation of organic groundwater contaminants. While other mechanisms like chemical transformation, dispersion, dilution, sorption and volatilization have also been identified, biodegradation is the major mechanism of reduction of contaminant mass in the subsurface (Azadpour-Keeley et al. 1999). In biodegradation processes, the enzymes produced by microbes are responsible for the degradation of the organic carbon, and this degradation is mostly a complex oxidation-reduction reaction (Azadpour-Keeley et al. 1999). Organic contaminants with a relatively high degree of oxidation are composed of carbon atoms or other elements present in their higher oxidation states, and are called as oxidizing agents or electron acceptors since their biodegradation pathways consist mainly of reductive transformation reactions in which the contaminants themselves get reduced. On the other hand, organic contaminants, such as petroleum hydrocarbons are composed of carbon atoms in their lower oxidation states, and are called as reducing agents or electron donors since their biodegradation pathways consist of oxidative transformation reactions in which the carbon atoms are oxidized. These redox reactions are catalyzed by the enzymes produced by indigenously present microbial populations in the subsurface, which harness the large amounts of energy released and utilize it for their metabolism and growth. The extents to which a contaminant degrades in the subsurface and the degradation mechanisms are highly dependent on the prevalent redox state of the aquifer.

1.1 In-Situ Bioremediation of BTEX Compounds

Benzene, toluene, ethyl-benzene and xylene isomers, collectively called as BTEX compounds, are highly soluble and toxic compounds (An 2004) released in the groundwater primarily due to gasoline and petroleum fuel spills, leakage from underground storage tanks and industrial effluents (Andreoni and Gianfreda 2007). These mono-aromatic hydrocarbons containing carbon atoms in lower oxidation states act as electron donors and are oxidized by the naturally occurring electron acceptors in the subsurface like dissolved oxygen (aerobic aquifers) or nitrate, sulfate, ferric iron, manganese and carbon dioxide (anaerobic aquifers). The electron acceptors thus act as oxidizing agents and get reduced in the process. Microorganisms in the subsurface are able to catalyze these redox reactions and utilize the mono-aromatic hydrocarbons as growth substrates in the presence of sufficient macro and micro nutrients and optimum environmental conditions for growth, thus enhancing the rates of natural attenuation (Schulze and Tiehm 2004; Salanitro et al. 1997; Villatoro-Monzon et al. 2003; Dou et al. 2008). In conditions where one or more of the required conditions like nutrient, electron acceptor or growth substrate availability are not met, they could be artificially provided in an engineered way to increase the natural biodegradation rates.

Aerobic oxidation of these contaminants results in the formation of substituted catechol intermediates, which are further cleaved by ortho- or meta-cleavage deoxygenases (Andreoni and Gianfreda 2007). Complete mineralization of these compounds via oxidation to carbondioxide has also been achieved by mixed cultures (Deeb and Alvarez-Cohen 2000). Anaerobic oxidation of toluene, ethylbenzene, and ortho- and meta-xylene isomers results in the formation of benzyl-CoA, a common intermediate metabolite, which gets further converted to acetyl-CoA and finally to carbon-dioxide (Chakraborty and Coates 2004). Complete anaerobic oxidation of the BTEX compounds to carbon-dioxide has also been successfully demonstrated by electron balances (Jahn et al. 2005). All these studies show that the BTEX compounds can be naturally degraded and completely mineralized by oxidative biotransformation

reactions, thus making in-situ bioremediation a viable strategy for achieving clean-up goals at contaminated sites.

1.2 Chlorinated Ethenes in Groundwater

Tetrachloroethene (PCE) and trichloroethene (TCE) are two of the most common and widespread groundwater contaminants in the United States (Westrick et al. 1984; US EPA 1994; Charbeneau 2000). They contain electronegative chlorine atoms, and hence the carbon atoms in both compounds are in higher oxidation states, in direct contrast to the BTEX compounds. Both PCE and TCE, degrade through a reductive transformation process, known as reductive dechlorination in which chlorine atoms are replaced by hydrogen atoms in a successive manner in the presence of appropriate electron donors and microbes capable of catalyzing the reaction. The reductive dechlorination process results in degradation of PCE to ethene via sequential formation of intermediates like TCE, dichloroethene (DCE) isomers and vinyl chloride (VC) (Vogel and McCarty 1985; Chapelle et al. 2003). DCE and VC are relatively less oxidized as compared to TCE and PCE, and can also undergo aerobic (Bradley and Chapelle 1996; 1998a, 1998b; Bradley et al. 1998a) as well as anaerobic oxidation (Bradley and Chapelle 1996; 1998b; Bradley et al. 1998a) similar to BTEX compounds. Aerobic cometabolism which results in complete mineralization of TCE, DCE and VC to carbon-dioxide has also been reported (Semprini et al. 1990; 1991; Semprini 1995) but both aerobic cometabolism and aerobic oxidation have limited applicability in in-situ remediation of chlorinated ethene contaminated sites (Chapelle et al. 2003).

1.2.1 Mechanism of Reductive Dechlorination

PCE and TCE primarily degrade through the reductive dechlorination process which is ubiquitous in strongly-reducing, anaerobic groundwater systems contaminated with the same. The process goes though a linear degradation pathway (Figure 1.1) which results in successive production of intermediates

dichloroethene (DCE) and vinyl chloride (VC) and finally the end-product ethene. Progressively stronger reducing conditions are required in the subsurface to transform the intermediates and end-products involved in such reductive degradation pathways due to their successively lower oxidation states reflected in their one electron or half reaction reduction potentials (Vogel et al. 1987). This frequently leads to the accumulation of recalcitrant transformation products like DCE and VC which are also highly toxic and carcinogenic. Thus, subsurface groundwater plumes arising due to the presence of TCE and PCE tend to persist for longer periods of time due to the lower rates of natural biodegradation of the intermediate and end-product compounds. The natural biodegradation rates of these recalcitrant compounds can be increased by addition of electron donors (e.g., hydrogen or organic carbon compounds). Organic carbon compounds also have the potential to act as primary growth substrates for the indigenous microbial populations. An alternative mechanism which could act complimentary to the reductive dechlorination of TCE and PCE is anaerobic oxidation of DCE and VC. Complete mineralization of VC and DCE to carbon-dioxide has been reported under manganese, ferric iron and sulfate reducing and methanogenic conditions (Bradley and Chapelle 1998b; Bradley et al. 1998b).

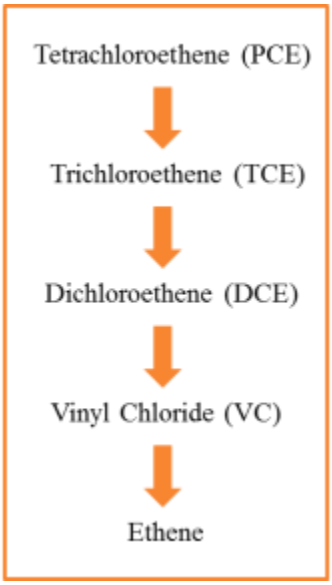

Figure 1.1. Linear reductive dechlorination pathway of PCE and TCE.

1.2.2 Kinetics of Reductive Dechlorination

A kinetic model based on modified Michaelis-Menten equations had been proposed and mathematical equations developed to describe the degradation kinetics of chlorinated ethenes via the reductive dechlorination process (Widdowson 2004). The equations included double Michaelis-Menten-type terms to account for inhibition and also incorporated microbial growth. They were also coupled to the prevailing terminal electron accepting processes (TEAPs) in the subsurface and the redox state of the aquifer. The model was further implemented in solute transport codes such as SEAM3D (Waddill and Widdowson 1998;, 2000).

1.3 Chlorinated Ethanes in Groundwater

1,1,2,2-tetrachloroethane (PCA) and 1,1,2-trichloroethane (TCA) are two common groundwater contaminants found at several military bases and industrial sites (U.S. EPA 1994). Both PCA and TCA, along with other chlorinated ethanes, have been classified as probable human carcinogens (U.S. EPA 2004). Both compounds contain carbon atoms in relatively oxidized state due to the presence of electronegative chlorine atoms similar to chlorinated ethenes, and are generally recalcitrant in normal environmental conditions due to their relatively low reduction potentials (Vogel et al. 1987).

PCA is known to biodegrade via a branched reductive transformation pathway consisting of two competing pathways (Figure 1.2) – (1) Hydrogenolysis, a reductive dechlorination process involving successive substitution of chlorine atoms by hydrogen atoms resulting in the sequential formation of 1,1,2-trichloroethane (1,1,2-TCA), 1,2-dichloroethane (1,2-DCA), chloroethane (CA) and ethane and (2) Dichloroelimination, another type of reductive dechlorination process involving the simultaneous release of two chlorine atoms from adjacent carbons thus resulting in the formation of alkenes like cis- and trans-1,2-DCE from PCA and VC from 1,1,2-TCA (Lorah and Olsen 1999). A third reductive transformation

process, Dehydrochlorination, involves the simultaneous release of hydrogen and chlorine atoms from adjacent carbons and also results in the formation of alkenes, but is considered to be an abiotic process (Chen et al. 1996; Lorah and Olsen 1999). All three reductive transformation processes have been inferred to occur naturally in the subsurface at field sites contaminated with PCA (Hunkeler et. al. 2005).

Such complex branched reductive degradation pathways like those of chlorinated ethanes like PCA and TCA and of nitroaromatic explosive compounds such as 2,4,6-trinitrotoluene (TNT) are in direct contrast to the linear reductive transformation pathway of chlorinated ethenes. The mathematical kinetic model developed earlier for the linear pathway of chlorinated ethenes (Widdowson 2004) has limited utility in describing the reductive degradation kinetics of such contaminants.

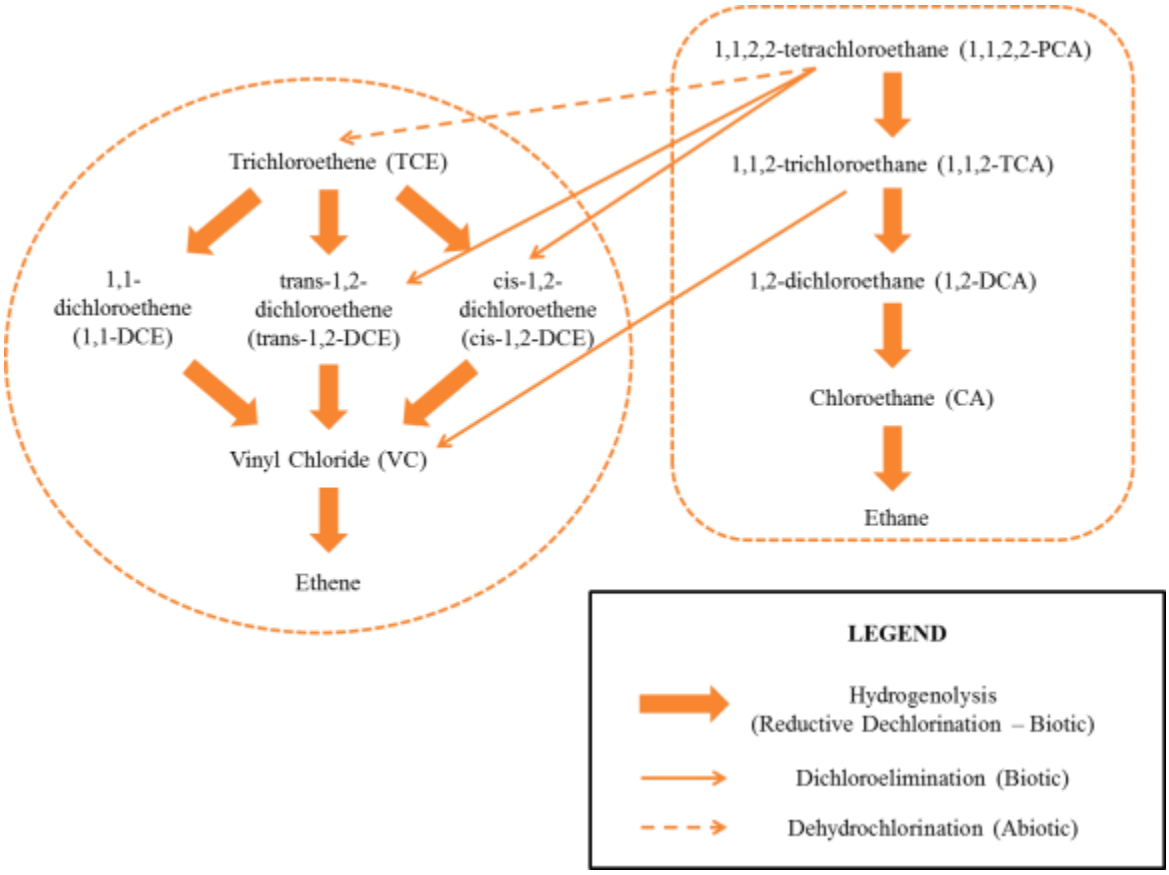

Figure 1.2. Branched reductive transformation pathway of 1,1,2,2-tetrachloroethane (PCA).

1.4 2,4,6-Trinitrotoluene (TNT)

2,4,6-Trinitrotoluene is a nitro-aromatic explosive compound widely found as a groundwater contaminant at former munitions manufacturing, handling and disposal military facilities active during the World Wars I and II (Pugh 1982; Spaulding and Fulton 1988). TNT is toxic and carcinogenic in nature and exposure to TNT has been recognized by the U.S. EPA as being harmful for public health and aquatic life (U.S. EPA 1988; ATSDR 1995).

1.4.1 Physical and Chemical Properties

TNT is highly soluble in water with a reported value of 94 mg/L at 20^0C in pure water at a pH of 7 (Prak and O'Sullivan 2006). TNT solubility increases with increasing temperatures and decreases with increasing ionic strength (Prak and O'Sullivan 2006). No significant variations in TNT solubility with changes in pH were found (Lynch et al. 2001). The reported value of density of TNT is 1.654 g/cm^3 which makes it heavier than water.

TNT contains three nitro groups symmetrically placed on the benzene ring which makes the nucleus highly electrophilic. The nitrogen atom in the nitro groups is highly electronegative, and the partial positive charge on it due to the polarization of the N-O bond makes it highly reducible (Preuss and Rieger 1995). Thus, even in oxidizing environments, the first transformation of TNT primarily involves reduction at one of the nitro groups. In vitro assays involving cell extracts obtained from various microorganisms and higher eukaryotes have showed that the reduction of the nitro groups occurs through successive transfers of two electrons along with sequential generation of nitroso, hydroxyl-amino and amino derivatives of the parent nitro-aromatic compound (Figure 1.3) (Esteve-Nunez et al. 2001).

The nitroso and hydroxyl-amino derivatives of TNT are also toxic since they are react with biological molecules like lipids, proteins and fatty acids and cause chemical mutagenesis and carcinogenesis (Carpenter et al. 1978). Previous studies have documented the toxic and carcinogenic effects of TNT and its nitroso, hydroxyl-amino and amino metabolites (Banerjee et al. 1999; Honeycutt et al. 1996). Successive reduction of the nitro groups to amino groups eventually culminates with the formation of 2,4,6-triaminotoluene (TAT) (Spain 1995) which is much less toxic (Schafer and Achazi 1999) and more biologically degradable (Esteve-Nunez et al. 2001).

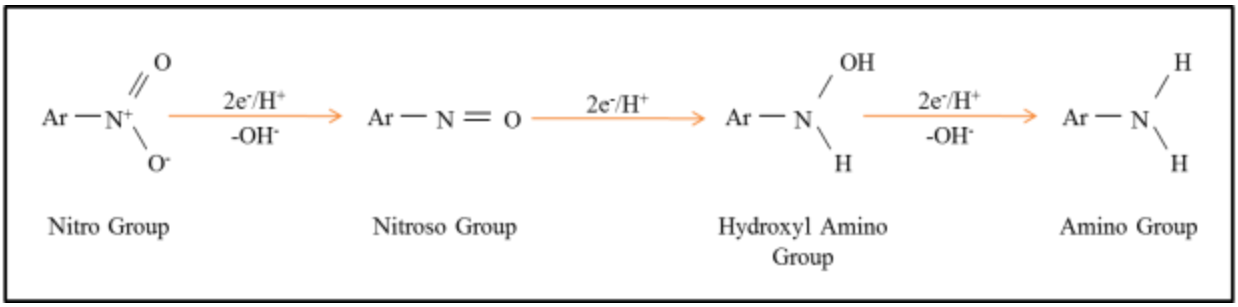

Figure 1.3. Sequential reduction of nitro group to nitroso, hydroxyl-amino and amino groups.

1.4.2 Reductive Transformation Pathway of TNT

Due to the strongly oxidizing nature of the nitro groups, TNT degrades through a reductive transformation process in which the nitro groups are successively reduced to amino groups in aerobic and anaerobic environments. The reduction of the first nitro group, which forms the first step in the reductive pathway, is known to occur at a higher rate than the subsequent steps (Hofstetter et al. 1999). Each successive substitution of a nitro group by an amino group via formation of nitroso and hydroxyl-amino derivatives reduces the electron deficiency of the nitro-aromatic compound, and consequently lowers the redox potential required for subsequent reduction of the remaining nitro groups (Figure 1.3) (Hofstetter et al. 1999). Formation of the end-product TAT requires strongly reducing conditions, which are normally not observed in aerobic or anaerobic environments.

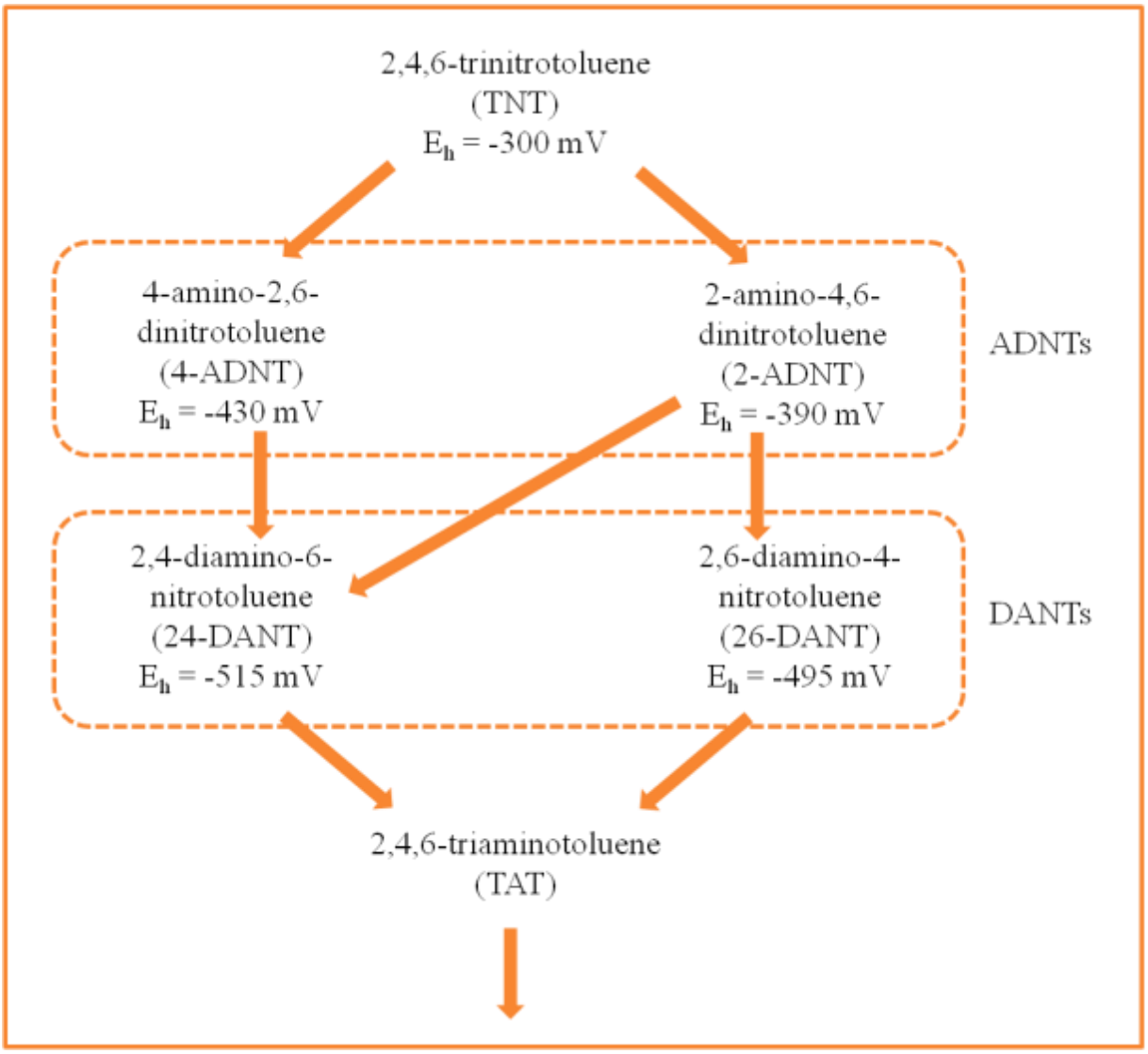

Figure 1.4. Reductive transformation pathway with redox potentials of TNT and each metabolite (redox potentials from Hofstetter et al. 1999).

A highly reducing anaerobic environment is preferred for TNT degradation, where all the nitro groups get sequentially reduced to and eventually substituted by amino groups by a reductive transformation process similar to reductive dechlorination. The reduction of TNT to TAT proceeds through a branched pathway and involves the formation of isomeric mono- and di- aminonitrotoluene intermediates like 2-amino-4,6-dinitrotoluene (2-ADNT), 4-amino-2,6-dinitrotoluene (4-ADNT), 2,4-diamino-6-nitrotoluene (2,4-DANT) and 2,6-diamino-4-nitrotoluene (2,6-DANT) (Figure 1.4) (Hwang et al. 2000; Esteve-Nunez et al.

2001). Among the isomeric intermediates, the para-position is more easily reduced than the ortho-position and hence, the 4-ADNT and 2,4-DANT isomers form the major products while 2-ADNT and 2,6-DANT are the minor products.

In aerobic or anaerobic environments, the reductive transformation of TNT is incomplete due to unavailability of stronger reducing conditions and results in the accumulation of ADNT and DANT isomers. In aerobic environments, in particular, these partially reduced compounds further react among themselves and condense to form recalcitrant azoxy-tetranitrotoluenes (Haïdour and Ramos 1996) which are more toxic and carcinogenic than TNT (Spanggord et al. 1995; George et al. 2001). Thus, aerobic environments for TNT degradation are highly unfavorable. In anaerobic oxidizing environments, carbon substrates like ethanol can be injected in an engineered way to create stronger reducing conditions in the subsurface and enhance the natural attenuation of accumulated recalcitrant ADNT and DANT isomers to TAT.

1.4.3. Sorption of TNT and its Metabolites

Sorption has been identified as a key process involved in the subsurface transport and fate of TNT and its metabolites (Myers and Townsend 1997). For soils rich in organic carbon content, the sorption affinity increases with the number of amino groups present on the aromatic ring. Both TAT and hydroxylaminodinitrotoluenes (HADNTs) were found to adsorb strongly and rapidly to humic acids, with the total sum of the concentrations of TNT and its metabolites dropping below 50% of the initial TNT concentration within the first ten hours. The sorption was found to be irreversible as neither TNT nor any of its metabolites could be desorbed from the soil matrix (Daun et al. 1998).

Soils rich in minerals like homoionic clays (e.g. montmorrilonitic clay) showed lower specific binding capacity for TNT and its metabolites. For such clays, fully reversible sorption was seen for TNT and the

two ADNT isomers, however 2,4-DANT showed only partially reversible sorption and TAT showed completely irreversible sorption (Daun et al. 1998). For TNT, ADNTs and DANTs, values of distribution coefficients have been determined with montmorrilonitic clay using linear adsorption isotherms (Daun et al. 1998). In the presence of 3.3% w/v clay, the total sum of concentrations of TNT and its metabolites was reported to drop to 50 – 60% of initial TNT concentration within 10 hours. In the presence of 10.3% w/v clay, the total dropped to around 30% of the initial TNT concentration (Daun et al. 1998). Both the above sorption experiments in the presence of humic acids and montmorrilonitic clay stress the importance of sorption as a competing process to reductive transformation responsible for the removal of TNT and its metabolites from the subsurface.

1.4.4 Kinetics of Reductive Transformation of TNT

The degradation kinetics of the branched reductive transformation pathway of TNT have been simulated traditionally only for TNT and not its metabolites. There have been prior attempts where pseudo first order kinetics have been used to describe TNT degradation assuming constant microbial biomass (Pavlostathis and Jackson 1999). Michaelis-Menten type kinetics which also assume constant microbial biomass have been more successfully used to model the anaerobic reductive TNT degradation pathway by incorporating different inhibition functions (Riefler and Smets 2002; Yin et al. 2005; Wang et al. 2010). Monod kinetics based equations have also been successfully used to simulate microbial growth along with Michaelis-Menten kinetics for TNT degradation (Admassu et al. 1998; Park et al. 2002). However, there is only one other study where the authors attempted to simulate the kinetics of the whole TNT degradation pathway along with its metabolites (Daun et al. 1999). The authors of the study used four different mathematical models involving cometabolic Monod and double substrate kinetic equations to describe TNT and its metabolites degradation but received only partial success in their attempts.

1.5 Research Objectives

In contrast to the chlorinated ethenes, other relatively oxidized contaminants including TNT and PCA are known to degrade through more complex reductive pathways. The extended Michaelis-Menten model presented earlier (Widdowson 2004) for simulating the reduction kinetics of chlorinated ethenes is not applicable in its current state to the degradation kinetics of branched reductive transformation pathways of TNT or chlorinated ethanes like PCA. The objective of this study is to present a modified and extended version of the mathematical model that is capable of simulating abstract complex reductive degradation schemas involving branched pathways and to validate it with prior published laboratory data.

In particular, the following three main research objectives were identified:

- To extend the mathematical model developed for the linear reductive dechlorination of chlorinated ethenes to branched reductive transformation pathways like those of TNT and PCA
- To validate the mathematical model by simulating the branched reductive degradation data of TNT and its metabolites.
- To incorporate the processes of microbial growth and sorption in the model and simulate TNT degradation data in the presence of both.

1.6 Benefits of the Proposed Kinetic Model

The extended Michaelis-Menten equations based kinetic model, once successfully validated, can be used to simulate the fate and transport of TNT and its metabolites in the subsurface. The kinetic model is compatible and easily integrable in solute transport codes like SEAM3D, and can be used to create well calibrated site specific solute transport models for TNT and its degradation products. Such well-calibrated site-specific solute transport models can then be further used to evaluate the Time of Remediation (TOR) scenarios associated with Monitored Natural Attenuation (MNA) or Enhanced Anaerobic Bioremediation

(EAB). The model can further be used for other contaminants such as TNT (e.g. PCA) which degrade through complex reductive transformation pathways.

1.7 References

Admassu, W., Sethuraman, A.V., Crawford, R., Korus, R.A., 1998. Growth Kinetics of *Clostridium bifermentans* and Its Ability to Degrade TNT Using an Inexpensive Alternative Medium. *Bioremediation Journal* 2, 17-28.

An, Y.J., 2004. Toxicity of benzene, toluene, ethylbenzene, and xylene (BTEX) mixtures to *Sorghum bicolor* and *Cucumis sativus*. *Bulletin of Environmental Contamination and Toxicology* 72, 1006-1011.

Andreoni, V., Gianfreda, L., 2007. Bioremediation and monitoring of aromatic-polluted habitats. *Applied Microbiology and Biotechnology* 76, 287-308.

Agency for Toxic Substances and Disease Registry (ATSDR), 1995. Toxicological profile for 2,4,6-trinitrotoluene (TNT). Atlanta, GA: U.S. Department of Health and Human Services, Public Health Service.

Azadpour-Keeley, A., Russell, H.H., Sewell, G.W., 1999. Microbial Processes Affecting Monitored Natural Attenuation of Contaminants in the Subsurface. *Ground Water Issue*, U.S. EPA 540/S-99/001, Office of Solid Waste and Emergency Response, Washington, DC.

Banerjee, H.N., Verma, M., Hou, L.H., Ashraf, M., Dutta, S.K., 1999. Cytotoxicity of TNT and its metabolites. *Yale Journal of Biology and Medicine* 72, 1-4.

Bradley, P.M., Chapelle, F.H., 1996, Anaerobic mineralization of vinyl chloride in Fe(III)-reducing, aquifer sediments. *Environmental Science and Technology* 30, 2084 – 2086.

Bradley, P.M., Chapelle, F.H., 1998a. Effect of contaminant concentration on aerobic microbial mineralization of DCE and VC in stream-bed sediments. *Environmental Science and Technology* 32, 553 – 557.

Bradley, P.M., Chapelle, F.H., 1998b. Microbial mineralization of VC and DCE under different terminal electron accepting conditions. *Anaerobe* 4, 81 – 87.

Bradley, P.M., Chapelle, F.H., Wilson, J.T., 1998a. Field and laboratory evidence for intrinsic biodegradation of vinyl chloride contamination in a Fe(III)-reducing aquifer. *Journal of Contamination Hydrology* 31, 111 – 127.

Bradley, P.M., Landmeyer, J.E., Dinicola, R.S., 1998b. Anaerobic oxidation of [1,2-14C] dichloroethene under Mn(IV)-reducing conditions. *Applied and Environmental Microbiology* 64, 1560 – 1562.

Carpenter, D. F., McCormick, N.J., Cornell, J.H., Kaplan, A., 1978. Microbial transformation of 14C-labeled 2,4,6-TNT in an activated-sludge system. *Applied and Environmental Microbiology* 35, 949-954.

Chakraborty, R., Coates, J.D., 2004. Anaerobic degradation of monoaromatic hydrocarbons. *Applied Microbiology and Biotechnology* 64, 437-446.

Chapelle, F.H., Widdowson, M.A., Brauner, J.S., Mendez III, E., Casey, C.C., 2003. Methodology for Estimating Times of Remediation Associated with Monitored Natural Attenuation. U.S. Geological Survey Water-Resources Investigation Report 03-4057, 51 pp.

Charbeneau, R.J., 2000. Groundwater Hydraulics and Pollutant Transport, 1st edition. Prentice Hall, Upper Saddle River, NJ.

Daun, G., Lenke, H., Reuss, M., Knackmuss, H.J., 1998. Biological Treatment of TNT-Contaminated Soil. 1. Anaerobic Cometabolic Reduction and Interaction of TNT and Metabolites with Soil Components. *Environmental Science and Technology* 32, 1956-1963.

Daun, G., Lenke, H., Knackmuss, H.J., Reuss, M., 1999. Experimental investigations and kinetic models for the cometabolic biological reduction of trinitrotoluene. *Chemical Engineering and Technology* 22, 308-313.

Deeb, R.A., Alvarez-Cohen, L., 2000. Aerobic Biotransformation of Gasoline Aromatics in MultiComponent Mixtures. *Bioremediation Journal* 4, 171-179.

Dou, J., Liu, X., Hu, Z., Deng, D., 2008. Anaerobic BTEX biodegradation linked to nitrate and sulfate reduction. *Journal of Hazardous Materials* 151, 720-729.

Esteve-Nunez, A., Caballero, A., Ramos, J.L., 2001. Biological Degradation of 2,4,6-Trinitrotoluene. *Microbiology and Molecular Biology Reviews* 65, 335-352.

George, S.E., Huggins-Clark, G., Brooks, L.R., 2001. Use of a Salmonella microsuspension bioassay to detect the mutagenicity of munitions compounds at low concentrations. *Mutation Research-Genetic Toxicology And Environmental Mutagenesis* 490, 45-56.

Haïdour, A., Ramos, J.L., 1996. Identification of products resulting from the biological reduction of 2,4,6-trinitrotoluene, 2,4-dinitrotoluene and 2,6-dinitrotoluene by *Pseudomonas sp. Environmental Science and Technology* 30, 2365-2370.

Hofstetter, T.B., Heijman, C.G., Haderlein, S.B., Holliger, C., Schwarzenbach, R.P., 1999. Complete Reduction of TNT and Other (Poly)nitroaromatic Compounds under Iron-Reducing Subsurface Conditions. *Environmental Science and Technology* 33, 1479-1487.

Honeycutt, M.E., Jarvis, A.S., McFarland, V.A., 1996. Cytotoxicity and mutagenicity of 2,4,6-trinitrotoluene and its metabolites. *Ecotoxicology and Environmental Safety* 35, 282-287.

Hwang, P., Chow, T., Adrian, N.R., 2000. Transformation of Trinitrotoluene to Triaminotoluene by Mixed Cultures Incubated under Methanogenic Conditions. *Environmental Toxicology and Chemistry* 19(4), 836-841.

Jahn, M.K., Haderlein, S.B., Meckenstock, R.U., 2005. Anaerobic Degradation of Benzene, Toluene, Ethylbenzene, and o-Xylene in Sediment-Free Iron-Reducing Enrichment Cultures. *Applied and Environmental Microbiology* 71, 3355-3358.

Myers, T.E., Townsend, D.M., 1997. Recent developments in formulating model descriptors for subsurface transformation and sorption of trinitrotoluene. *Annals of the New York Academy of Sciences* 829, 219-229.

Park, C., Kim, T.H., Kim, S., Lee, J., Kim, S.W., 2002. Biokinetic Parameter Estimation for Degradation of 2,4,6-Trinitrotoluene (TNT) with *Pseudomonas putida* KP-T201. *Journal of Bioscience and Bioengineering* 94, 57-61.

Pavlostathis, S.G., Jackson, G.H., 1999. Biotransformation of 2,4,6-Trinitrotoluene in *Anabaena Sp.* Cultures. *Environmental Toxicology and Chemistry* 18, 412-419.

Prak, D.J.L., O'Sullivan, D.W., 2006. Solubility of 2,4-Dinitrotoluene and 2,4,6-Trinitrotoluene in Seawater. *Journal of Chemical Engineering Data* 51, 448-450

Preuss, A., Rieger, P.G., 1995. Anaerobic transformation of 2,4,6-TNT and other nitroaromatic compounds. p. 69-85. In J. C. Spain (ed.), Biodegradation of nitroaromatic compounds. Plenum Press, New York, N.Y..

Pugh, D.L., 1982. Milan Army Ammunition Plant Contamination Survey. USATHAMA Report DRXTH-FR-8213, U.S. Army Toxic and Hazardous Materials Agency, Aberdeen Proving Ground, Aberdeen, MD.

Riefler, R.G., Smets, B.F., 2002. NAD(P)H:Flavin Mononucleotide Oxidoreductase Inactivation during 2,4,6-Trinitrotoluene Reduction. *Applied and Environmental Microbiology* 68, 1690-1696.

Salanitro, J.P., Wisniewski, H.L., Byers, D.L., Neaville, C.C., Schroder, R.A., 1997. Use of Aerobic and Anaerobic Microcosms to Assess BTEX Biodegradation in Aquifers. *Ground Water Monitoring and Remediation* 17, 210-221.

Semprini, L., 1995. In situ bioremediation of chlorinated solvents. *Environmental Health Perspective* 103, 101 – 105.

Semprini, L., Roberts, P.V., Hopkins, G.D., McCarty, P.L., 1990. A field evaluation of in situ biodegradation of chlorinated ethenes, Part 2 — Results of biostimulation and biotransformation experiments. *Ground Water* 28, 715 – 727.

Semprini, L., Hopkins, G.D., Roberts, P.V., Grbic-Galic, D., McCarty, P.L., 1991. A field evaluation of in situ biodegradation of chlorinated ethenes, Part 3 — Studies of competitive inhibition. *Ground Water* 29, 239 – 250.

Schafer, R., Achazi, R.K., 1999. The toxicity of soil samples containing TNT and other ammunition derived compounds in the enchytraeid and collembola-biotest. *Environmental Science and Pollution Research* 6, 213-219.

Schulze, S., Tiehm, A., 2004. Assessment of microbial natural attenuation in groundwater polluted with gasworks residues. *Water Science and Technology* 50, 347-353.

Spain, J.C., 1995. Biodegradation of nitroaromatic compounds. *Annual Review of Microbiology* 49, 523-555.

Spaulding, R.F., Fulton, J.W., 1988. Groundwater munition residues and nitrate near Grand Island, Nebraska, U.S.A. *Journal of Contaminant Hydrology* 2, 139-153.

Spanggord, R.J., Stewart, K.R., Riccio, E.S., 1995. Mutagenicity of tetranitroazoxytoluenes: a preliminary screening in *Salmonella typhimurium* strains TA100 and TA100NR. *Mutation Research-Environmental Mutagenesis And Related Subjects* 335, 207-211.

U.S. EPA, 1994. Common Chemicals Found at Superfund Sites. EPA 540/R-94/044. Office of Emergency and Remedial Response. Washington, DC.

U.S. EPA, 1998. Health Advisory on Trinitrotoluene, Office of Drinking Water, Washington DC.

U.S. EPA, 2004. Edition of the Drinking Water Standards and Health Advisories. EPA 822/R-04/005. Office of Drinking Water, Washington DC.

Villatoro-Monzón, W.R., Mesta-Howard, A.M., Razo-Flores, E., 2003. Anaerobic biodegradation of BTEX using Mn(IV) and Fe(III) as alternative electron acceptors. *Water Science and Technology* 48, 125-131.

Vogel, T.M., McCarty, P.L., 1985. Biotransformation of Tetrachloroethylene to Trichloroethylene, Dichloroethylene, Vinyl Chloride, and Carbon Dioxide under Methanogenic Conditions. *Applied and Environmental Microbiology* 49, 1080-1083.

Vogel, T.M., Criddle, C.S., McCarty, P.L., 1987. Transformation of halogenated aliphatic-compounds. *Environmental Science and Technology* 21, 722 – 736.

Waddill, D.W., Widdowson, M.A., 1998. A three-dimensional model for subsurface transport and biodegradation. *Journal of Environmental Engineering-ASCE* 124, 336-344.

Waddill, D.W., Widdowson, M.A., 2000. SEAM3D: A numerical model for three-dimensional solute transport and sequential electron acceptor-based bioremediation in groundwater. ERDC/EL TR-00-X, U.S. Army Engineer Research and Development Center, Vicksburg, MS, 89 pp.

Wang, Z., Ye, Z., Zhang, M., Bai, X., 2010. Degradation of 2,4,6-trinitrotoluene (TNT) by immobilized microorganism-biological filter. *Process Biochemistry* 45, 993-1001.

Westrick, J.J., Mello, J.W., Thomas, R.F., 1984. The groundwater supply survey. *Journal - American Water Works Association* 76, 52-59.

Widdowson, M.A., 2004. Modeling natural attenuation of chlorinated ethenes under spatially varying redox conditions. *Biodegradation* 15, 435-451.

Yin, H., Wood, T.K., Smets, B.F., 2005. Reductive transformation of TNT by Escherichia coli resting cells:kinetic analysis. *Applied Microbiology and Biotechnology* 69, 326-334.

Chapter 2

Mathematical Modeling of Reductive Transformation Kinetics of Branched Degradation Pathways of Groundwater Contaminants

Ankit Gupta[a], Mark A. Widdowson[a]

[a] The Charles E. Via, Jr. Department of Civil and Environmental Engineering, Virginia Tech, Blacksburg, Virginia

2.1 Abstract

Chlorinated ethenes such as 1,1,2,2-tetrachloroethene and 1,1,2-trichloroethene have been shown to degrade via a linear reductive transformation pathway under reducing conditions by the microbially-mediated reductive dechlorination process (Vogel and McCarty 1985; Chapelle et al. 2003). Their degradation kinetics has been successfully modeled by Michaelis-Menten type equations (e.g., Widdowson 2004). The mathematical equations have been successfully validated and implemented in solute transport codes such as SEAM3D. Other contaminants such as 2,4,6-trinitrotoluene (TNT) and 1,1,2,2-tetrachloroethane (PCA) are also known to degrade in anaerobic aquifers through microbially-mediated reductive transformation processes. However, TNT and PCA degrade through much more complex reductive transformation pathways which involve branching. For both TNT and PCA, the degradation pathways involve formation of multiple daughter products by competing reductive transformations of a single parent compound as well as formation of a single daughter product from degradation of multiple parent compounds. With the objective of simulating the attenuation and transport of such contaminants, a mathematical model was developed to enable kinetic modeling of complex

branched degradation pathways. The mathematical model was successfully validated against experimental time-dependent concentration data obtained for TNT and its metabolites degradation from two prior experimental laboratory studies, both in the presence and absence of sorption (Daun et al. 1998; Hwang et al. 2000). High R-square values were obtained between the model-predicted and observed concentration data. The proposed mathematical kinetic model is also compatible with solute transport codes to create site-specific transport models which can be used to evaluate remediation scenarios associated with natural and enhanced anaerobic bioremediation.

2.2 Introduction

Biodegradation is the primary process in the subsurface responsible for the natural attenuation of organic groundwater contaminants. While other mechanisms such as chemical transformation, dispersion, dilution, sorption and volatilization have also been identified, it forms the major mechanism of reduction of contaminant mass in the subsurface. In biodegradation processes, the enzymes produced by the microbes are responsible for the degradation of the organic carbon, and this degradation is mostly a complex oxidation-reduction reaction (Azadpour-Keeley et al. 1999). For petroleum hydrocarbons, which are composed of carbon atoms in their lower oxidation states, the biodegradation pathways consist of transformation reactions in which the carbon atoms are oxidized. These compounds act as electron donors and are oxidized by naturally occurring electron acceptors in the subsurface such as dissolved oxygen (aerobic aquifers), nitrates, sulfates, ferric iron, manganese oxides (Mn^{4+}) and carbon dioxide (anaerobic aquifers) (Schulze and Tiehm 2004; Salanitro et al. 1997; Villatoro-Monzon et al. 2003; Dou et al. 2008).

Organic contaminants in which carbon atoms or other elements are present in their higher oxidation states, often act as oxidizing agents or electron acceptors and their dominant biodegradation pathways consist of reductive transformation reactions in which the oxidized elements get reduced. In most cases, the oxidized organic contaminants either act as the terminal electron acceptors or as the primary growth

substrates required for microbial metabolism and provide the microbes with energy for their growth which results in higher rates of reductive transformation while in other cases, the process is cometabolic in nature (Azadpour-Keeley et al. 1999; Chapelle et al. 2003). Cometabolism is defined as the transformation of a non-growth substrate by either growing cells in the presence of a growth substrate or by resting cells in the absence of a growth substrate (Criddle 1993). Common examples of contaminants degrading through reductive transformation pathways are chlorinated ethenes including 1,1,2,2-tetrachloroethene (PCE) and 1,1,2-trichloroethene (TCE); chlorinated ethanes including 1,1,2,2-tetrachloroethane (PCA) and 1,1,2-trichloroethane (TCA); and nitroaromatic explosive compounds such as 2,4,6-trinitrotoluene (TNT). Progressively stronger reducing conditions are required to transform the intermediates and end-products involved in the degradation pathways due to their successively lower oxidized states (reflected in their one electron or half reaction reduction potentials) (Vogel et al. 1987; Hofstetter et al. 1999). In aquifers that are not strongly reducing, accumulation of recalcitrant transformation products, which frequently are highly toxic and carcinogenic in nature, can occur. The biodegradation rates of these recalcitrant compounds can be increased by injecting in to the subsurface organic carbon compounds which act as electron donors and primary growth substrates for the indigenous microbial populations (Grindstaff 1998).

PCE and TCE are two of the most widely occurring contaminants in groundwater (Charbaneau 2000). Chlorinated ethenes primarily degrade through a reductive transformation process in which they act as electron acceptors and are sequentially dechlorinated by replacing a chlorine atom with a hydrogen atom. This reductive dechlorination process is microbially catalyzed and goes through a linear degradation pathway resulting in successive production of intermediates dichloroethene (DCE) isomers (1,2-cis-DCE, 1,2-trans-DCE and 1,1-DCE), vinyl chloride (VC) and the end-product ethene (Vogel and McCarty 1985; Chapelle et al. 2003). Widdowson (2004) proposed a mathematical model based on Michaelis-Menten type equations to describe the degradation kinetics of chlorinated ethenes via the reductive dechlorination process. The equations were coupled to the redox state and the prevailing terminal electron accepting

processes (TEAPs) in a groundwater system. Furthermore, the model was implemented in solute transport codes like SEAM3D (Waddill and Widdowson 1998; Waddill and Widdowson 2000) for the development of solute transport models at chloroethene-contaminated sites. However, other contaminants such as TNT and PCA are known to degrade through more complex reductive pathways, and the extended Michaelis-Menten kinetic model proposed for reductive chlorination of chloroethenes provides limited utility in trying to simulate their degradation kinetics.

Recently, much focus has been directed towards the bioremediation of TNT plumes in soil and groundwater. Exposure to TNT has been recognized by the USEPA as harmful for human and aquatic life (U.S. EPA 1988; ATSDR 1995). TNT degradation in aerobic and anaerobic environments proceeds through a reductive transformation process where each nitro group is sequentially reduced to an amino group. The extent of reduction is dependent on the reducing potential of the system and could result in reduction of one, two or all three nitro groups (McCormick et al. 1976). In aerobic or anaerobic oxidizing environments, the reductive transformation of TNT is incomplete due to unavailability of stronger reducing conditions and results in the accumulation of mono- and di- aminonitrotoluene isomers (Boopathy et al. 1994; Drzyzga et al. 1998). In oxidizing environments, these partially reduced compounds further react among themselves and condense to form recalcitrant azoxy-tetranitrotoluenes (McCormick et al. 1976; Haïdour and Ramos 1996) which are more toxic and carcinogenic than TNT (Spanggord et al. 1995; George et al. 2001). A highly anaerobic reducing environment is thus preferred for TNT degradation, where all the nitro groups get sequentially reduced to and eventually substituted by amino groups by the reductive transformation process (Spain 1995). The process eventually culminates with the formation of 2,4,6-triaminotoluene (TAT) which is much less toxic (Schafer and Achazi 1999) and more biologically degradable (Esteve-Nunez et al. 2001) than TNT. The reduction of TNT to TAT proceeds through a branched pathway in contrast to the linear reductive pathway of chlorinated ethenes and involves the formation of isomeric mono- and di- aminonitrotoluene intermediates like 2-amino-4,6-dinitrotoluene (2-ADNT), 4-amino-2,6-dinitrotoluene (4-ADNT), 2,4-diamino-6-nitrotoluene (2,4-

DANT) and 2,6-diamino-4-nitrotoluene (2,6-DANT) (Figure 2.1) (Hwang et al. 2000; Esteve-Nunez et al. 2001).

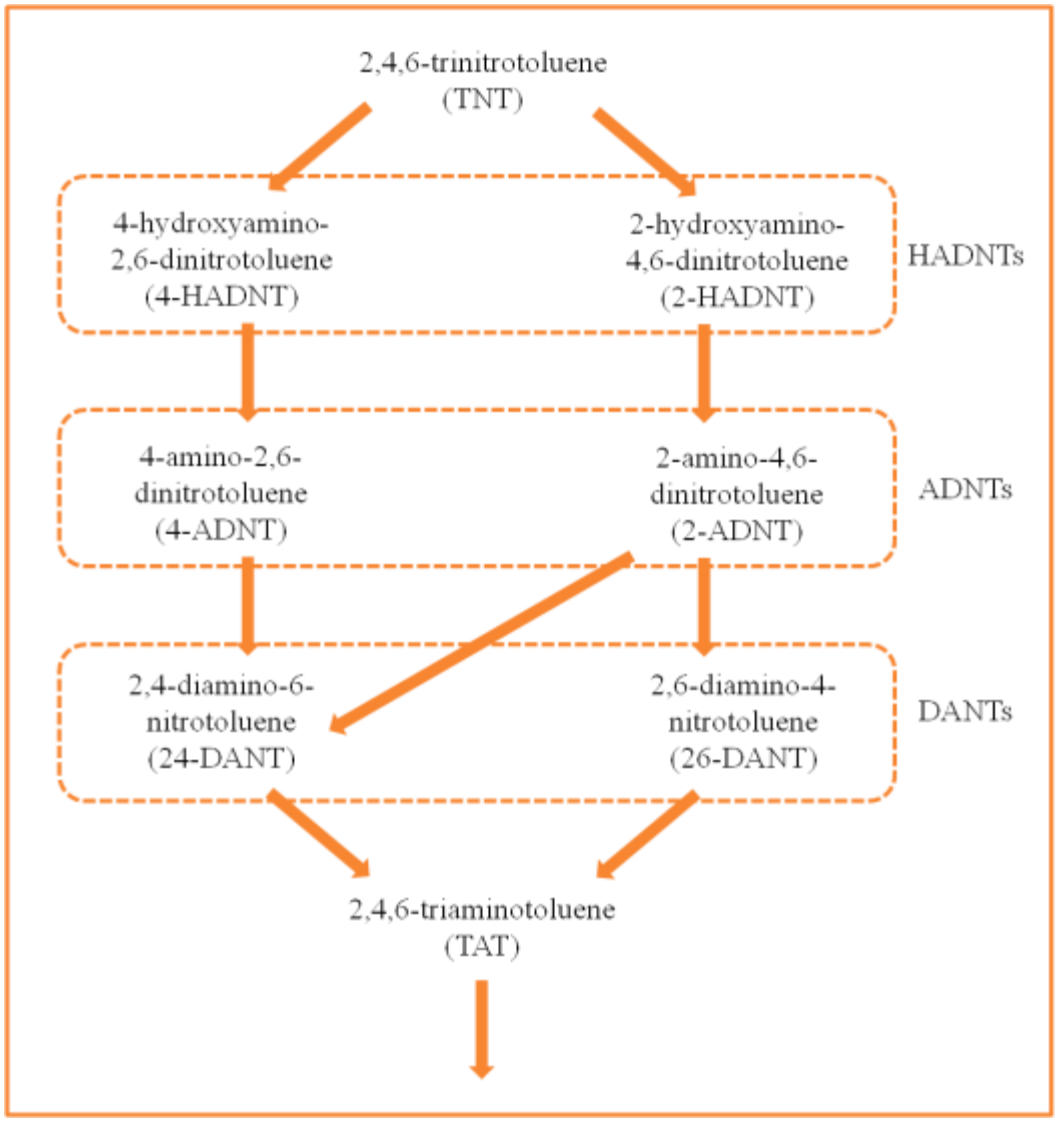

Figure 2.1. Branched reductive degradation pathway of TNT.

Another example of a complex branched reductive degradation pathway is that of chlorinated ethanes (e.g., PCA). Tetrachloroethane is known to biodegrade via two competing pathways: (1) Hydrogenolysis, which is a reductive dechlorination process involving successive substitution of chlorine atoms by hydrogen atoms resulting in the sequential formation of 1,1,2-TCA, 1,2-dichloroethane (1,2-DCA),

chloroethane (CA) and ethane; and (2) Dichloroelimination, which is another type of reductive dechlorination process involving the simultaneous release of two chlorine atoms from adjacent carbons resulting in the formation of alkenes like cis- and trans-1,2-DCE from PCA and VC from 1,1,2-TCA (Lorah and Olsen 1999). A third reductive transformation process, dehydrochlorination, involves the simultaneous release of hydrogen and chlorine atoms from adjacent carbons and also results in the formation of alkenes, but is considered to be an abiotic process (Chen et al. 1996; Lorah and Olsen 1999). All three reductive transformation processes have been observed to occur naturally in the subsurface at field sites contaminated with PCA (Hunkeler et. al. 2005).

Prior attempts at simulating the degradation kinetics of the branched reductive transformation pathway of TNT have not addressed the fate of its metabolites. Pseudo-first order kinetics assuming constant biomass concentration had been used earlier to describe TNT degradation in microbial systems (Pavlostathis and Jackson 1999). More recent investigations have successfully used Michaelis-Menten type kinetics with different inhibition functions for modeling anaerobic TNT degradation assuming constant biomass concentrations (Riefler and Smets 2002; Yin et al. 2005; Wang et al. 2010). Some studies have also successfully used Monod kinetics to simulate microbial growth coupled with Michaelis-Menten-type kinetics to describe TNT degradation (Admassu et al. 1998; Park et al. 2002). Daun et al. (1999) employed four different cometabolic mathematical models involving Monod, simple double substrate and complex competitive double substrate kinetic equations to describe the complete TNT degradation pathway. The results showed limited success in simulating the observed TNT concentration data with only the simple Monod model for co-substrates while the other three models proved unsuccessful.

A review of the literature points to a gap in the ability to mathematically represent such biotransformation processes known to occur at contaminated sites. The objective of this research is to develop a mathematical kinetic model capable of simulating complex schemes for contaminant degradation pathways that involve branched reductive transformation reactions (e.g., TNT and PCA). The following

study presents the kinetic model development as well as validation results with experimental data obtained from two prior published lab studies describing TNT degradation, both in the presence and absence of sorption. Although the model is validated using data from one contaminant group, the aim in developing this mathematical model is a non-prescriptive framework that provides sufficient flexibility for application to other contaminants and degradation pathways.

2.3 Model Development

Figure 2.2 shows an example abstract scheme of a branched reductive degradation pathway. Compound C1 is the original source contaminant parent compound which is biotransformed to three intermediate daughter products C2, C3 and C4. The arrows in the pathway show the microbially catalyzed reductive transformation reactions responsible for the production of daughter compounds from parent compounds. C5, C8, C9, C10 and C11 form the final end-products of the degradation scheme and will accumulate in the system. C6 is an intermediate daughter product of C2 and the parent compound of end-products C8 and C9. Similarly, C7 is the intermediate daughter product of C3 and C4 and the parent compound of end-products C10 and C11. The intermediate compounds C2, C3, C4, C6 and C7 will accumulate transiently in the system because their concentrations would decrease as they degrade to their respective daughter products. The daughter products produced from the same parent compound like C2, C3 and C4 from C1 can be isomers of each other with different chemical structures or possess completely different chemical formulas.

Two types of branching can be differentiated in such a branched pathway:

1. A parent compound degrading to multiple daughter compounds (e.g., C1 to C2, C3 and C4; C2 to C5 and C6; C6 to C8 and C9; C7 to C10 and C11)
2. A daughter compound being generated from multiple parent compounds (e.g., C7 from C3 and C4).

Both types of branching need to be addressed to successfully extend a mathematical model designed for a linear pathway to a branched pathway.

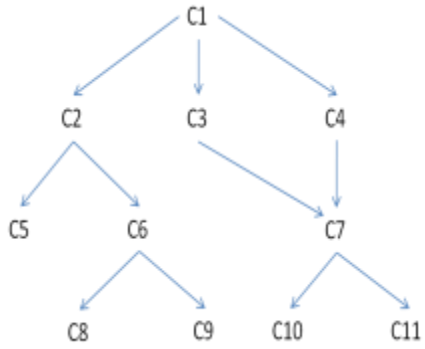

Figure 2.2. An example abstract schema of a branched reductive degradation pathway.

The mass balance equation for a compound *lc* in the aqueous phase in the presence of biodegradation and sorption can be written as

$$\frac{dC_{lc}^{aq}}{dt} = R_{source,lc}^{bio} - R_{sink,lc}^{bio,EA} - \frac{\rho_b dC_{lc}^{s}}{\theta dt} \quad (1)$$

where C_{lc}^{aq} is the aqueous phase concentration of the compound *lc* [ML^{-3}], *t* is the time [T], $R_{source,lc}^{bio}$ is the rate of production of the compound *lc* [$ML^{-3}T^{-1}$], $R_{sink,lc}^{bio,EA}$ is the rate of degradation of the compound *lc* [$ML^{-3}T^{-1}$], ρ_b is the bulk density of the solution [ML^{-3}], C_{lc}^{s} is the sorbed phase concentration of the compound *lc* [MM^{-1}] and θ is the dimensionless porosity. The equation is rearranged by taking the sorption term to the left hand side, assuming linear equilibrium isotherm for the sorption and introducing the distribution coefficient as

$$\left(1 + \frac{\rho_b K_{d,lc}}{\theta}\right) \frac{dC_{lc}^{aq}}{dt} = R_{source,lc}^{bio} - R_{sink,lc}^{bio,EA} \quad (2)$$

where $K_{d,lc}$ is the dimensionless distribution coefficient for the linear isotherm of compound *lc*. Other sorption models (non-linear equilibrium and kinetic) may be substituted for the linear model depending on site conditions, contaminants of interest and available data.

The formulation of the rate of degradation of a parent compound remains the same irrespective of the number of daughter products. The modified Michaelis-Menten kinetic equation for the rate of degradation of a compound *lc* ($R_{sink,lc}^{bio,EA}$) as presented earlier (Widdowson 2004) is

$$R_{sink,lc}^{bio,EA} = \frac{f_{lc} M_{red}}{\theta} v_{lc}^{max,EA} \left[\frac{\bar{C}_{lc}}{\bar{K}_{lc}^{EA} + \bar{C}_{lc}} \right] I_{lc,li} I_{lc,lj} \quad (3a)$$

where M_{red} is the total reducing microbial population density present in the aquifer [ML^{-3}], f_{lc} is the dimensionless fraction of the total reducing microbial population responsible for the reductive transformation of compound *lc*, $v_{lc}^{max,EA}$ is the maximum specific rate of reductive degradation for the compound *lc* [T^{-1}], $\bar{C}_{lc}$ is the effective concentration (defined as the difference between the aqueous phase concentration and the minimum concentration at which biodegradation occurs) of the compound *lc* [ML^{-3}], $\bar{K}_{lc}^{EA}$ is the effective half saturation constant for the compound *lc* [ML^{-3}] (defined as the aqueous phase concentration at which the rate of degradation is half of the maximum specific rate of degradation) and $I_{lc,li}$ and $I_{lc,lj}$ are inhibition functions defined as

$$I_{lc,li} = \prod_{li} \left[\frac{K_{lc,li}}{K_{lc,li} + \bar{E}_{li}} \right] \quad (3b)$$

$$I_{lc,lj} = \prod_{lj} \left[\frac{K_{lc,lj}}{K_{lc,lj} + \bar{C}_{lj}} \right] \quad (3c)$$

In the inhibition functions presented above, $I_{lc,li}$ represents the inhibition of the degradation of compound *lc* by the indigenous electron acceptors (li) present in the subsurface and $I_{lc,lj}$ represents inhibition of the same by other compounds in the degradation pathway (lj). Here, $\overline{E}_{li}$ is the effective concentration of the electron acceptor li [ML^{-3}], $\overline{C}_{lj}$ is the effective concentration of the inhibitor compound lj [ML^{-3}] and $K_{lc,li}$ and $K_{lc,lj}$ are the inhibition coefficients [ML^{-3}].

To address the first type of branching where a parent compound degrades to multiple daughter compounds, a branching coefficient was introduced in the model equations. The branching coefficient ($\xi^{dau}_{lc,lp}$) is defined as the fraction of the total rate of degradation of a parent compound *lp* that leads to the formation of a specific daughter compound *lc*. The sum of all branching coefficients for a parent compound should not exceed one for 100% mass balance, and it has a default value of one if only one daughter product is being generated by the degradation of the parent compound. Thus, the dimensionless daughter product generation coefficient ($\zeta^{dau}_{lc,lp}$) is now redefined as

$$\zeta^{dau}_{lc,lp} = \xi^{dau}_{lc,lp}\ \sigma^{dau}_{lc,lp} \tag{4}$$

where $\sigma^{dau}_{lc,lp}$ [MM^{-1}] is the stoichiometric coefficient derived from the parent-daughter reaction stoichiometry. The rate of production of the daughter compound *lc* from the parent compound *lp* ($R^{bio}_{source,lc,lp}$) then becomes

$$R^{bio}_{source,lc,lp} = \zeta^{dau}_{lc,lp}\ R^{bio,\ EA}_{sink,lp} = \xi^{dau}_{lc,lp}\ \sigma^{dau}_{lc,lp}\ R^{bio,\ EA}_{sink,lp} \tag{5}$$

To address the second form of branching where a single daughter degradation product could be formed by degradation of multiple parent compounds, the different rates of production are summed over all the parent compounds

$$R^{bio}_{source,lc} = \sum_{lp} R^{bio}_{source,lc,lp} = \sum_{lp} \xi^{dau}_{lc,lp} \, \sigma^{dau}_{lc,lp} \, R^{bio,\,EA}_{sink,lp} \qquad (6)$$

The set of equations (2), (3a), (3b), (3c) and (6) presented above can completely simulate the reductive biodegradation kinetics for an abstract branched pathway as shown in the Figure 2.2. For reductive dechlorination of chlorinated ethenes, specifying a value of unity for the branching ratios and including inhibition of daughter product degradation by the immediate parent compound reverts the modified equations back to the original equations put forward (Widdowson 2004).

2.4 Model Validation Methodology

To validate the model on a lab scale, two prior published bench scale studies of TNT degradation were chosen. The first study, conducted by Daun et. al. (1998), investigated the reductive degradation of TNT in the absence and presence of montmorillonitic clay to study the sorption of TNT and its different reduction products to soil components. The mixed culture used in the experiments was obtained from a continuous fixed bed culture grown in the presence of glucose and TNT. The fixed bed culture had originally been taken from a sewage plant. Bioreactors containing mineral medium and known concentrations of glucose and TNT were inoculated with the bacterial culture. The clay was added before the inoculum in experiments conducted in the presence of clay. Concentrated glucose solution was added regularly at periodic intervals. Sequential reduction of TNT to TAT along with stepwise formation of the intermediates including hydroxyaminodinitrotoluenes (HADNTs), ADNTs and DANTs was observed, both in the presence and absence of clay. Sorption of TNT and its degradation products was also

observed in the presence of clay, which makes sorption an important factor to consider while evaluating the fate and transport and time of remediation at TNT contaminated field sites.

The second study, conducted by Hwang et al. (2000), investigated the anaerobic reductive degradation of TNT by a mixed culture incubated under methanogenic conditions. The culture was obtained from the biofilm at a wastewater treatment plant that received explosives manufacturing wastewater. Slurry containing the biofilm and wastewater from the industrial wastewater treatment plant was added to serum bottles containing TNT and a basal salts medium. Glucose at 10 mM was added as a co-substrate to boost the microbial activity since methane production had decreased substantially over the course of time before the start of the experiment. Nearly complete stoichiometric degradation of TNT to TAT via stepwise reduction of the nitro groups was observed along with formation of all the isomeric intermediates involved in the TNT degradation pathway like 2-ADNT, 4-ADNT, 2,4-DANT and 2,6-DANT. Due to the relatively low amount of organic matter in the serum bottles, the authors concluded negligible sorption to the aqueous matrix.

For both studies, the experimental data was obtained by digitizing the published concentration-time graphs using the Engauge Digitizer v4.1 free software. The differential equations (2), (3a), (3b), (3c) and (6) were converted to finite-difference formulations and solved by employing an explicit solution using small time steps (Δt). The solution was programmed in Microsoft Office Excel 2007. The decrease in concentration for a compound *lc* due to biotransformation in a time interval Δt was calculated using the finite difference formulations of equations (3a) and (3b) as

$$\Delta C_{lc}^{sink,\Delta t} = \min\left\{\frac{v_{lc}^{max,EA}\, C_{lc}^{t}\, M_{red}\, \Delta t}{(K_{lc}^{EA} + C_{lc}^{t})\theta}\ \prod_{lp}\frac{K_{lc,lp}}{K_{lc,lp} + C_{lp}^{t+\Delta t}},\ C_{lc}^{t}\right\} \quad (7)$$

where the parameters f_{lc} and $I_{lc,li}$ were set as one due to lack of sufficient data to evaluate them.

The amount the compound *lc* formed in the time interval Δt by degradation of its parent compounds was calculated using the finite difference formulation of equation (6) as

$$\Delta C_{lc}^{source,\Delta t} = \sum_{lp} \xi_{lc,lp}^{dau} \sigma_{lc,lp}^{dau} (C_{lp}^{t} - C_{lp}^{t+\Delta t}) \quad (8)$$

The concentration of a compound *lc* after Δt time was, thus calculated using the finite difference formulation of equation (2) as

$$C_{lc}^{t+\Delta t} = C_{lc}^{t} + \frac{\Delta C_{lc}^{source,\Delta t} - \Delta C_{lc}^{sink,\Delta t}}{\left(1 + \frac{\rho_b K_{d,lc}}{\theta}\right)} \quad (9)$$

For the Daun et al. (1998) study, microbial growth during the exponential growth period was also factored in the above equations. In a similar experiment presented in the study, the authors measured optical density and observed an exponential increase during the initial few hours of the experiment. Optical density is directly correlated to and used to estimate the microbial activity using proportionality constants determined from experimental calibration curves. An initial lag phase in the degradation of TNT was also apparent in both the presence and absence of clay and was attributed to the growth in TNT reducing microbial activity within the exponential growth time frame of the total microbial population. The optical density data was plotted with time on a semi-log graph, and the growth rate constant was determined by fitting an exponential trendline. The initial microbial density (M_{red}) in equation (7) was determined using the given proportionality constant and the initial optical density and allowed to increase exponentially using the rate constant for the initial duration of the experiments, after which it was kept constant. The finite-difference formulation for calculating M_{red} at any given time t during the initial duration is

$$M_{red,t+\Delta t} = M_{red,t0}\, e^{k(t+\Delta t)} \qquad 0 \le t \le 6 \text{ hours} \quad (10)$$

Equation (10) along with (7), (8) and (9) was used to simulate the TNT degradation data in the absence of sorption presented in the Daun et al. (1998) study. The maximum specific rates of degradation, half saturation constants, inhibition coefficients and the daughter product branching ratios wherever applicable were used as calibration parameters. A sensitivity analysis was also performed for each compound to minimize the number of calibration parameters by identifying the correlated and excluding the insensitive calibration parameters. The stoichiometric coefficients were determined based on reaction stoichiometry and corresponding molecular weights. The porosity (θ) was set as one and the distribution coefficients for each compound were set to zero due to the absence of clay in the first part of the experiments. The total duration of experiments was 285 hours and successively increasing time step intervals of 0.1, 0.2 and 1 hours were used for a total of 430 time steps.

In the sorption experiments conducted in the presence of montmorillonitic clay, Daun et al. (1998) reported that 44.2 g (dry weight) of clay was dissolved in 1.33 L aqueous solutions of TNT, glucose and mineral medium. The bulk density of the solution was thus calculated as (44.2 g)/(1330 mL) which is equal to 0.033 g/mL. They also determined the distribution coefficients for each of the intermediate compounds except for HADNTs, 2,6-DANT and TAT. The porosity was calculated as

$$\theta = 1 - \frac{V_S}{V_T} \tag{11}$$

where the total volume of the solution (V_T) was taken as 1.33 L. The total volume of solids (V_s) was calculated by dividing the dry weight of clay with the density of dry clay (2.6 g/mL, Chitale et. al. 2000) as (44.2 g)/(2.6 g/mL) which comes out to be 17.0 mL. Thus the calculated porosity used in the model was 0.99.

The compatibility of the mathematical model presented above with the process of sorption was then validated by fitting the equations (7), (8), (9) and (10) to the TNT degradation data obtained from experiments conducted in the presence of montmorillonitic clay in the Daun et al. study. The distribution coefficients for HADNTs, ADNTs and DANTs were used as calibration parameters along with the calculated values of porosity and bulk density. The maximum specific rates of degradation were also used as calibration parameters for TNT and all of its metabolites. A sensitivity analysis was again performed for the calibration parameters for each compound, namely the maximum specific rates of degradation and distribution coefficients. The total duration of experiments in the presence of sorption was 285 hours, similar to the experiments in the absence of sorption, and correspondingly similar successively increasing time step intervals of 0.1, 0.2 and 1 hours were used for a total of 430 time steps.

The basic set of equations (7, 8 and 9) was used to simulate the TNT degradation data presented in the Hwang et al. (2000) study. For each compound *lc*, the maximum specific rate of degradation ($v_{lc}^{max,EA}$), the half saturation constant (K_{lc}^{EA}), the inhibition coefficients ($K_{lc,lp}$) and the daughter product branching ratios ($\xi_{lc,lp1}^{dau}$) where applicable were used as calibration parameters. The porosity (θ) was set as one and the distribution coefficients for each compound were set to zero since the experiments were conducted in a completely aqueous medium. Due to the lack of any data in the study regarding the values of microbial density or optical density during the course of the experiment, the microbial density was set to the resting cells density value obtained earlier in the Daun et al. 1998 study. Since a considerable period of time had elapsed before the experimental data used herein was collected in the Hwang et al. 2000 study, the microbial cells were assumed to be in a resting or stationary stage and the microbial density was kept constant throughout the course of the simulations for all the compounds. The stoichiometric coefficients ($\sigma_{lc,lp}^{dau}$) were determined based on a 1:1 parent-daughter molar ratio and corresponding molecular weights. A sensitivity analysis was also performed similar to that in the Daun et al. study for the model calibration

parameters for all compounds. The total duration of experiments was 30 days, and a time step interval of 0.1 day was used for a total of 350 time steps.

The goodness of fit of the model equations to the experimental data was evaluated by calculating the coefficient of determination R^2 for each graph. Measures of goodness of fit like R^2 summarize the discrepancy between experimental or observed values and model predicted values. R^2 compares the unexplained variance in the model fit to the data (variance of the model errors) with the total variance in the dataset. It varies in values from zero to one, and the closer the value of R^2 is to one, the better the fit of the model equations to the experimental data. The value of R^2 for each instance was calculated as:

$$R^2 = 1 - \frac{SS_{err}}{SS_{tot}} \tag{12}$$

where SS_{err} and SS_{tot} are the residual and total sum of squares each calculated as

$$SS_{err} = \sum_i (y_i - f_i)^2 \text{ and } SS_{tot} = \sum_i (y_i - \bar{y})^2 \tag{13}$$

where y_i are the observed or experimental values, f_i are the modeled or predicted values and $\bar{y}$ is the mean of the observed data calculated as

$$\bar{y} = \frac{1}{n} \sum_i^n y_i \tag{14}$$

where n is the number of observations.

The values of the calibration parameters in the model were determined by varying them in order to achieve the smallest value of the residual sum of squares and evaluating the best visual fit to the data. A

smaller value of the residual sum of squares would translate into a value of R^2 closer to one and signifies lower errors between the model-predicted and observed experimental values. The built in solver add-in in Microsoft Office Excel 2007 was used to vary the calibration parameter values along with manual calibration wherever needed. A sensitivity analysis was performed for all the model calibration parameters by varying them and plotting the corresponding changes in the residual sum of squares in graphs called spider curves. For parameters insensitive to model calibration, variations in their value did not result in any change in the residual sum of squares, thus giving horizontal straight curves parallel to the x-axis. These variables were excluded from the model calibration process. For sensitive parameters, the curves were inclined to the horizontal axis, and the shape of the curve gave an insight into whether the relationship was linear or not. Variables highly correlated to each other produce overlapping curves, which makes identification of a unique set of values for the correlated parameters difficult. The spider curves provide an easy way to identify such correlated parameters and allow us to identify if a unique solution set of model calibration parameters is determinable or not.

2.5 Results and Discussion

2.5.1 Case Study I – Modeling of Daun et al. 1998 (In absence of clay)

Figure 2.3 shows the experimental and model-predicted concentrations with time for TNT and its degradation products and the total mole balance in the absence of montmorillonitic clay as presented in Daun et al. 1998. The total sum of the molar concentrations of TNT and its degradation products in the absence of clay decreased in the initial few hours of the experiment, but then increased back close to the original value and remained constant till it finally decreased gradually with the formation and degradation of TAT. The initial drop in the total molar concentration was attributed to the absence of analytical standards for the pure isomers of HADNTs by the authors of the study. The gradual decrease in the total mole balance with the formation of TAT is due to further degradation of TAT to unidentified compounds.

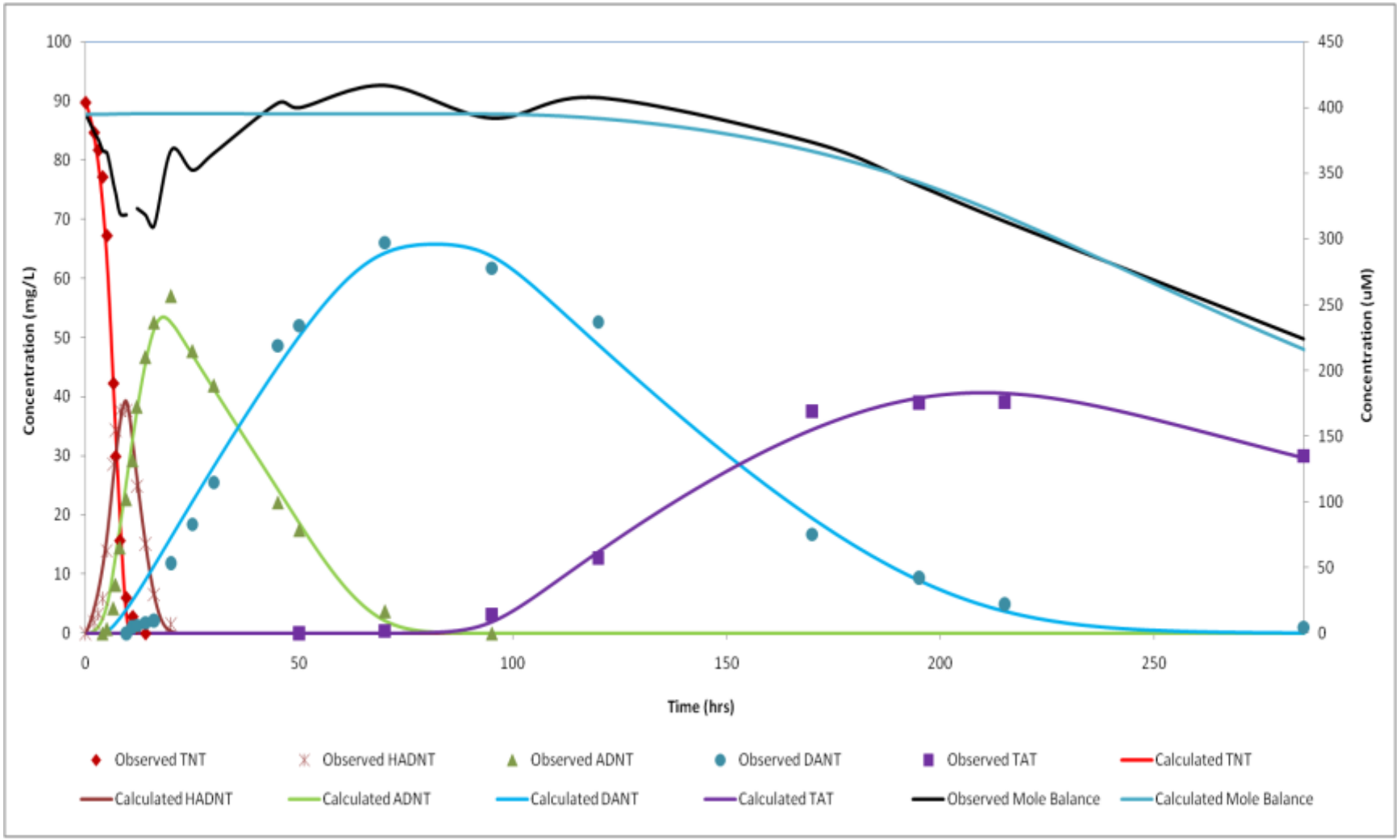

Figure 2.3. Experimentally determined concentrations of TNT and its degradation products and the total mole balance in the absence of clay with time and associated model fits (Case Study I).

Figure 2.4 presents the semi-log graph of the optical density vs. time data. An exponential trendline was fitted to the optical density data and the microbial growth rate constant was determined as 0.3489 hr^{-1}. The trendline fitted to the exponential growth phase showed a high correlation to the measured optical density data (r-square value of 0.99). The corresponding microbial density was calculated using the reported proportionality constant of 3.9 L/g. Thus the microbial density was initially calculated to be 5.08 mg/L and allowed to increase exponentially for the observed lag period in TNT degradation to a final constant value of 41.21 mg/L. Figure 2.4 also shows the microbial density vs. time plotted on the secondary axis.

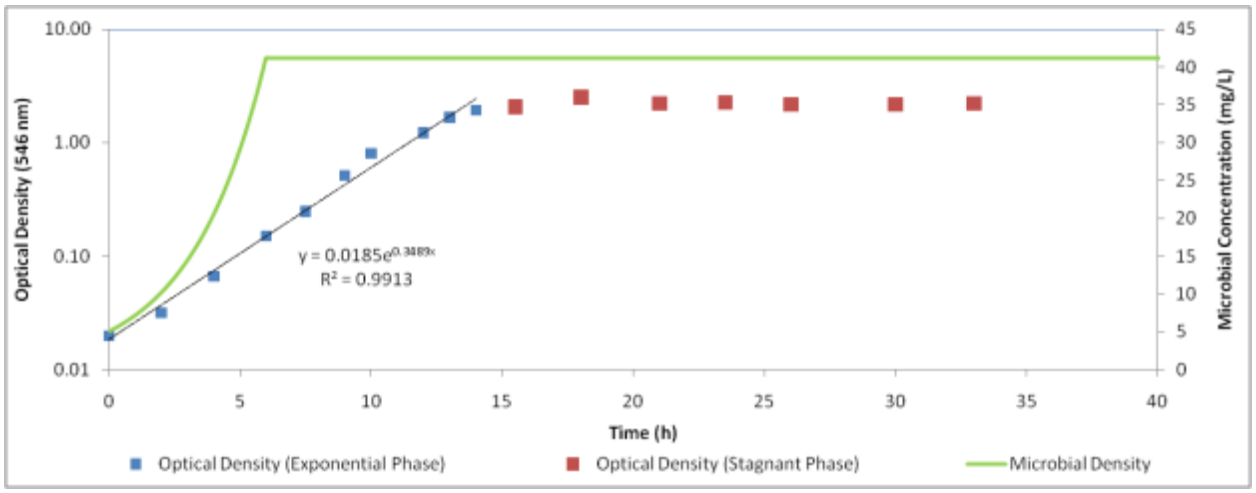

Figure 2.4. Optical Density (measured at 546 nm) and microbial density with time.

To account for the observed initial drop in the total molar concentration, a proxy HADNT isomeric compound was added to the TNT degradation pathway being modeled (Figure 2.4). The branching coefficient for the observed HADNT compounds was determined by model calibration to the experimentally determined HADNT concentrations with time. The branching coefficient for the proxy HADNT compounds was calculated by keeping the sum of both branching coefficients as one. The concentrations of the proxy HADNT compounds were calculated with time by subtracting the observed total molar concentrations with time from the initial total molar concentration. The other model

parameters for the proxy HADNT compounds were then determined by calibrating the model to the calculated concentrations with time. The branching coefficients were set to one for all the remaining compounds where the parent compound's degradation led to the formation of a single daughter compound.

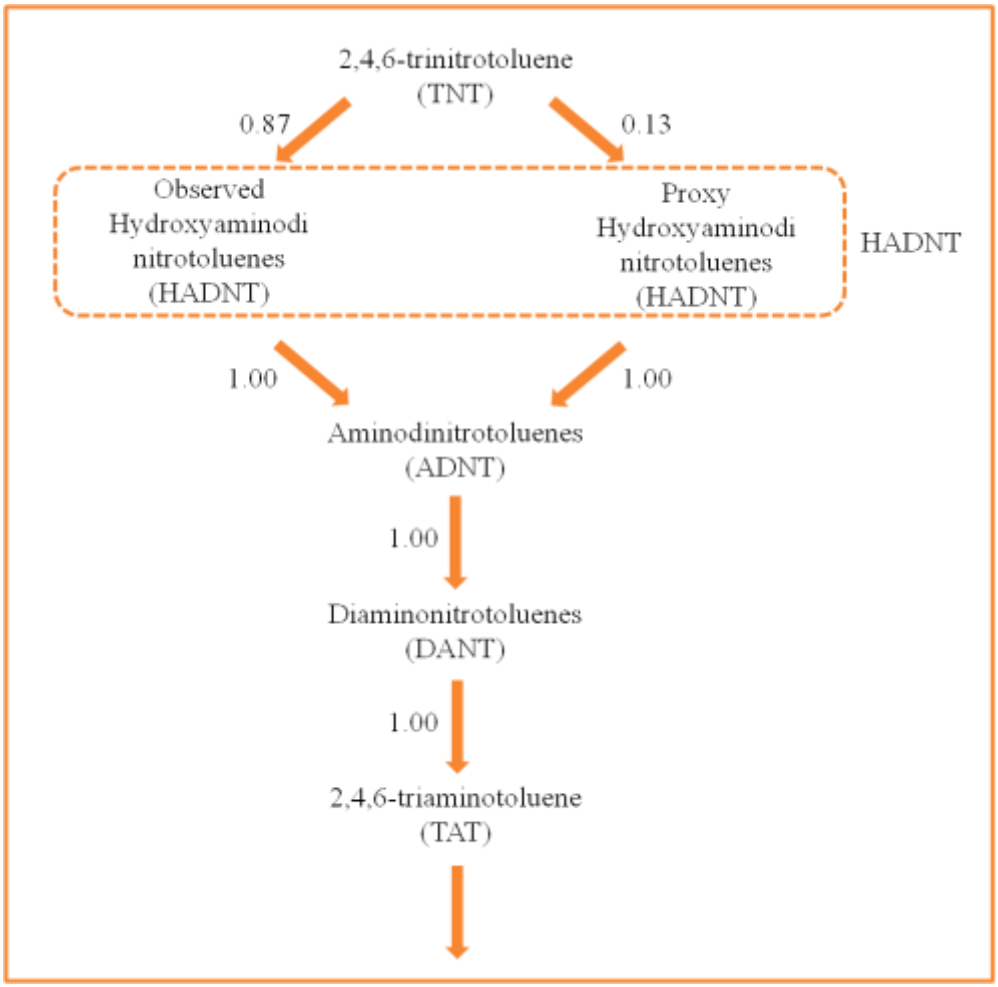

Figure 2.5. TNT degradation schema with branching coefficients in absence of clay (Case Study I)

The concentrations of all the isomers of each aminonitrotoluene have been summed together since they coeluted in the experiment and their individual concentrations were not determined in the study. Table 2.1 shows the parameter values and the associated r-square values for each compound. Sensitivity analysis was performed for each compound's model calibration parameters. The insensitive calibration parameters

have been highlighted with a grey shaded background while the calibration parameters have been differentiated from the experimentally determined parameters by bold style font in Table 2.1. Model fits to experimental data and the results of sensitivity analysis for each individual compound are shown in Appendix (Figures A.1 to A.12).

Table 2.1. Values of model parameters and R-square values (Case Studies I & II)

Parameter		Units	TNT	HADNT	ADNT	DANT	TAT
Without Sorption	Maximum Specific Rate of Degradation ($v_{lc}^{max,EA}$)	/hr	**0.42**	**0.197**	**0.04**	**0.02**	**0.011**
	Half Saturation Constant (K_{lc}^{EA})	mg/L	**5.74**	**9.63**	**8**	**13.36**	**40**
	Initial Microbial Density ($M_{red,t0}$)	mg/L	5.08				
	Microbial Growth Rate Constant (k)	/hr	0.3489				
	Porosity (θ)	--	1.00				
	Branching Coefficient ($\xi_{lc,lp}^{dau}$)	--	--	**0.87**	1.00	1.00	1.00
	Inhibition Coefficient ($K_{lc,lp}$)	mg/L	--	1000	1000	**0.01**	**21.54**
	Number of Calibration Parameters	--	2	3	2	3	3
	R-Square	--	1.00	0.98	0.98	0.97	1.00
With Sorption*	Maximum Specific Rate of Degradation ($v_{lc}^{max,EA}$)	/hr	**0.326**	**0.3**	**0.017**	**0.014**	**0.003**
	Branching Coefficient ($\xi_{lc,lp}^{dau}$)	--	--	0.48	1.00	1.00	1.00
	Porosity (θ)	--	0.99				
	Bulk Density (ρ_b)	g/L	0.033				
	Distribution Coefficient ($K_{d,lc}$)	L/Kg	6.22	**9.61**	**3.07**	**7.86**	--
	Number of Calibration Parameters	--	1	2	2	2	1
	R-Square	--	1.00	0.92	0.96	0.98	1.00

* The half saturation constants, microbial growth parameters and inhibition coefficients remain the same

Excellent correlation was observed between the model derived and experimentally determined concentrations of TNT and its degradation products with time. This is apparent in the very good fits observed in the graphs and the range of values obtained for the r-square values for each graph (0.97 – 1.00). The model calibration determined maximum specific rates of degradation decrease from TNT to

TAT along the reductive degradation pathway. The rates correlates well with the increasing one electron reduction potentials along the degradation pathway as determined experimentally in prior published studies (Hofstetter et al. 1999).

The inhibition constants for inhibition of HADNT's degradation by TNT and ADNT's degradation by HADNT were found to be insensitive to model calibration. However, the inhibition constants for inhibition of DANT's and TAT's degradation were sensitive to the model calibration, and the degradation of DANTs was found to be strongly inhibited by the presence of ADNTs, as is evident in the very low value of 0.01 for the DANT inhibition constant. This correlates well with the fact that the authors determined the reduction of DANT to be the overall rate-limiting step of the reduction of TNT to TAT in the experimental study.

The concentration of TAT was observed to decrease after reaching a plateau in the final hours of the experiment indicating further degradation of TAT to compounds unidentified in the study. The model parameters associated with TAT degradation like the maximum specific rate, the half saturation constant and the inhibition coefficient due to DANT's presence were all found to be sensitive to model calibration for TAT. The total molar balance calculated in the model also correlates well with the experimental total molar balance and decreases with the formation of TAT thus providing further evidence of TAT's degradation.

2.5.2 Case Study II – Modeling of Daun et al. 1998 (In presence of clay)

Figure 2.6 shows the experimental and model-predicted concentrations with time for TNT and its degradation products and the total mole balance in the presence of montmorillonitic clay as presented in

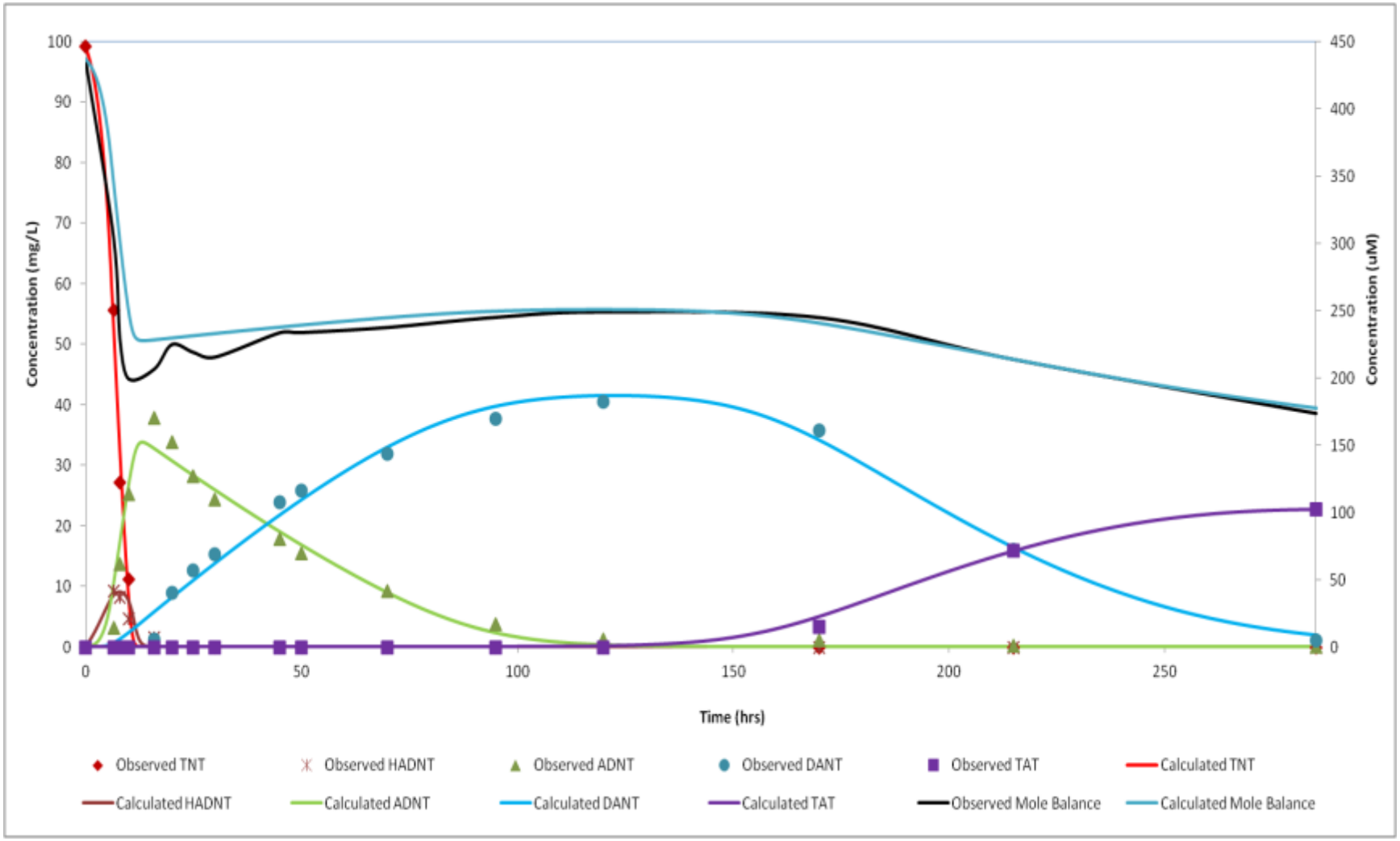

Figure 2.6. Experimentally determined concentrations of TNT and its degradation products and the total mole balance in the presence of clay with time and associated model fits (Case Study II)

Daun et al. (1998). The total sum of the molar concentrations of TNT and its degradation products in the presence of clay decreased in the initial few hours of the experiment and then remained nearly constant till it finally decreased gradually with the formation and degradation of TAT. The systemic decrease in the sum of concentrations of all the degradation products of TNT in the presence of clay was attributed to the irreversible sorption of HADNT intermediates to montmorillonitic clay. The gradual decrease in the total mole balance with the formation of TAT is due to further degradation of TAT, similar to what was observed in the absence of clay.

To account for the permanent drop in the total molar concentration with the irreversible sorption of HADNT intermediates, the fraction of total HADNT formed that disappeared from the system was determined by subtracting the maximum total molar concentration observed later in the experiment from the initial total molar concentration. Thus, in the TNT degradation pathway being modeled (Figure 2.7), an additional sink component corresponding to the irreversible sorption of HADNT was also added. The concentrations of the proxy HADNT compounds were calculated with time by subtracting the observed total molar concentration from the maximum total molar concentration. The branching coefficients for the observed and proxy HADNT compounds were determined by multiplying the branching coefficients determined earlier in the absence of clay with the fraction of HADNTs not irreversibly bound to the clay.

Table 2.1 shows the parameter values and the associated r-square values for each compound. The half saturation constants, microbial growth parameters and the inhibition constants for each compound remained the same as determined previously in the absence of clay. For TNT, model calibration was successfully achieved by only using the maximum specific rate of degradation as the calibration parameter and using the value of linear sorption isotherm distribution coefficient determined experimentally by the authors in separate adsorption-desorption experiments. For HADNTs, ADNTs and DANTs, both the maximum specific rates of degradation and the linear sorption isotherm distribution coefficients were used as calibration parameters and were determined by calibrating the model to the

experimentally observed concentrations with time in the presence of clay. For TAT, the maximum specific rate of degradation was the only calibration parameter since sorption was not modeled because the authors reported complete irreversible sorption of TAT to montmorillonitic clay.

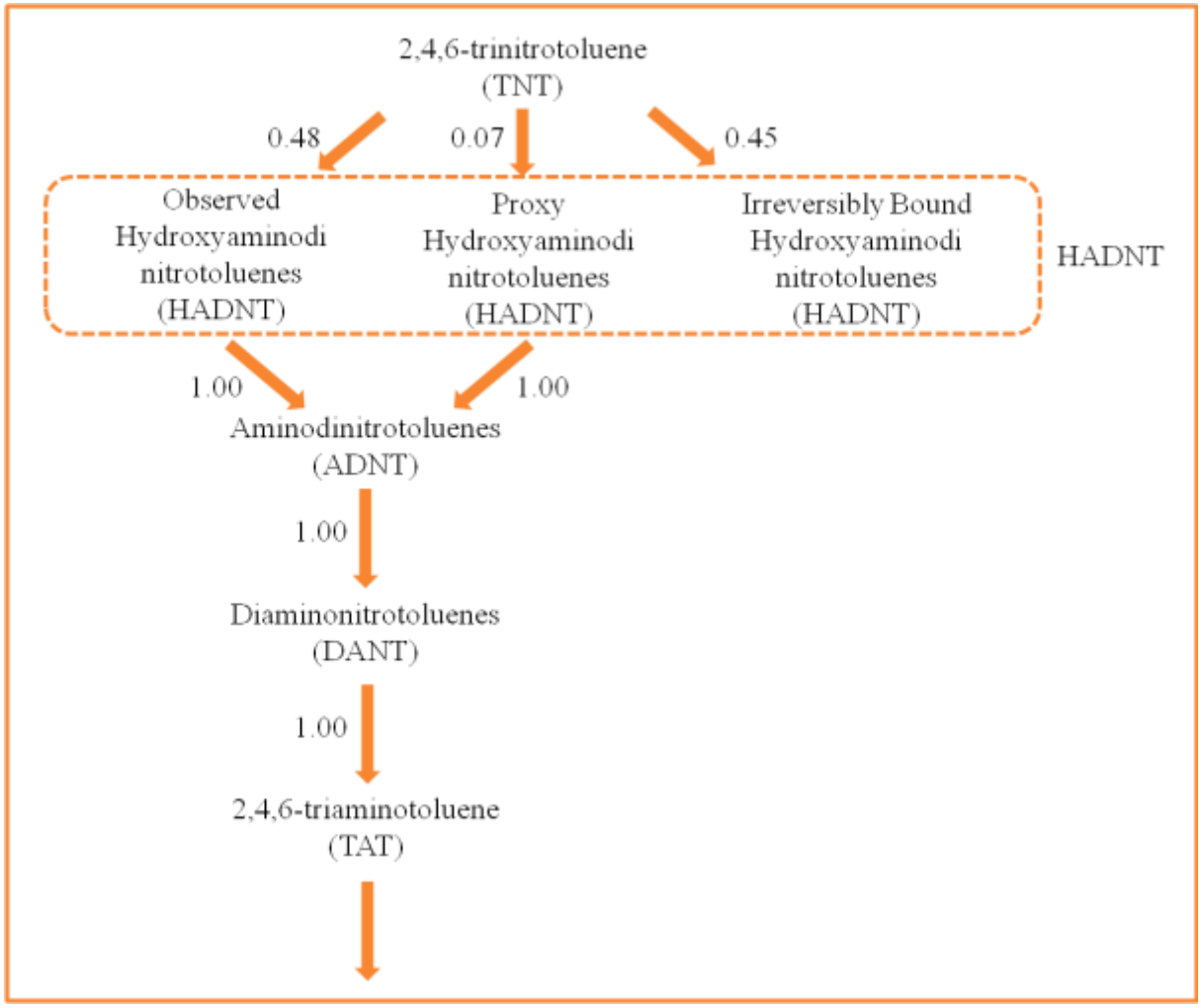

Figure 2.7. TNT degradation schema with branching coefficients in presence of clay (Case Study II)

Sensitivity analysis was performed for each compound's model calibration parameters. The calibration parameters have been differentiated from the experimentally determined parameters by bold font style in Table 2.1. Model fits to experimental data and the results of sensitivity analysis for each individual compound are shown in Appendix (Figures A.13 to A.23).

Calibration of the mathematical model in the presence of sorption to clay was successful for all the degradation products. Very good model fits to the observed concentrations were obtained as indicated by the range of r-square values (0.92 – 1.00). The maximum specific rates of degradation decreased along the pathway from TNT to TAT in a trend similar to that observed in the absence of clay. With the exception of HADNTs, the maximum specific rates of degradation were all lower in the presence of sorption as compared to those in the absence of sorption. This is expected since sorption to soils and sediments often results in reduced bioavailability for microbial metabolism and correspondingly reduced biodegradability of organic contaminants (Wszolek and Alexander 1979; Ogram et al. 1985).

The model calibration determined value of distribution coefficient of ADNTs (3.07 L/Kg) falls within the distribution coefficients of 2-ADNT (5.26 L/Kg) and 4-ADNT (1.77 L/Kg) experimentally determined by the authors of the Daun et al. 1998 study. For DANTs, the model calibration determined distribution coefficient (7.86 L/Kg) is higher than that determined experimentally in the study (1.80 L/Kg). However, it should be noted that the mathematical model presented herein assumes an equilibrium linear isotherm sorption model, while hysteresis between the adsorption and desorption isotherms indicating only partially reversible sorption was observed for 2,4-DANT in the study. For HADNTs, rapid sorption to montmorrilonitic clay was reported in the study, and the permanent decrease observed in total molar concentration with their formation makes them good candidates for irreversible sorption. However, adsorption-desorption experiments evaluating reversible vs. irreversible sorption were not performed and the distribution coefficient was not determined experimentally for HADNTs in the study. The model calibration determined value of distribution coefficient for HADNTs (9.61 L/Kg) is higher than those determined for TNT and its other metabolites, which correlates well with the observed strong sorption tendency of HADNTs.

2.5.3 Case Study III – Modeling of Hwang et al. 2000

Figure 2.8 shows the observed and simulated concentration vs. time data for TNT and all its degradation products and the total mole balance as presented in Hwang et al. 2000. The total molar amount of TNT and its derivatives drops initially and remains low for the first six hours, but then increases back close to the original sum for a short period of time after which it decreases steadily. The drop in the total mass in the initial few hours of the experiment was attributed to the lack of standards and analytical testing for the nitroso and hydroxylaminodinitrotoluenes. The gradual decrease in the total mass observed in the later part of the experiment is due to further degradation of TAT to unidentified products similar to that observed in the Daun et al. 1998 study.

The drop in the total molar amount of TNT and its metabolites observed initially was accounted for by introducing a proxy ADNT isomeric compound similar to the proxy HADNT isomeric compound that was introduced in the modeling of the Daun et al. 1998 study. The TNT degradation pathway being modeled for the Hwang et al. 2000 study which includes the proxy isomeric ADNT compound is shown in Figure 2.9. The branching coefficients for TNT's degradation to 2-ADNT and 4-ADNT and for 2-ADNT's degradation to 2,4-DANT and 2,6-DANT were determined by model calibration to the experimentally determined concentrations with time. The concentration of the proxy isomeric ADNT compound with time was calculated by subtracting the observed total molar amount with time from the initial total molar amount. The corresponding branching coefficient for the proxy ADNT isomer was calculated by subtracting the sum of the branching coefficients of 2-ADNT and 4-ADNT from one. The other model parameters for the proxy isomeric ADNT compound were then evaluated by model calibration to the calculated concentrations with time. For the remaining metabolites of TNT, wherever the parent compound's degradation led to the formation of a single daughter compound, the branching coefficients were all set to one.

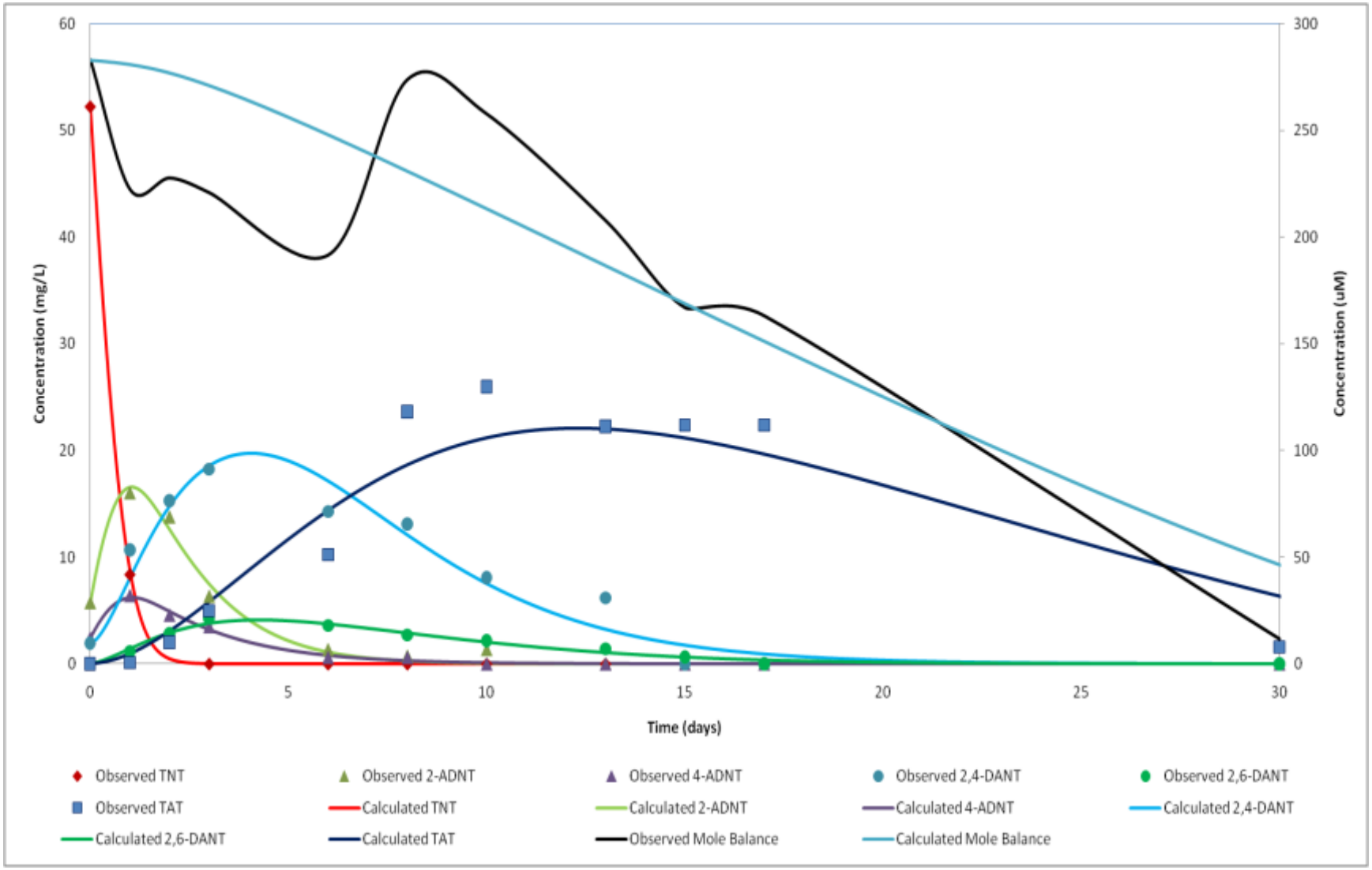

Figure 2.8. Experimentally determined concentrations of TNT and its degradation products and the total mole balance with time and associated model fits (Case Study III)

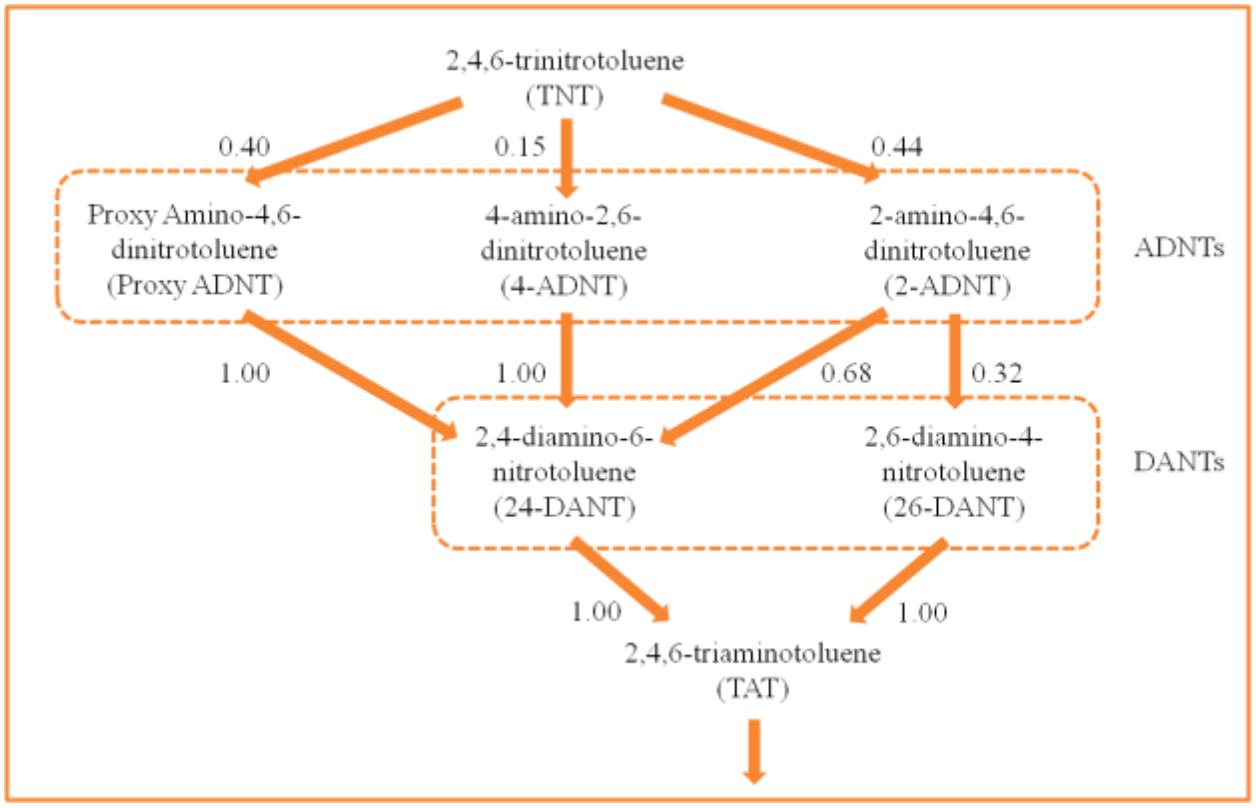

Figure 2.9. TNT degradation schema with branching coefficients (Case Study III)

The parameter values and the associated r-square values for each compound are presented in Table 2.2. Sensitivity analysis was also performed for each compound's model calibration parameters. The inhibition constants defined in the degradation pathway were found to be insensitive from the sensitivity analysis results and their inclusion in the model did not improve the model fit or the r-square values. The insensitive calibration parameters and the sensitive calibration parameters have been differentiated from the experimentally determined parameters by shaded backgrounds and bold style fonts in Table 2.2 in a manner similar to Table 2.1. The concentration vs. time graphs showing the model fits to experimental data and the results of sensitivity analysis for each individual compound are in Appendix (Figures A.24 to A.37). The model-predicted concentrations of TNT and its degradation products at different time points correlate very well with the experimentally determined concentrations as is evident from the r-squares for each individual curve (range: 0.92 – 1.00).

Table 2.2. Values of model parameters and R-Square values (Case Study III)

Parameter	Units	TNT	2-ADNT	4-ADNT	2,4-DANT	2,6-DANT	TAT
Maximum Specific Rate of Degradation ($v_{lc}^{max,EA}$)	/hr	**0.109**	**0.023**	**0.019**	**0.013**	**0.0011**	**0.0014**
Half Saturation Constant (K_{lc}^{EA})	mg/L	**40**	**34.2**	**40**	**40**	**3.52**	**3.22**
Microbial Density (M_{red})	mg/L	41.74*					
Branching Coefficient ($\xi_{lc,lp1}^{dau}$)	--	--	**0.44**	**0.15**	**0.68**	**0.32**	1.00
Branching Coefficient ($\xi_{lc,lp2}^{dau}$)	--	--	--	--	1.00	--	1.00
Inhibition Coefficient ($K_{lc,lp1}$)	mg/L	--	1000	1000	1000	1000	--
Inhibition Coefficient ($K_{lc,lp2}$)	mg/L	--	--	--	1000	--	--
Number of Calibration Parameters	--	2	3	3	3	3	2
R-Square	--	1.00	0.99	0.99	0.94	0.97	0.92

* The microbial density was assumed to be equal to the resting cells population determined from the Daun et al. 1998 study

The model calibration determined maximum specific rates of degradation decreased with increasing substitution of nitro groups with amino groups along the degradation pathway. This correlates well with the fact that progressively increasing reducing conditions are required for reduction of each nitro group to an amino group (Hofstetter et. al. 1999). The decreasing trend in the rates also correlates well with that observed in the modeling of the Daun et al. 1998 study and the one electrode reduction potentials experimentally determined for each compound in prior published studies (Hofstetter et. al. 1999). The only exceptions are the DANTs where the model determined degradation rate of 2,6-DANT is lower than that of 2,4-DANT, whereas the one-electron reduction potential is higher for 2,4-DANT.

The maximum specific rates of degradation determined for the Hwang et al. 2000 study are lower than those determined for the Daun et al. 1998 study for TNT and all of its degradation products. This is also reflected in the duration of the experiments since it took 17 days from the start of the experiments for the TNT, ADNTs and DANTs to completely degrade to TAT in the Hwang et al. 2000 study as compared to 12 days in the Daun et al. 1998 study. An important difference in the experimental conditions leading to the lowering of rates in the Hwang et al. 2000 study could be the availability of the co-substrate glucose,

Table 2.3. Comparison of model calibration determined kinetic parameters for TNT degradation and experimental conditions for Case Studies I, II and III with prior published studies.

Publication	Vmax (mg TNT/mg biomass/hr)	Ks (mg/L)	Initial TNT Concentration (uM)	Aerobic/ Anaerobic	Growth Substrate	Electron Donor Availability	Sorption Matrix
Hwang et al. 2000*	0.109*	40*	230	Anaerobic	Sludge containing biofilm and wastewater initially, glucose 10 mM added later to boost the microbial activity	Low amount of glucose and organic matter	Organic matter in sludge, but sorption not observed
Daun et al. 1998 (without Sorption)*	0.42*	5.74*	400	Anaerobic	Glucose fed continuously throughout the course of the experiment with concentration starting from 5 mM to finally 40 mM	Excess availability of Glucose	None
Daun et al. 1998 (with Sorption)*	0.326*	5.74*	440				Montmorillonitic clay as mineral soil component, low in organic carbon
Admassu et al. 1998	0.84	2.02	968.6	Anaerobic	An optimized rich growth substrate containing corn steep liquor and molasses as carbon and nitrogen source	Excess availability of growth substrate	None
Yin et al. 2005	0.68	28.68	50 - 400	Anaerobic	20 mM glycerol	Excess glycerol available	None

* The kinetic parameters for TNT degradation for these experimental studies have been determined from model calibration.

which was added periodically in the Daun et al. 1998 experiments to avoid microbial growth limitations arising due to its availability. Table 2.3 presents a comparison of the model calibration determined kinetic parameters for TNT degradation in the Daun et al. 1998 and Hwang et al. 2000 studies with prior published results along with a comparison of the experimental conditions.

2.6 Conclusions

This study presented a kinetic model based on the Michaelis-Menten kinetic equations for simulating the complex branched reductive degradation pathways of groundwater contaminants such as TNT. It was further shown that the mathematical model can be easily modified to include key features of biodegradation pathways in the subsurface like parent-daughter inhibition, microbial growth and sorption to the aquifer matrix. The model was successfully validated with experimental datasets describing TNT and its derivatives' degradation and formation through a branched pathway, both in the presence and absence of sorption to natural soil components like clay.

It is useful to develop kinetic models which incorporate contaminant reductive transformation processes from a regulatory point of view to achieve cleanup goals at contaminated sites. The proposed model will provide the capability to simulate the kinetics of the reductive biodegradation process of such contaminants in the presence of other important processes in the subsurface like sorption, advection, dispersion and diffusion and will allow the creation of site-specific solute transport models which can be further used to evaluate the impacts of remediation activities at the sites. The validated model can be integrated with a solute transport code and used to create a calibrated solute transport model, which can then be used to simulate the transport and attenuation of TNT and other contaminants in groundwater.

2.7 References

Admassu, W., Sethuraman, A.V., Crawford, R., Korus, R.A., 1998. Growth Kinetics of *Clostridium bifermentans* and Its Ability to Degrade TNT Using an Inexpensive Alternative Medium. *Bioremediation Journal* 2, 17-28.

Agency for Toxic Substances and Disease Registry (ATSDR), 1995. Toxicological profile for 2,4,6-trinitrotoluene (TNT). Atlanta, GA: U.S. Department of Health and Human Services, Public Health Service.

Azadpour-Keeley, A., Russell, H.H., Sewell, G.W., 1999. Microbial Processes Affecting Monitored Natural Attenuation of Contaminants in the Subsurface. *Ground Water Issue*, U.S. EPA 540/S-99/001, Office of Solid Waste and Emergency Response, Washington, DC.

Boopathy, R., Manning, J., Montemagno, C., Kulpa, C., 1994. Metabolism of 2,4,6-Trinitrotoluene by a *Pseudomonas* Consortium under Aerobic Conditions. *Current Microbiology* 28, 131-137.

Chapelle, F.H., Widdowson, M.A., Brauner, J.S., Mendez III, E., Casey, C.C., 2003. Methodology for Estimating Times of Remediation Associated with Monitored Natural Attenuation. U.S. Geological Survey Water-Resources Investigation Report 03-4057, 51 pp.

Charbeneau, R.J., 2000. Groundwater Hydraulics and Pollutant Transport, 1st edition. Prentice Hall, Upper Saddle River, NJ.

Chen, C., Puhakka, J.A., Ferguson, J.F., 1996. Transformations of 1,1,2,2-Tetrachloroethane under methanogenic conditions. *Environmental Science and Technology* 30, 542-547.

Chitale, D.V., Sigal, R., Halliburton Energy Services, 2000. NMR Characterization of the Water Adsorbed by Montmorillonite: Impact on the Analysis of Porosity Logs. SPE/AAPG Western Regional Meeting, 19-22 June 2000, Long Beach, California

Criddle, C.S., 1993. The Kinetics of Cometabolism. *Biotechnology and Bioengineering* 41, 1048-1056.

Daun, G., Lenke, H., Reuss, M., Knackmuss, H.J., 1998. Biological Treatment of TNT-Contaminated Soil. 1. Anaerobic Cometabolic Reduction and Interaction of TNT and Metabolites with Soil Components. *Environmental Science and Technology* 32, 1956-1963.

Daun, G., Lenke, H., Knackmuss, H.J., Reuss, M., 1999. Experimental investigations and kinetic models for the cometabolic biological reduction of trinitrotoluene. *Chemical Engineering and Technology* 22, 308-313.

Dou, J., Liu, X., Hu, Z., Deng, D., 2008. Anaerobic BTEX biodegradation linked to nitrate and sulfate reduction. *Journal of Hazardous Materials* 151, 720-729.

Drzyzga, O., Bruns-Nagel, D., Gorontzy, T., Blotevogel, K.H., Gemsa, D., Low, E.V., 1998. Mass Balance Studies with ^{14}C-Labeled 2,4,6-Trinitrotoluene (TNT) Mediated by an Anaerobic *Desulfovibrio* Species and an Aerobic *Serratia* Species. *Current Microbiology* 37, 380-386.

Esteve-Nunez, A., Caballero, A., Ramos, J.L., 2001. Biological degradation of 2,4,6-trinitrotoluene. *Microbiology and Molecular Biology Reviews* 65, 335-352.

George, S.E., Huggins-Clark, G., Brooks, L.R., 2001. Use of a Salmonella microsuspension bioassay to detect the mutagenicity of munitions compounds at low concentrations. *Mutation Research-Genetic Toxicology And Environmental Mutagenesis* 490, 45-56.

Grindstaff, M., 1998. Bioremediation of Chlorinated Solvent Contaminated Groundwater. U.S. EPA Technology Innovation Office, National Network of Environmental Management Studies Fellowship.

Haïdour, A., Ramos, J.L., 1996. Identification of products resulting from the biological reduction of 2,4,6-trinitrotoluene, 2,4-dinitrotoluene and 2,6-dinitrotoluene by *Pseudomonas sp. Environmental Science and Technology* 30, 2365-2370.

Hofstetter, T.B., Heijman, C.G., Haderlein, S.B., Holliger, C., Schwarzenbach, R.P., 1999. Complete Reduction of TNT and Other (Poly)nitroaromatic Compounds under Iron-Reducing Subsurface Conditions. *Environmental Science and Technology* 33, 1479-1487.

Hunkeler, D., Aravena, R., Berry-Spark, K., Cox, E., 2005. Assessment of Degradation Pathways in an Aquifer with Mixed Chlorinated Hydrocarbon Contamination Using Stable Isotope Analysis. *Environmental Science and Technology* 39, 5975-5981.

Hwang, P., Chow, T., Adrian, N.R., 2000. Transformation of Trinitrotoluene to Triaminotoluene by Mixed Cultures Incubated under Methanogenic Conditions. *Environmental Toxicology and Chemistry* 19(4), 836-841.

Lorah, M.M., Olsen, L.D., 1999. Degradation of 1,1,2,2-Tetrachloroethane in a freshwater tidal wetland: Field and laboratory evidence. *Environmental Science and Technology* 33, 227-234.

McCormick, N.G., Feeherry, F.E., Levinson, H.S., 1976. Microbial transformation of 2,4,6-trinitrotoluene and other nitroaromatic compounds. *Applied and Environmental Microbiology* 31, 949-958.

Ogram, A.V., Jessup, R.E., Ou, L.T., Rao, P.S.C., 1985. Effects of Sorption on Biological Degradation Rates of (2,4-Dichlorophenoxy)acetic Acid in Soils. *Applied and Environmental Microbiology* 49, 582-587.

Park, C., Kim, T.H., Kim, S., Lee, J., Kim, S.W., 2002. Biokinetic Parameter Estimation for Degradation of 2,4,6-Trinitrotoluene (TNT) with *Pseudomonas putida* KP-T201. *Journal of Bioscience and Bioengineering* 94, 57-61.

Pavlostathis, S.G., Jackson, G.H., 1999. Biotransformation of 2,4,6-Trinitrotoluene in *Anabaena Sp.* Cultures. *Environmental Toxicology and Chemistry* 18, 412-419.

Riefler, R.G., Smets, B.F., 2002. NAD(P)H:Flavin Mononucleotide Oxidoreductase Inactivation during 2,4,6-Trinitrotoluene Reduction. *Applied and Environmental Microbiology* 68, 1690-1696.

Salanitro, J.P., Wisniewski, H.L., Byers, D.L., Neaville, C.C., Schroder, R.A., 1997. Use of Aerobic and Anaerobic Microcosms to Assess BTEX Biodegradation in Aquifers. *Ground Water Monitoring and Remediation* 17, 210-221.

Schafer, R., Achazi, R.K., 1999. The toxicity of soil samples containing TNT and other ammunition derived compounds in the enchytraeid and collembola-biotest. *Environmental Science and Pollution Research* 6, 213-219.

Schulze, S., Tiehm, A., 2004. Assessment of microbial natural attenuation in groundwater polluted with gasworks residues. *Water Science and Technology* 50, 347-353.

Spain, J.C., 1995. Biodegradation of nitroaromatic compounds. *Annual Review of Microbiology* 49, 523-555.

Spanggord, R.J., Stewart, K.R., Riccio, E.S., 1995. Mutagenicity of tetranitroazoxytoluenes: a preliminary screening in *Salmonella typhimurium* strains TA100 and TA100NR. *Mutation Research-Environmental Mutagenesis And Related Subjects* 335, 207-211.

USEPA, 1998. Health Advisory on Trinitrotoluene, Office of Drinking Water, Washington DC.

Villatoro-Monzón, W.R., Mesta-Howard, A.M., Razo-Flores, E., 2003. Anaerobic biodegradation of BTEX using Mn(IV) and Fe(III) as alternative electron acceptors. *Water Science and Technology* 48, 125-131.

Vogel, T.M., McCarty, P.L., 1985. Biotransformation of Tetrachloroethylene to Trichloroethylene, Dichloroethylene, Vinyl Chloride, and Carbon Dioxide under Methanogenic Conditions. *Applied and Environmental Microbiology* 49, 1080-1083.

Vogel, T.M., Criddle, C.S., McCarty, P.L., 1987. Transformation of halogenated aliphatic-compounds. *Environmental Science and Technology* 21, 722 – 736.

Waddill, D.W., Widdowson, M.A., 1998. A three-dimensional model for subsurface transport and biodegradation. *Journal of Environmental Engineering-ASCE* 124, 336-344.

Waddill, D.W., Widdowson, M.A., 2000. SEAM3D: A numerical model for three-dimensional solute transport and sequential electron acceptor-based bioremediation in groundwater. ERDC/EL TR-00-X, U.S. Army Engineer Research and Development Center, Vicksburg, MS, 89 pp.

Wang, Z., Ye, Z., Zhang, M., Bai, X., 2010. Degradation of 2,4,6-trinitrotoluene (TNT) by immobilized microorganism-biological filter. *Process Biochemistry* 45, 993-1001.

Widdowson, M.A., 2004. Modeling natural attenuation of chlorinated ethenes under spatially varying redox conditions. *Biodegradation* 15, 435-451.

Wszolek, P.C., Alexander, M., 1979. Effect of desorption rate on the biodegradation of n-alkylamines bound to clay. *Journal of Agricultural and Food Chemistry* 27, 410–414.

Yin, H., Wood, T.K., Smets, B.F., 2005. Reductive transformation of TNT by Escherichia coli resting cells:kinetic analysis. *Applied Microbiology and Biotechnology* 69, 326-334.

Chapter 3

Conclusions

This research presents a novel approach to simulating microbially-mediated reductive transformation of contaminants degrading through branched pathways, including explosives (e.g., 2,4,6-trinitrotoluene (TNT)), chlorinated ethenes and ethanes and other classes of regulated compounds. While kinetic models have been successfully developed and applied to linear reductive transformation pathways (e.g. reductive dechlorination of chlorinated ethenes), there is a lack of kinetic models capable of completely describing complex branched reductive transformation pathways which has led prior attempts to traditionally focus only on simulating the degradation of the source parent contaminant compound. The kinetic model presented herein, although validated for only one contaminant group, has been developed with a non-prescriptive framework that provides enough flexibility for application to other contaminants and provides the capability to simulate the complete branched reductive transformation pathways including the source parent compound and all its metabolites.

It is useful to develop kinetic models which incorporate contaminant reductive transformation processes from a regulatory point of view to achieve cleanup goals at contaminated sites. The proposed model will provide the capability to simulate the kinetics of the reductive biodegradation process of such contaminants in the presence of other important processes in the subsurface like sorption, advection, dispersion and diffusion and will allow the creation of site-specific solute transport models which can be further used to evaluate the impacts of remediation activities at the sites. The validated model can be integrated with a solute transport code and used to create a calibrated solute transport model, which can then be used to simulate the transport and attenuation of TNT and other contaminants in groundwater.

The three main research objectives identified at the start of the proposed study were achieved in the following way:

- The mathematical kinetic model based on Michaelis-Menten equations developed previously for the linear reductive dechlorination pathway of chlorinated ethenes (Widdowson 2004) was extended to the branched reductive transformation pathway of TNT. The branching in the pathway was accounted for by introducing user-defined branching coefficients which also allowed for the incorporation of variations in the total mass balance from the system.

- The proposed mathematical model was successfully validated for the branched reductive transformation pathway of TNT. Model-predicted concentrations of TNT and its isomeric degradation products matched well with experimentally determined concentrations with time from prior published laboratory scale studies of TNT degradation (Hwang et al. 2000; Daun et al. 1998).

- Exponential phase microbial growth during the initial lag period of TNT degradation and sorption in the presence of soils and sediments was also incorporated in the kinetic model. Sorption was implemented using a linear equilibrium adsorption isotherm. The model was successfully validated for reductive transformation of TNT in the presence of sorption as a competing process and microbial growth during the initial lag phase of TNT degradation, and model-derived concentrations of TNT and its metabolites correlated well with experimentally determined concentrations from a previously published soil column lab study (Daun et al. 1998).

Further research work would include incorporating the kinetic model in a solute transport code like SEAM3D. SEAM3D (Sequential Electron Acceptor Model, 3 Dimensional) is a numerical code designed to simulate the flow and degradation of multiple solutes in a three-dimensional, anisotropic and

heterogeneous domain. An evaluation of the kinetic model in the presence of spatially varying redox conditions in the subsurface and inhibition of reductive transformation of contaminant compound and its metabolites by the varying availability of naturally occurring electron acceptors like dissolved oxygen, nitrates, ferric iron etc. remains to be addressed before it can be incorporated in the solute transport code. Further research could also involve explicitly testing and validating the kinetic model for other contaminants like PCA and TCA which also degrade through similar branched reductive transformation pathways.

Appendix A – Individual Model Calibration & Sensitivity Results

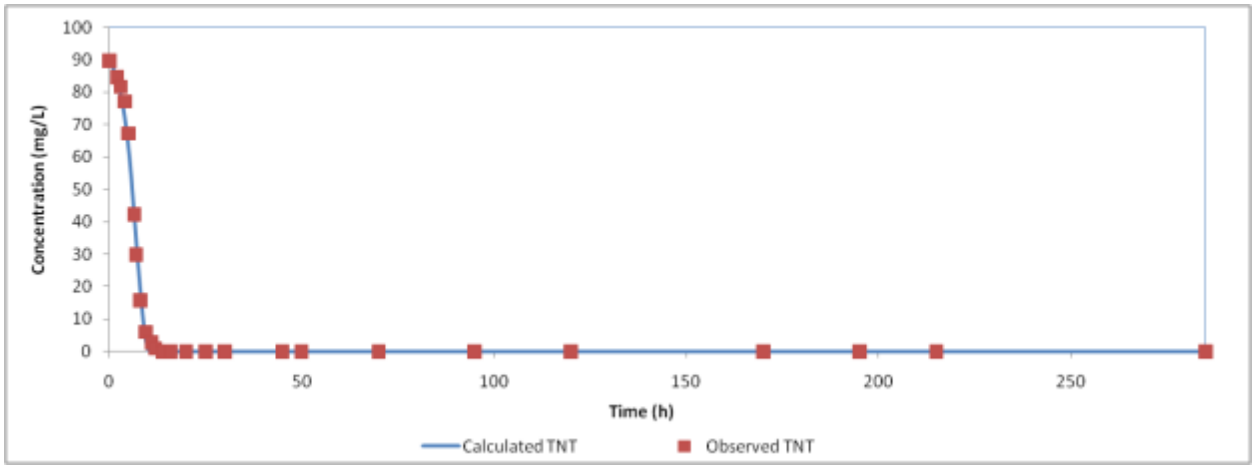

Figure A.1. Experimental and Model Predicted TNT Concentrations with Time (Case Study I)

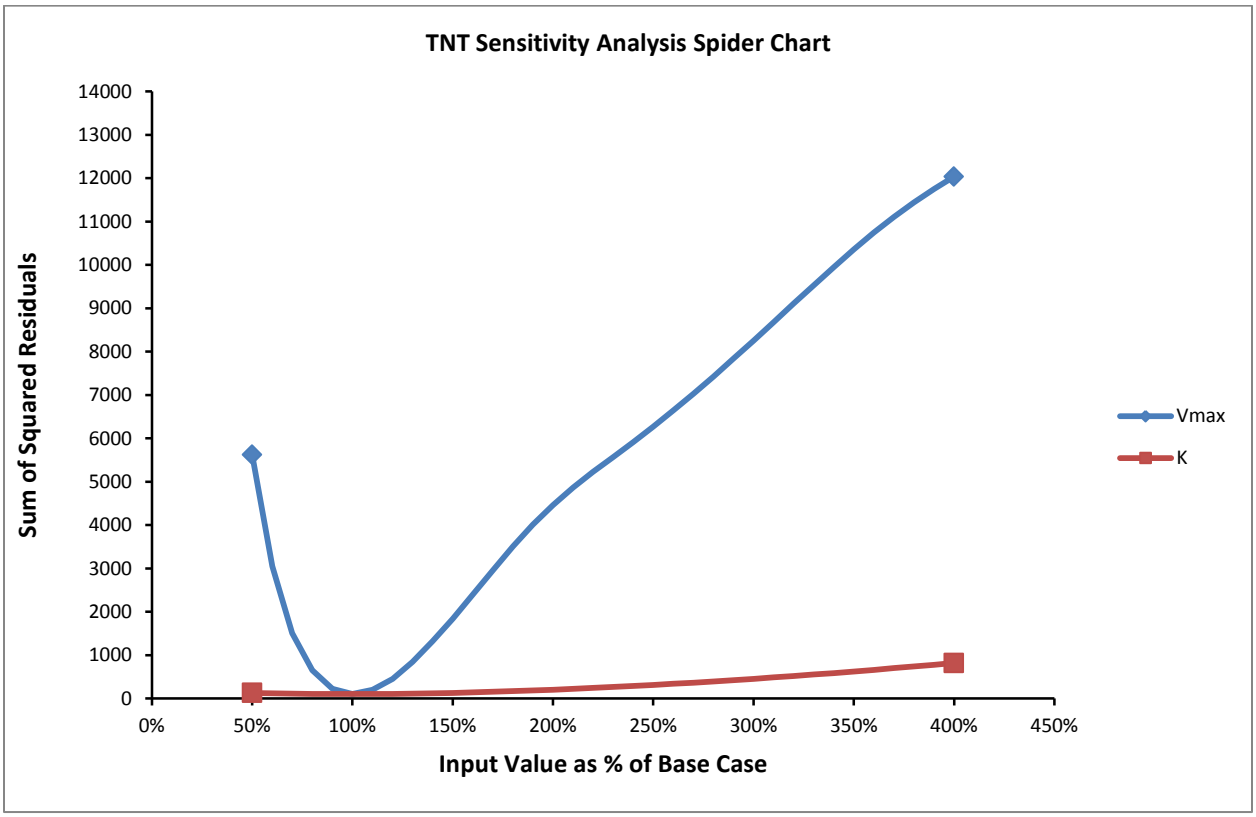

Figure A.2. TNT Model Parameters Sensitivity Analysis Results (Case Study I)

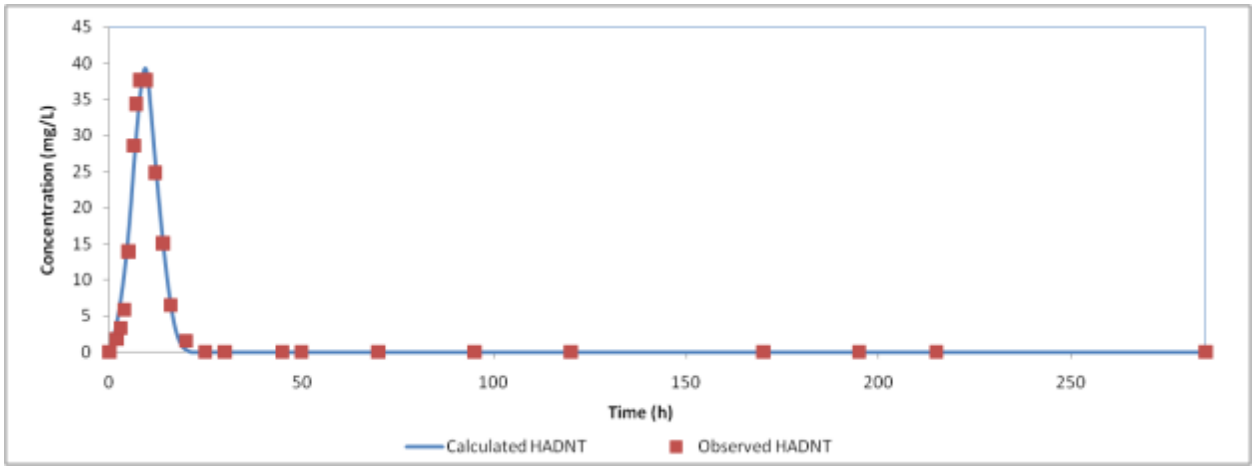

Figure A.3. Experimental and Model Predicted HADNT Concentrations with Time (Case Study I)

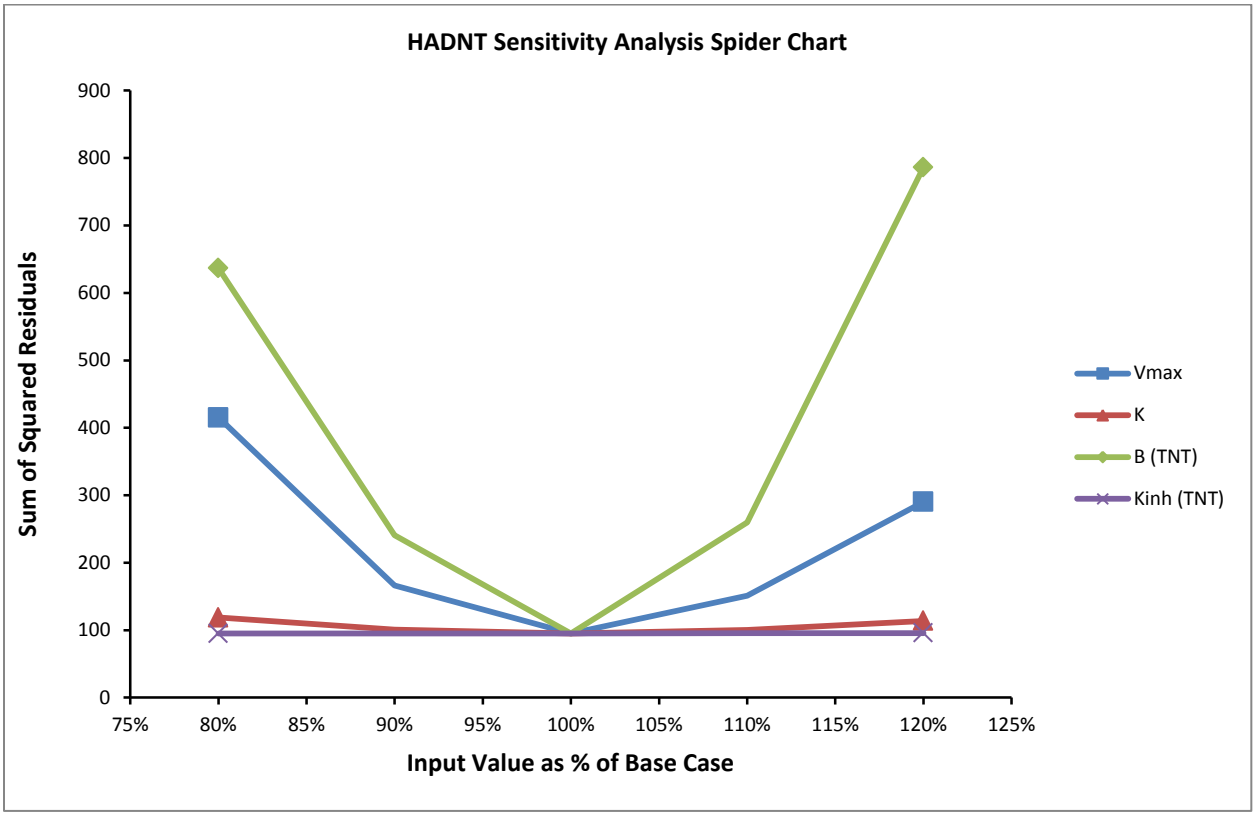

Figure A.4: HADNT Model Parameters Sensitivity Analysis Results (Case Study I)

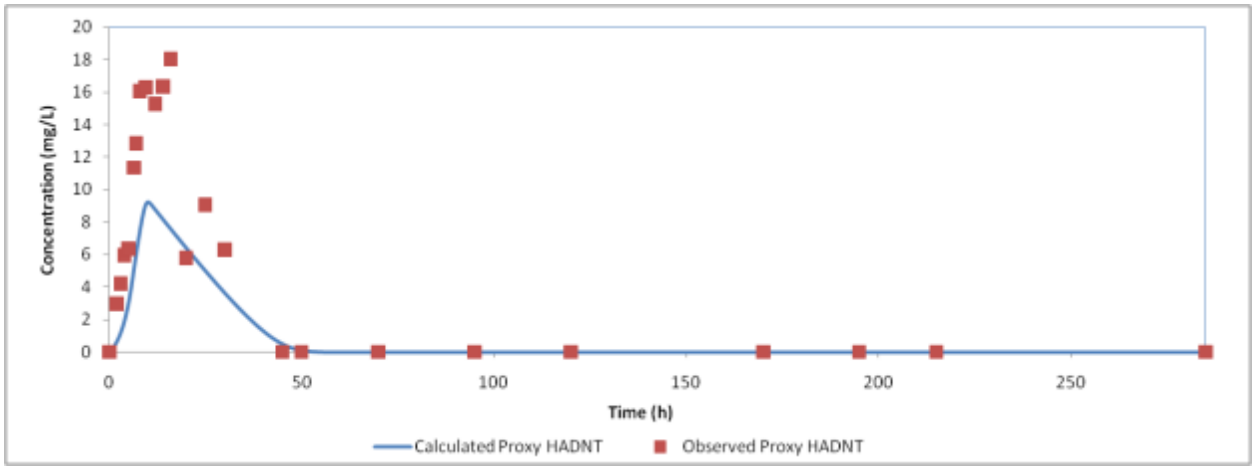

Figure A.5. Experimental and Model Predicted Proxy HADNT Concentrations with Time (Case Study I)

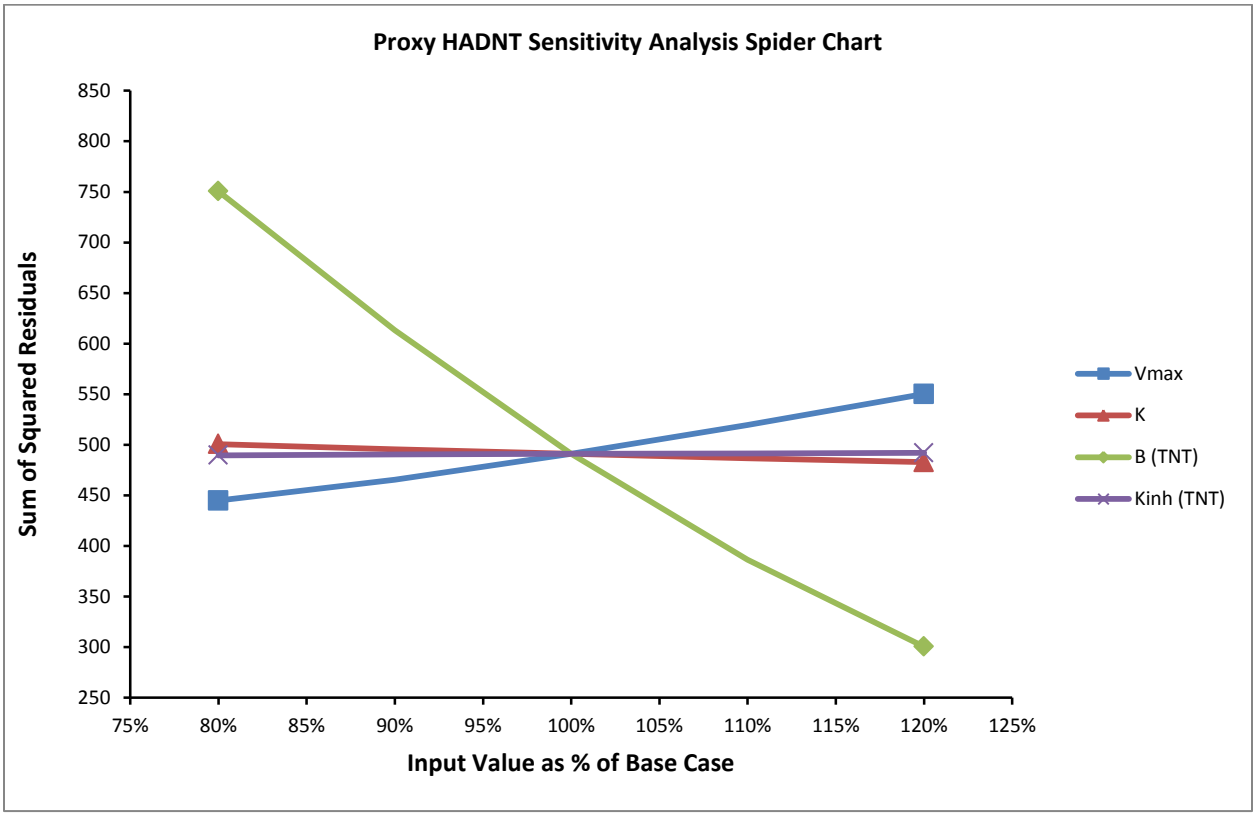

Figure A.6. Proxy HADNT Model Parameters Sensitivity Analysis Results (Case Study I)

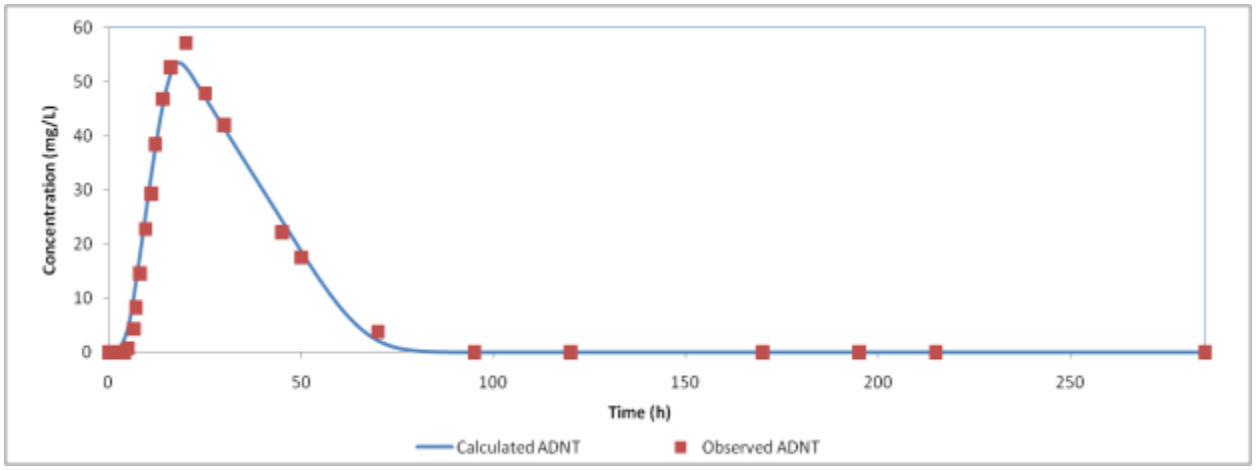

Figure A.7. Experimental and Model Predicted ADNT Concentrations with Time (Case Study I)

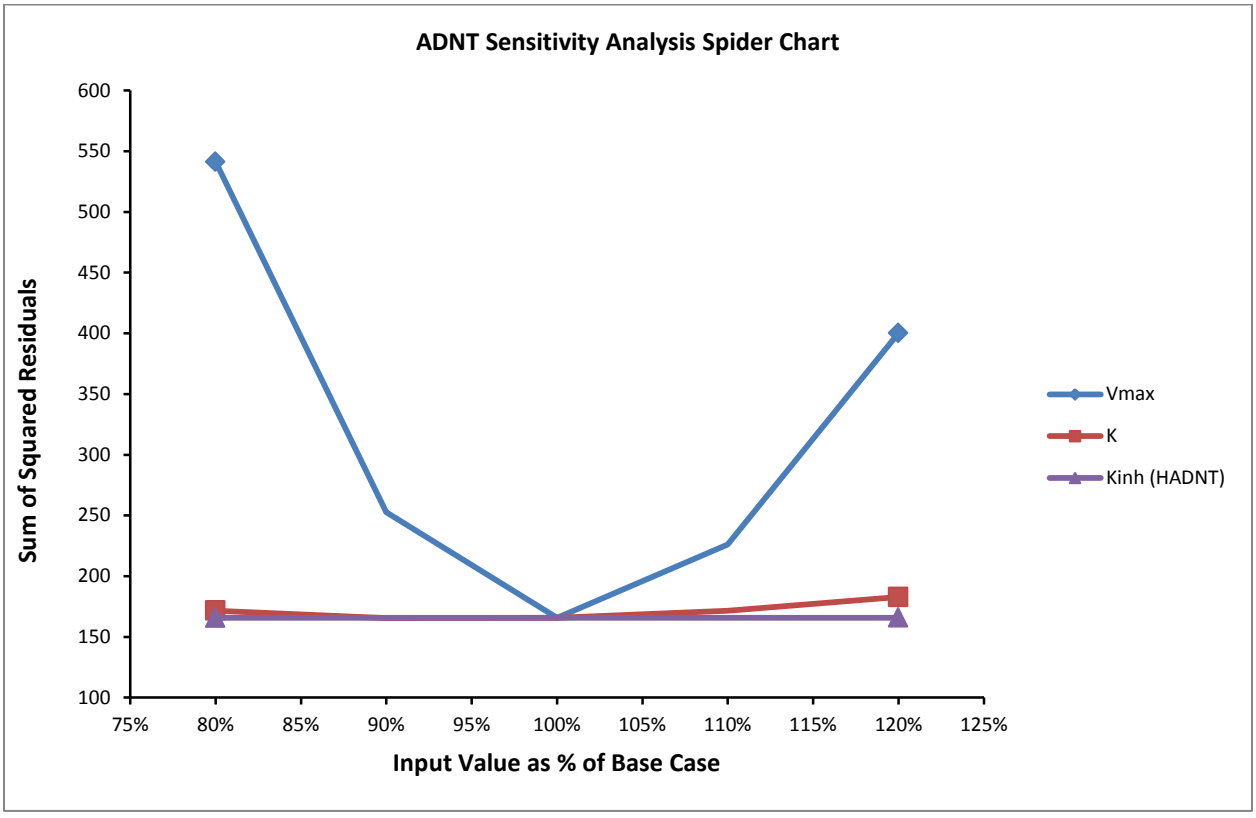

Figure A.8. ADNT Model Parameters Sensitivity Analysis Results (Case Study I)

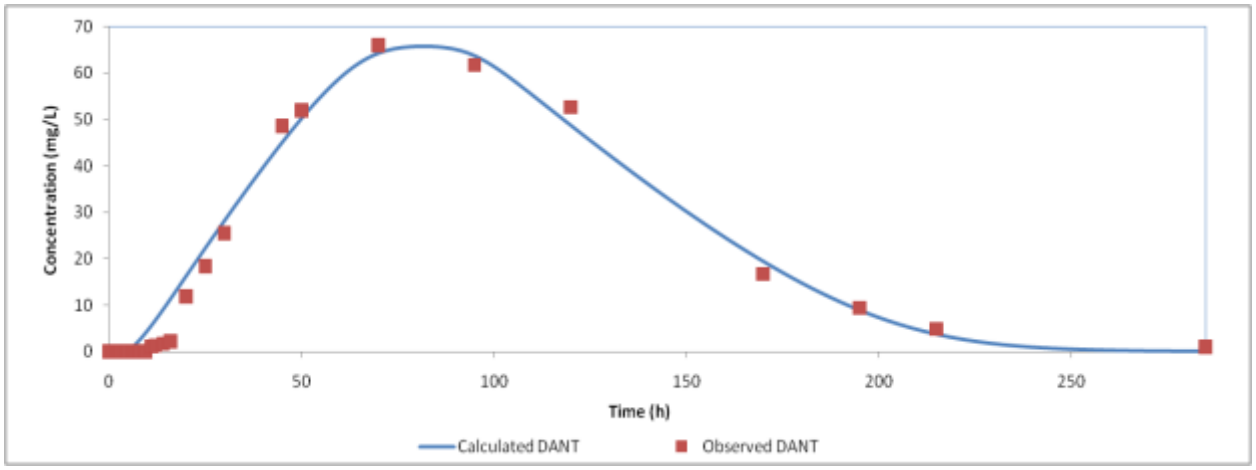

Figure A.9. Experimental and Model Predicted DANT Concentrations with Time (Case Study I)

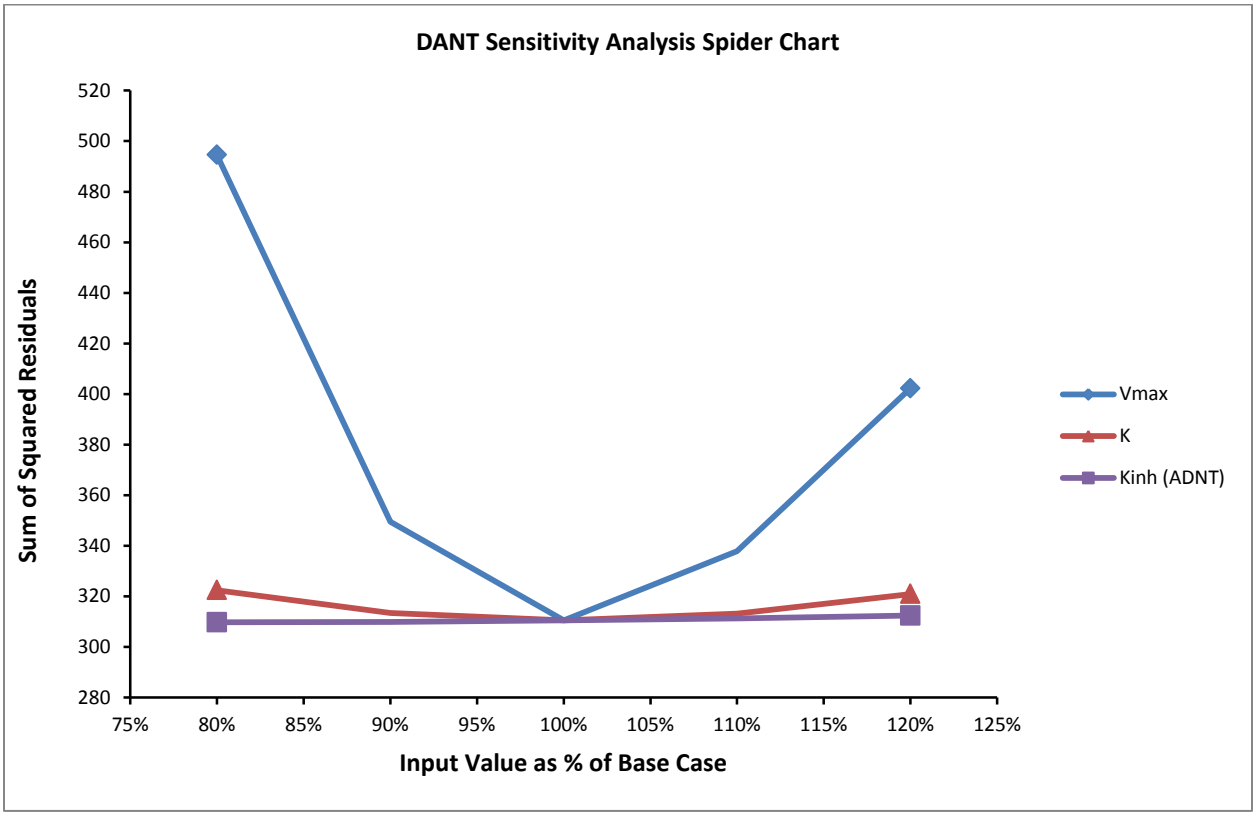

Figure A.10. DANT Model Parameters Sensitivity Analysis Results (Case Study I)

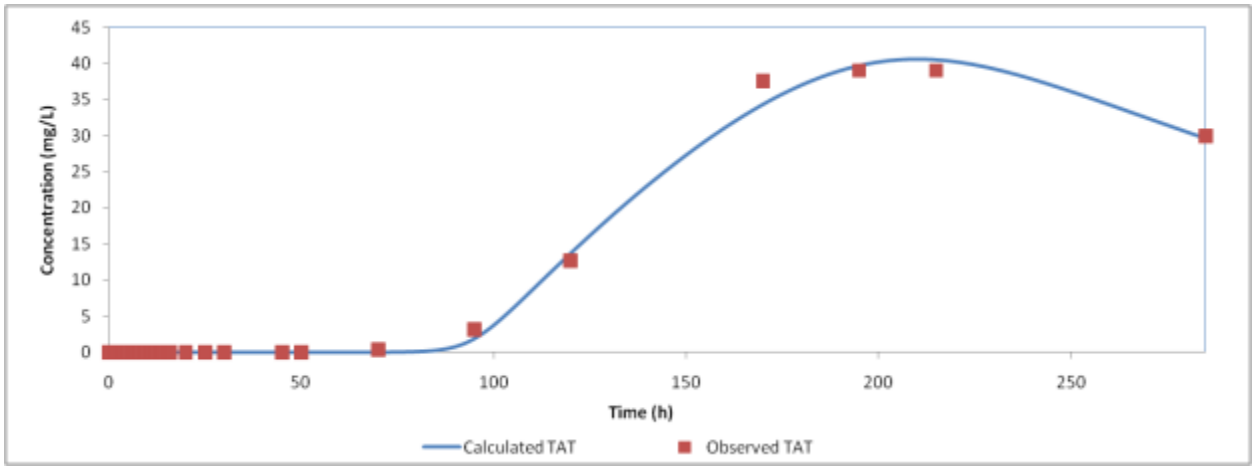

Figure A.11. Experimental and Model Predicted TAT Concentrations with Time (Case Study I)

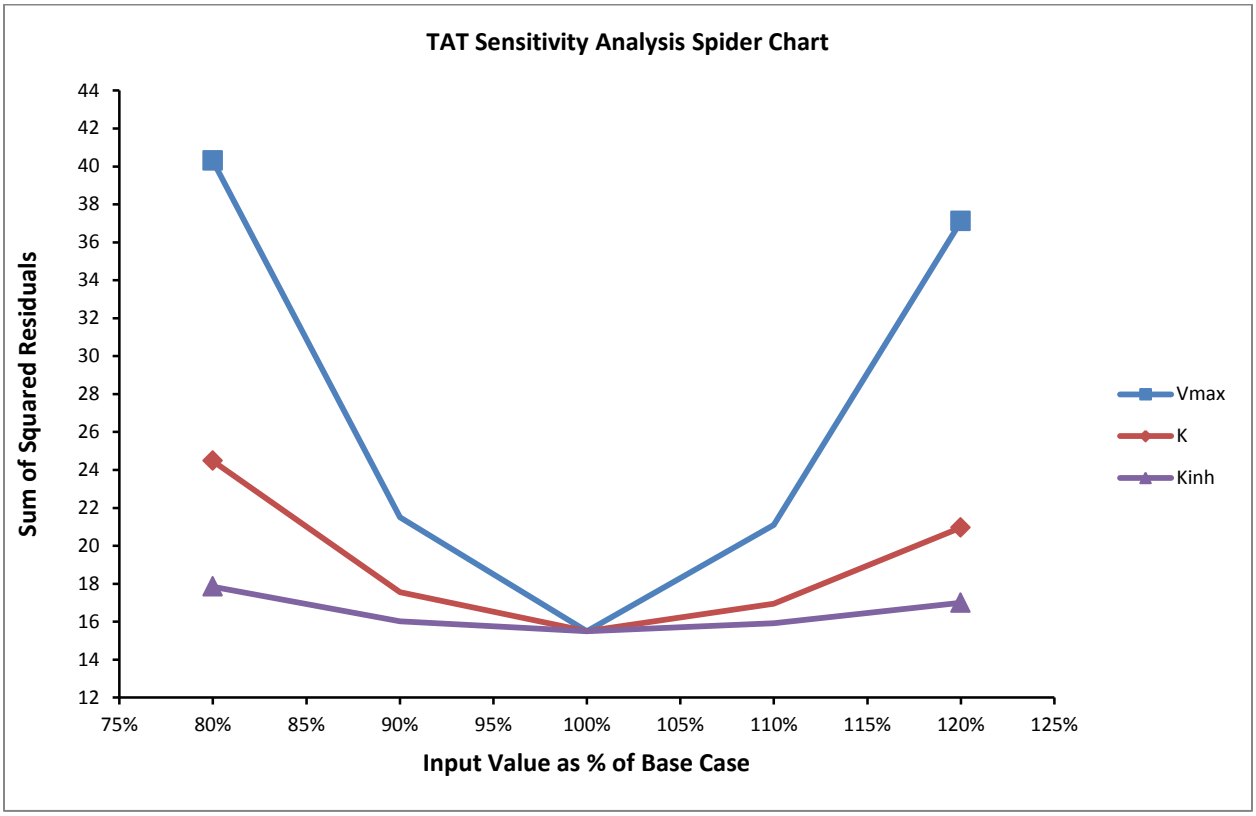

Figure A.12. TAT Model Parameters Sensitivity Analysis Results (Case Study I)

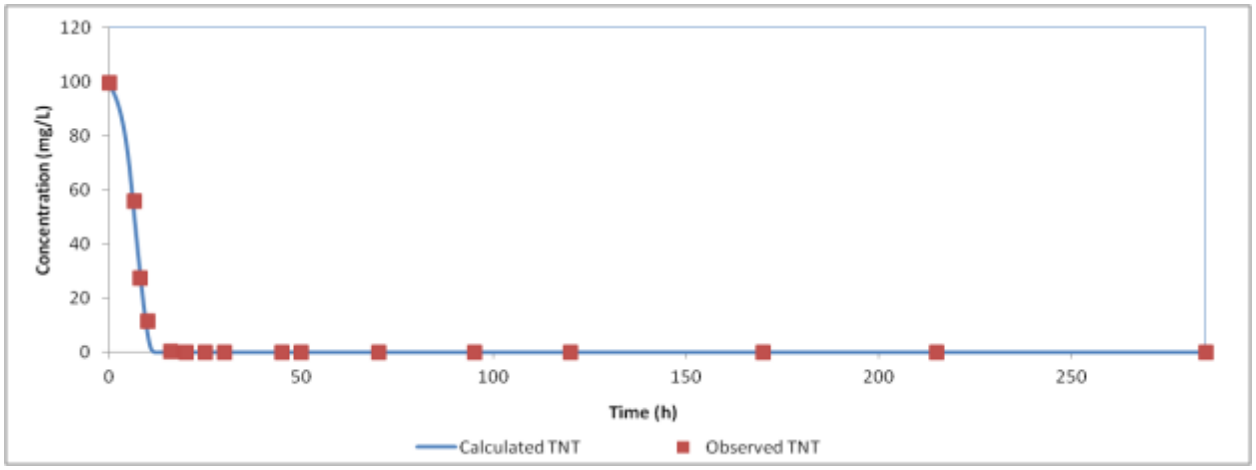

Figure A.13. Experimental and Model Predicted TNT Concentrations with time (Case Study II)

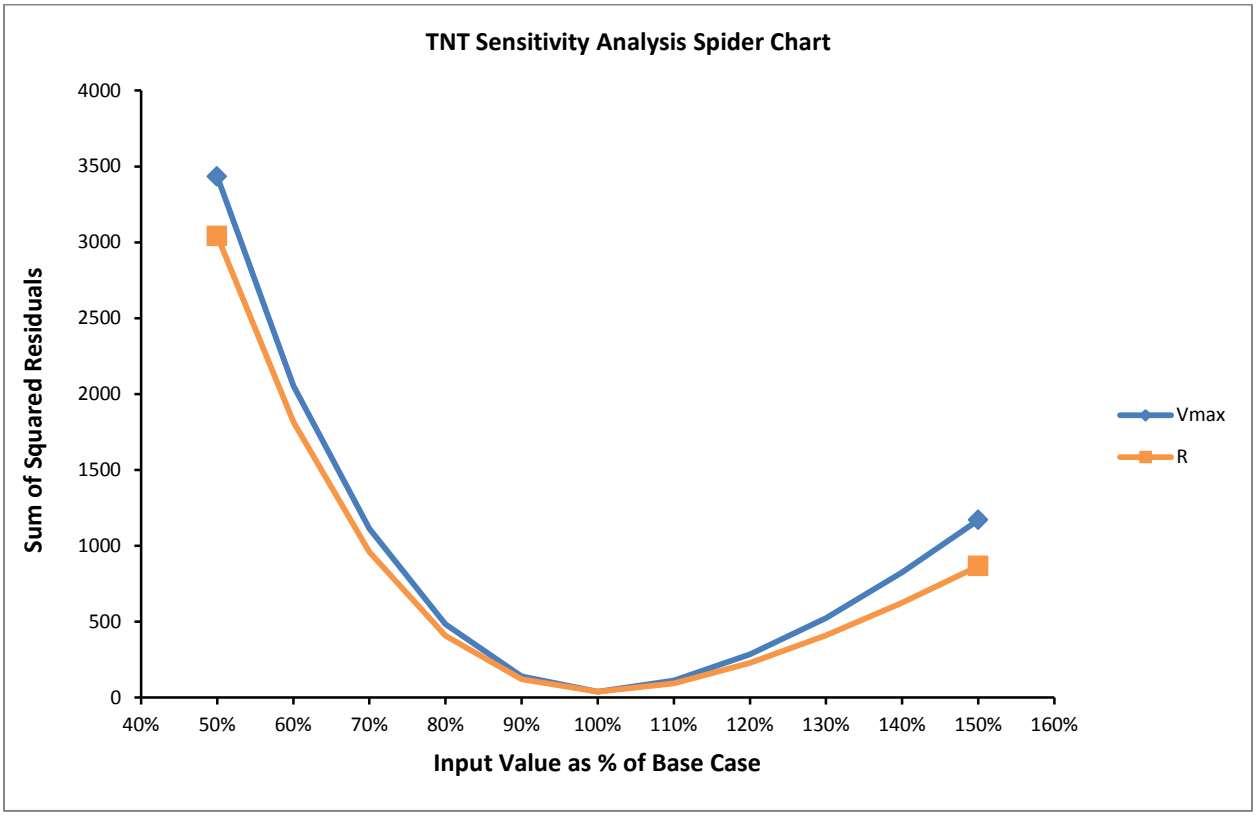

Figure A.14. TNT Model Parameters Sensitivity Analysis Results (Case Study II)

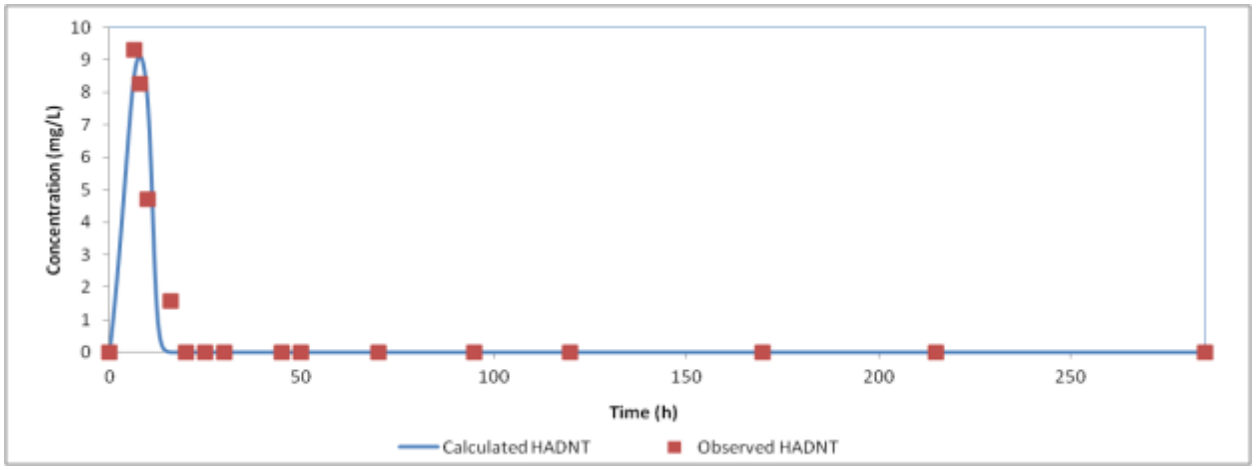

Figure A.15. Experimental and Model Predicted HADNT Concentrations with time (Case Study II)

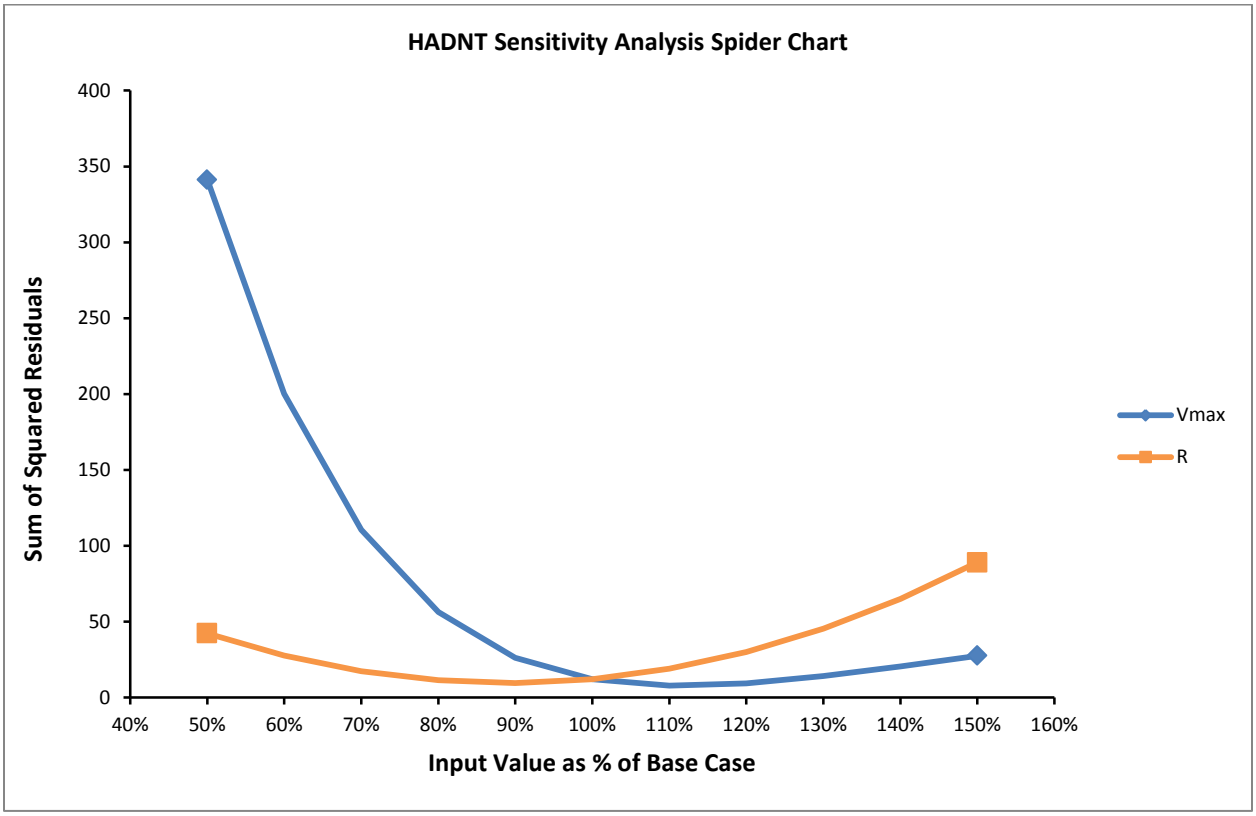

Figure A.16. HADNT Model Parameters Sensitivity Analysis Results (Case Study II)

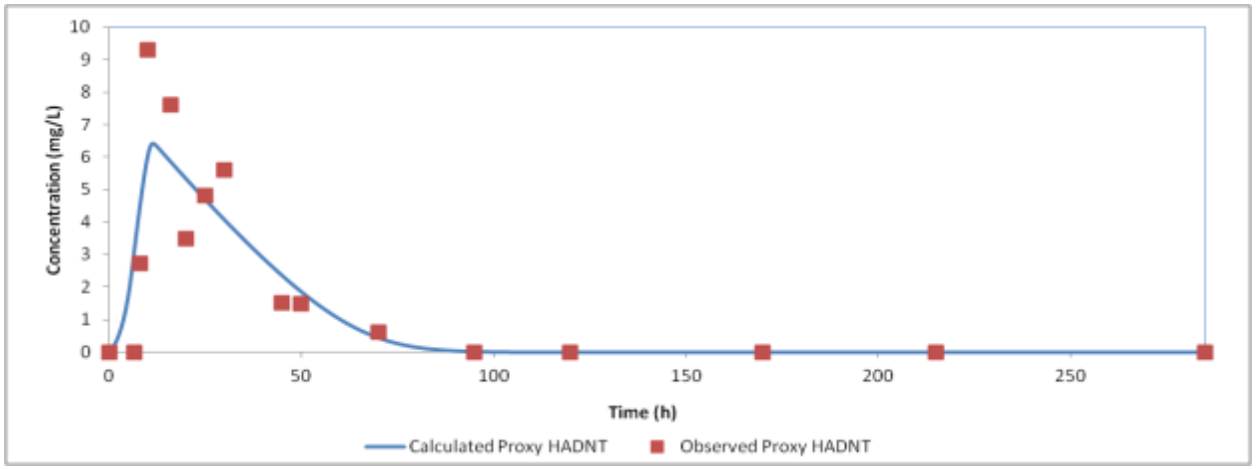

Figure A.17. Experimental and Model Predicted Proxy HADNT Concentrations with Time (Case Study II)

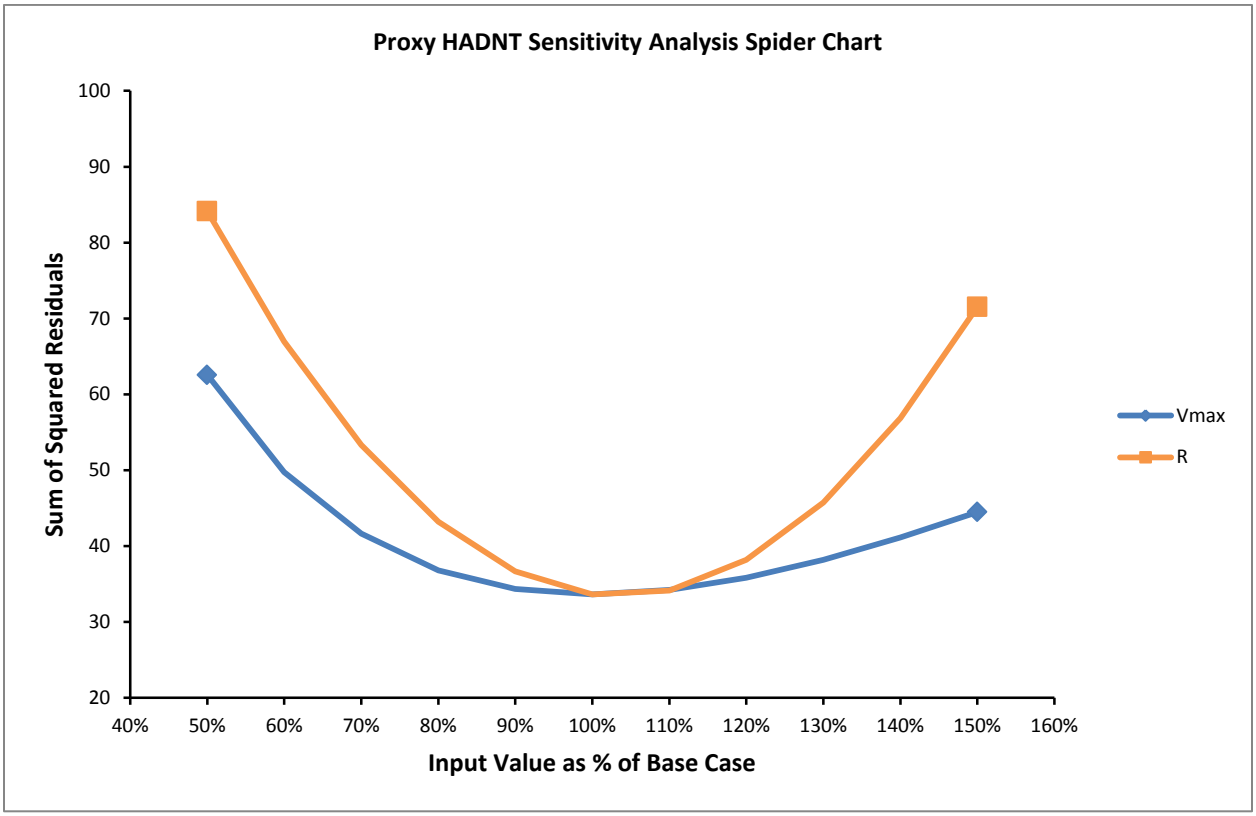

Figure A.18. Proxy HADNT Model Parameters Sensitivity Analysis Results (Case Study II)

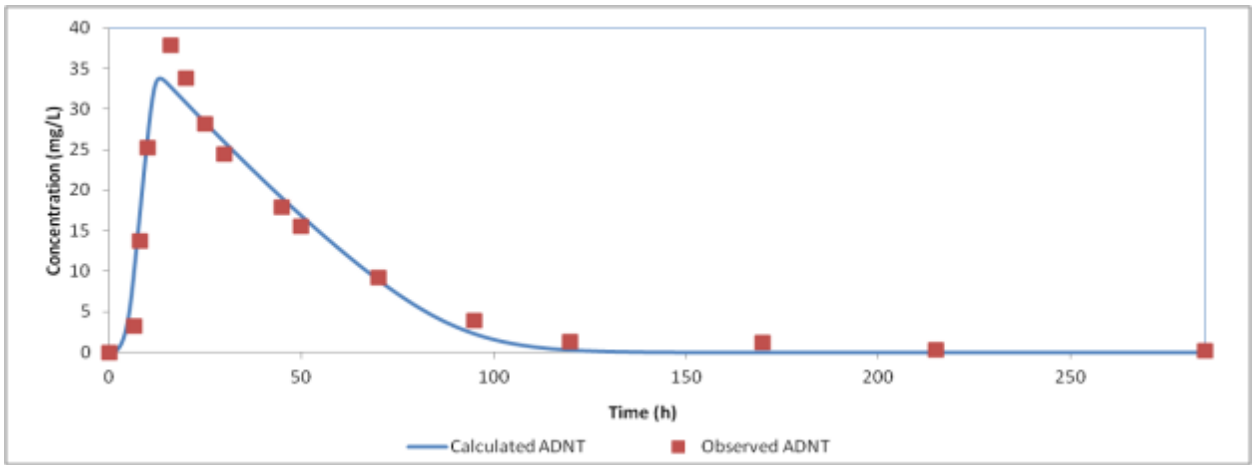

Figure A.19. Experimental and Model Predicted ADNT Concentrations with time (Case Study II)

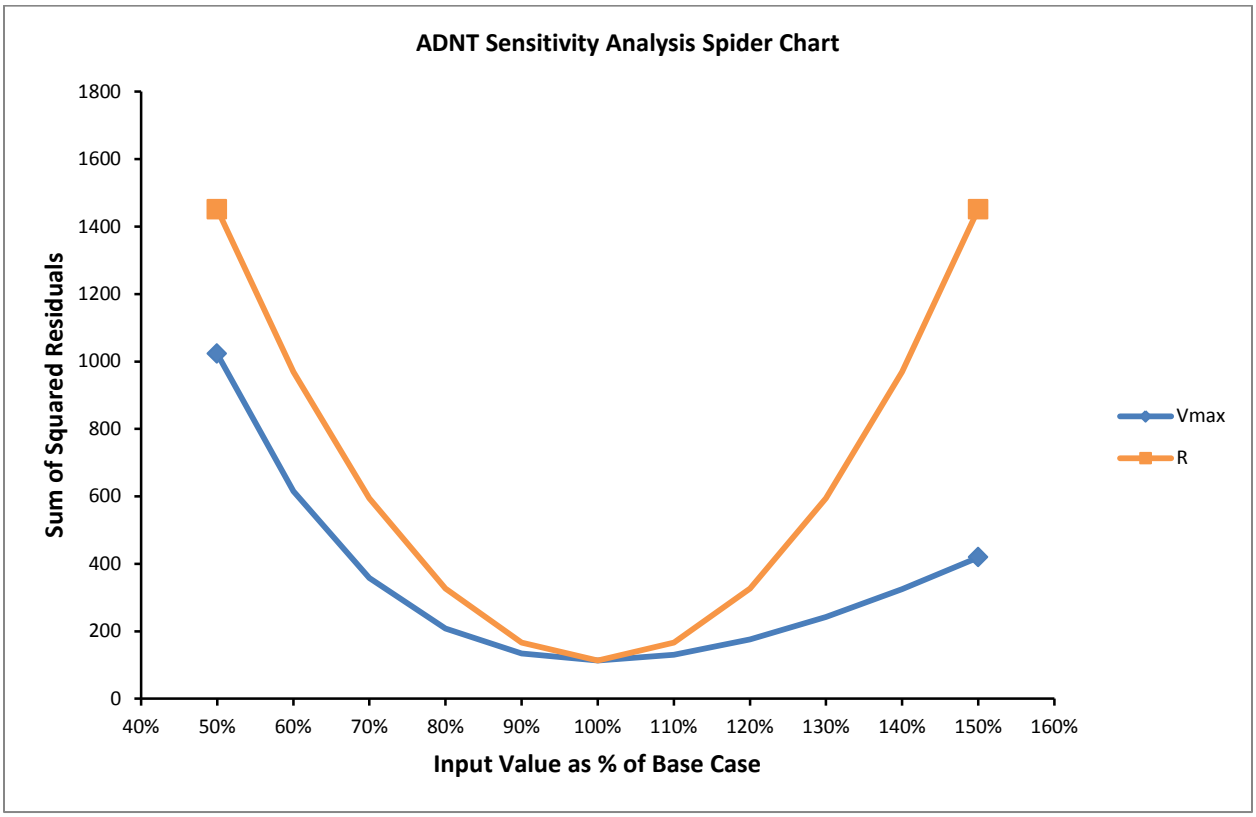

Figure A.20. ADNT Model Parameters Sensitivity Analysis Results (Case Study II)

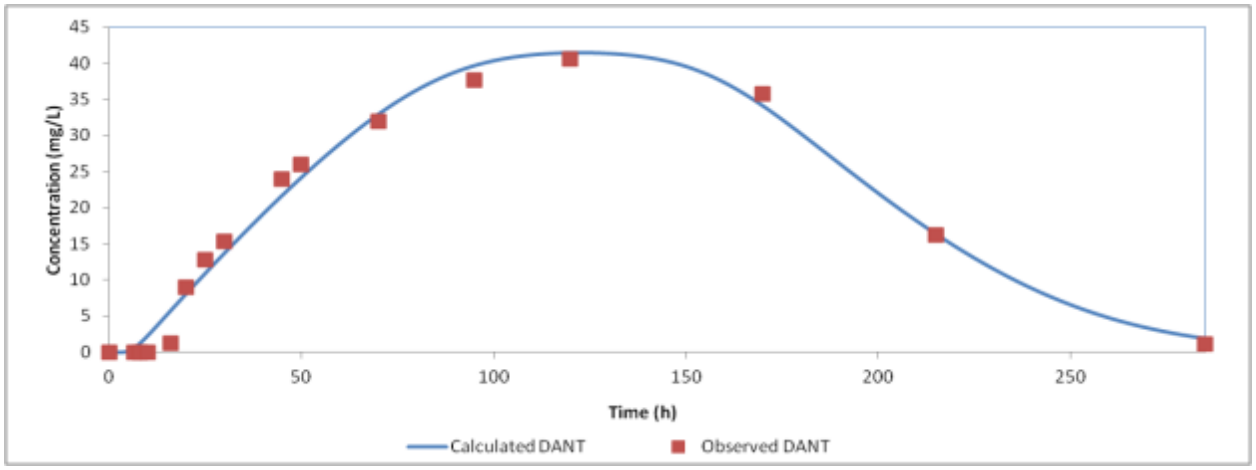

Figure A.21. Experimental and Model Predicted DANT Concentrations with time (Case Study II)

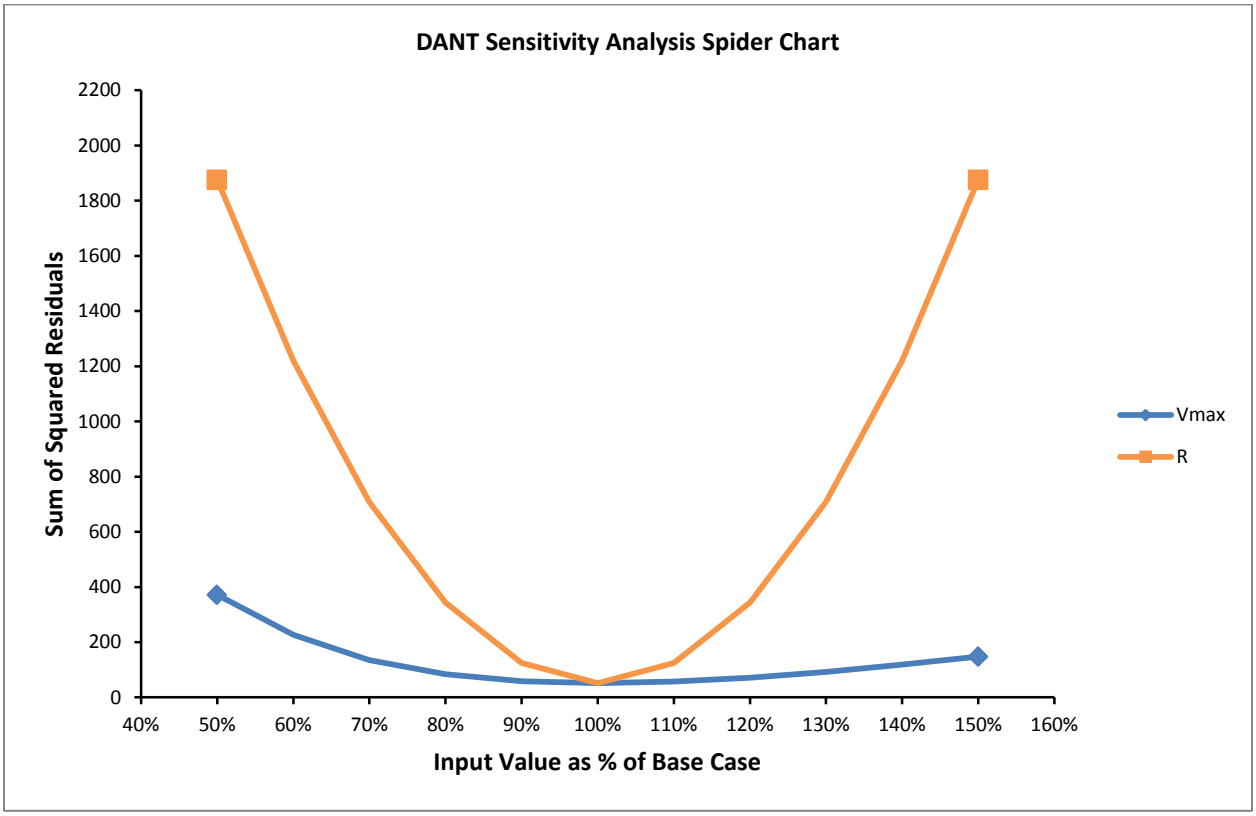

Figure A.22. DANT Model Parameters Sensitivity Analysis Results (Case Study II)

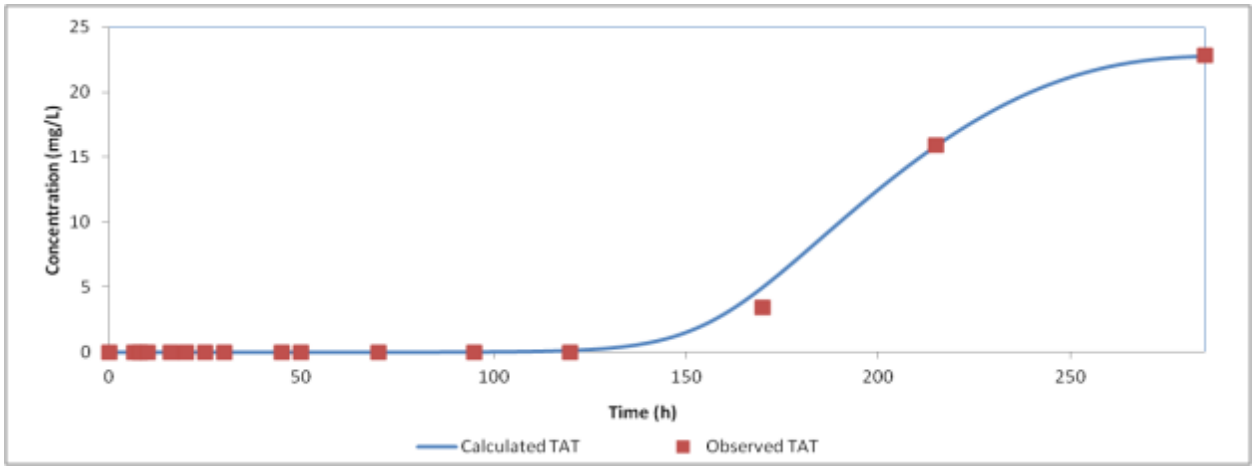

Figure A.23. Experimental and Model Predicted TAT Concentrations with time (Case Study II)

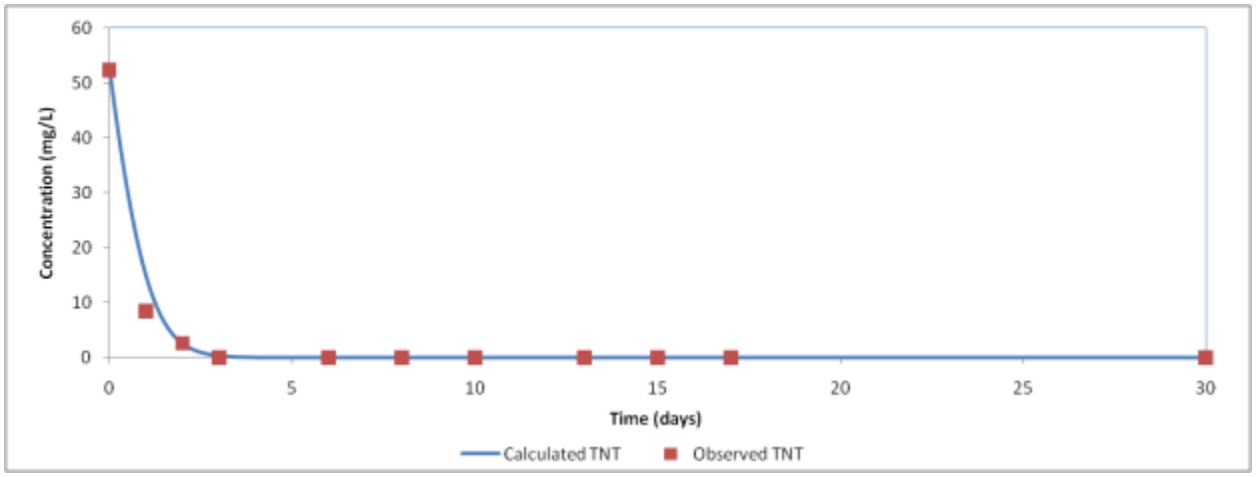

Figure A.24. Experimental and Model Predicted TNT Concentrations with Time (Case Study III)

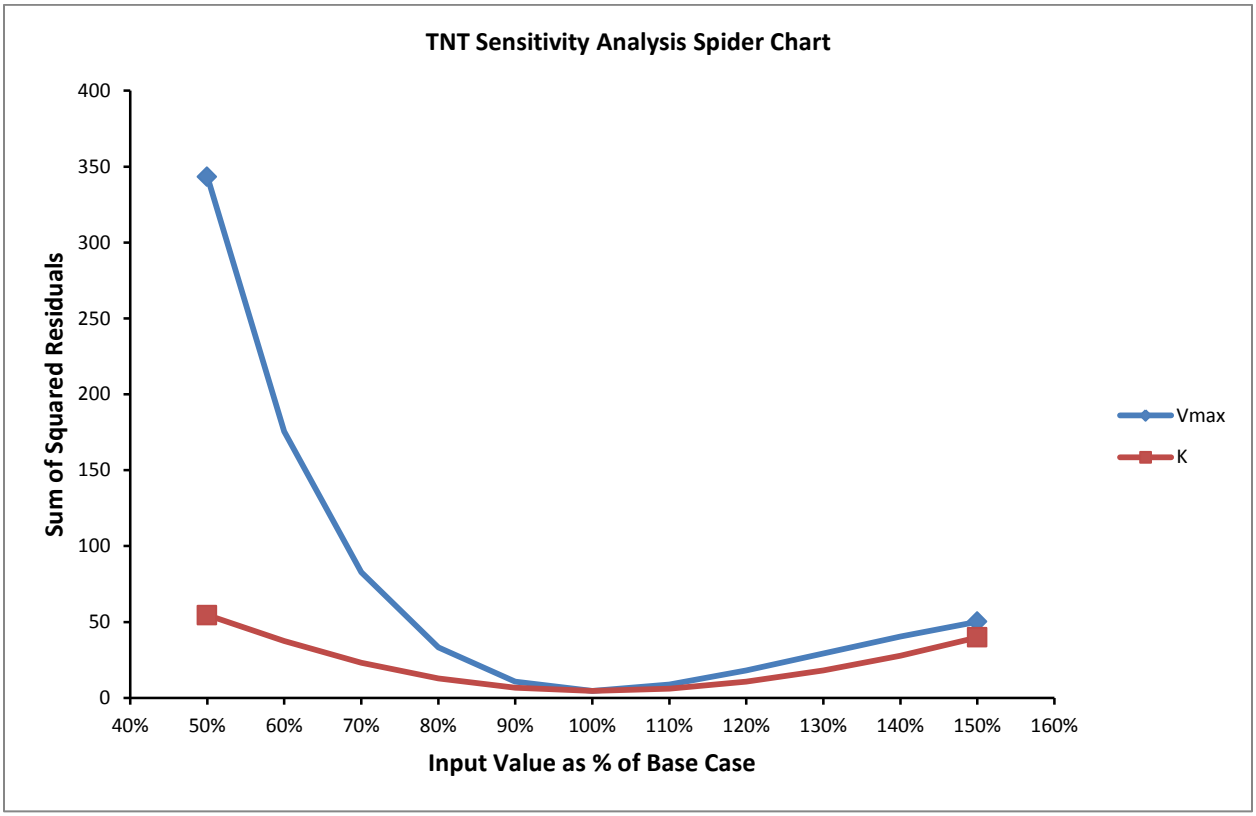

Figure A.25. TNT Model Parameters Sensitivity Analysis Results (Case Study III)

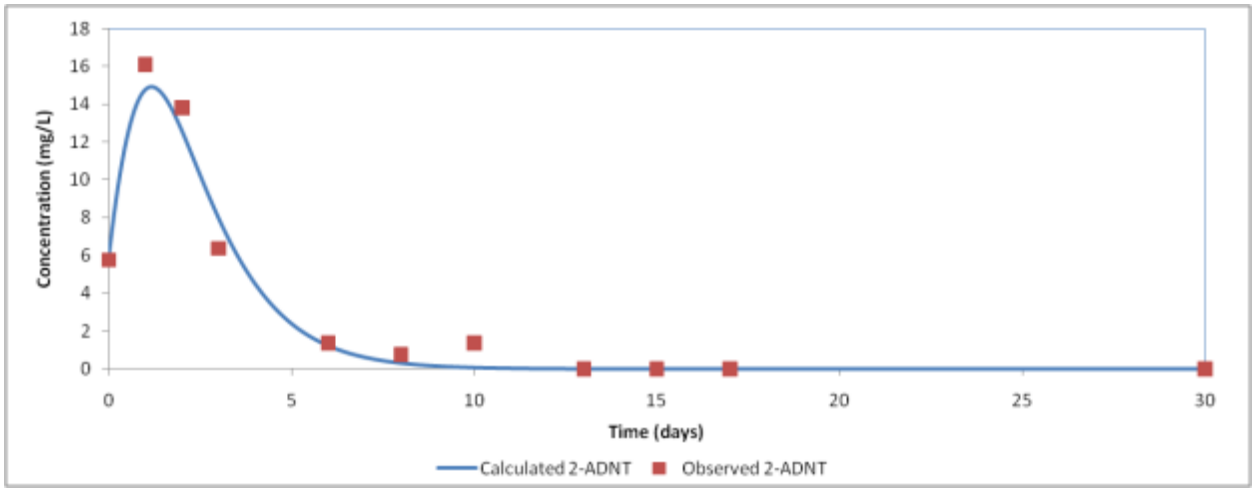

Figure A.26. Experimental and Model Predicted 2-ADNT Concentrations with Time (Case Study III)

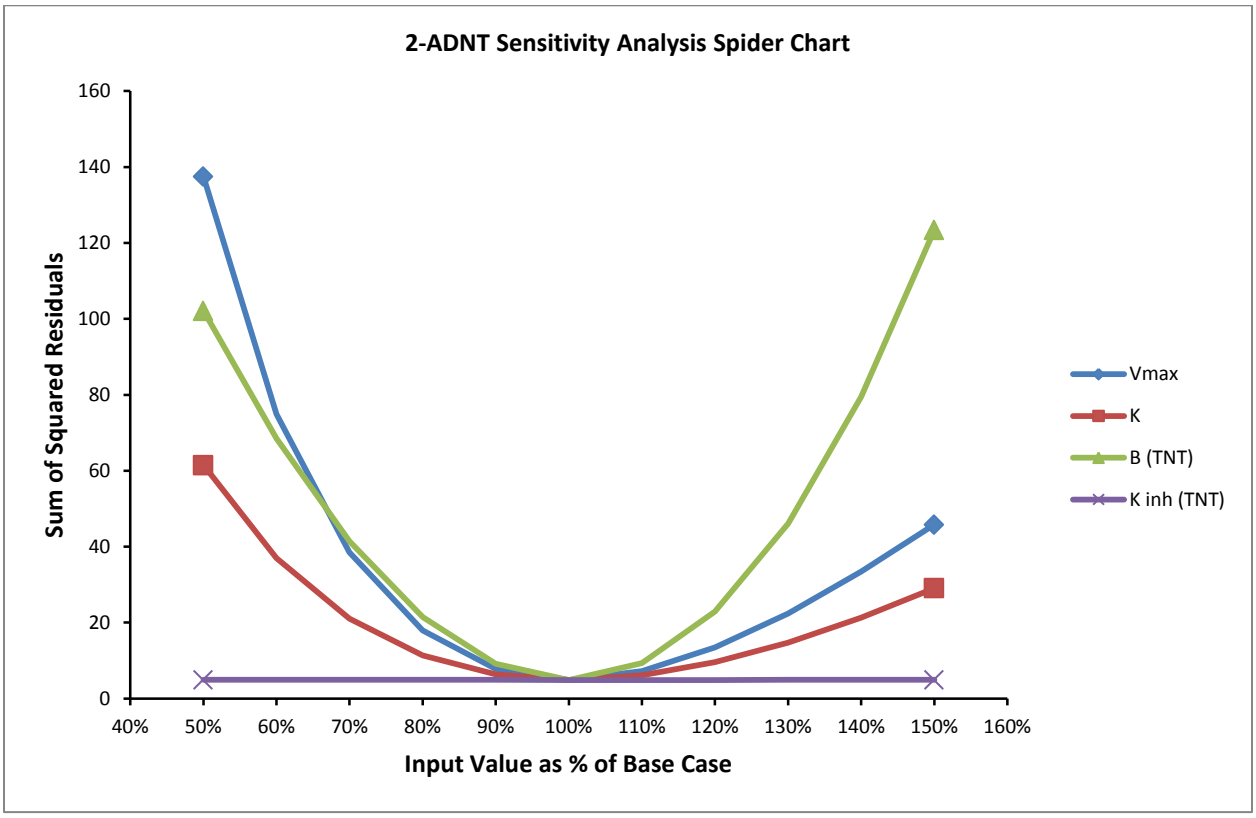

Figure A.27. 2-ADNT Model Parameters Sensitivity Analysis Results (Case Study III)

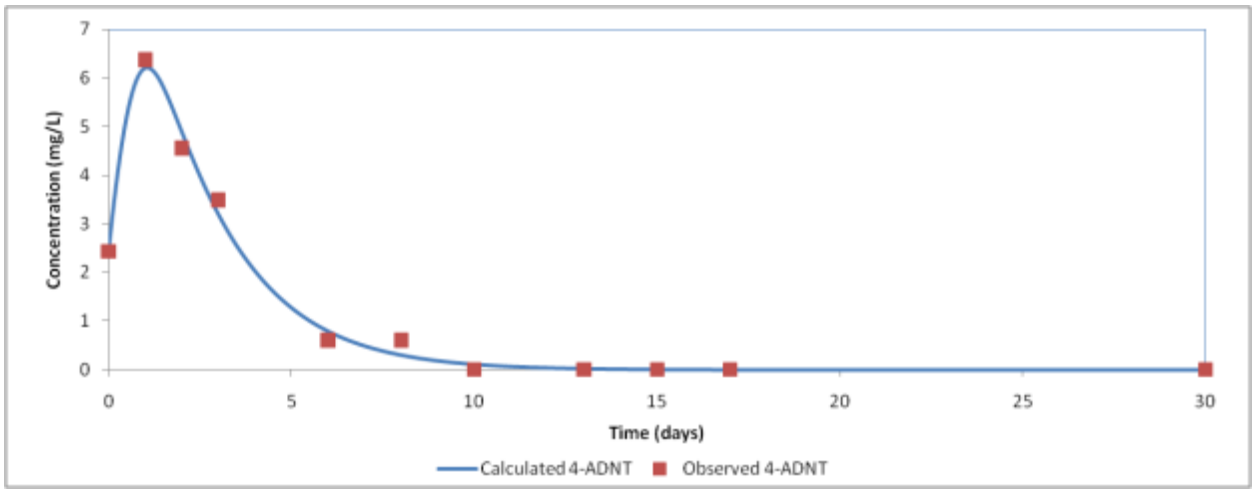

Figure A.28. Experimental and Model Predicted 4-ADNT Concentrations with Time (Case Study III)

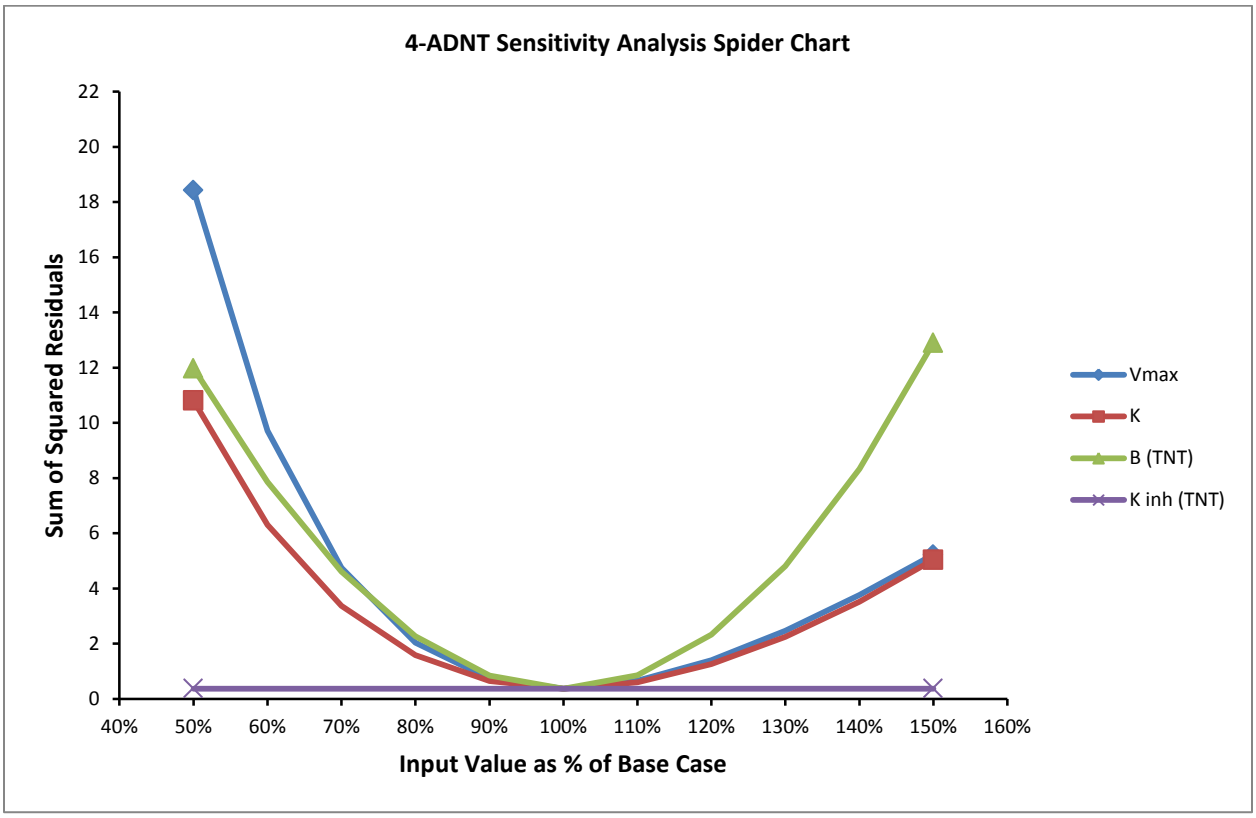

Figure A.29. 4-ADNT Model Parameters Sensitivity Analysis Results (Case Study III)

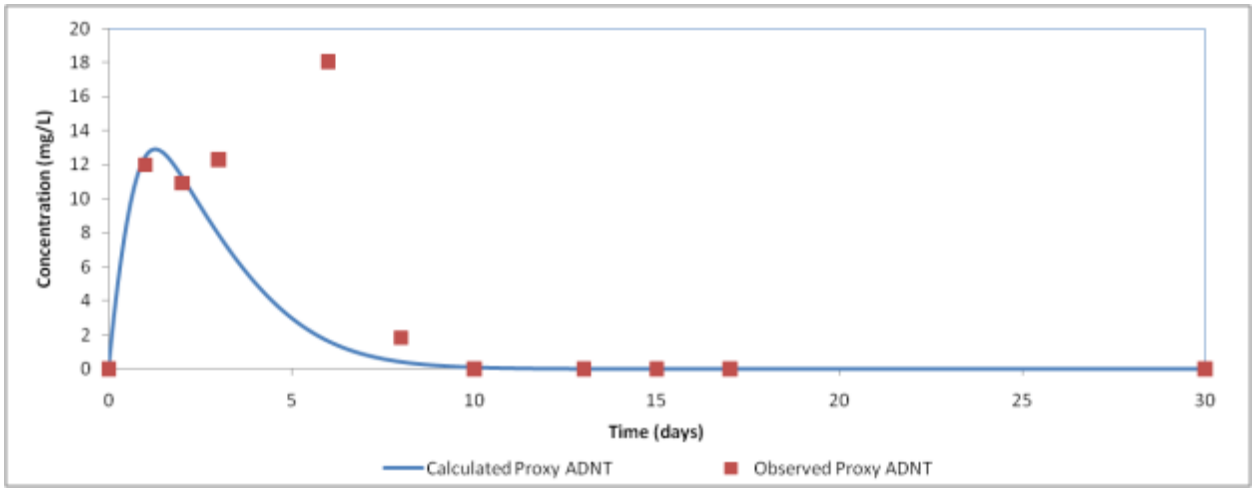

Figure A.30. Experimental and Model Predicted Proxy ADNT Concentrations with Time (Case Study III)

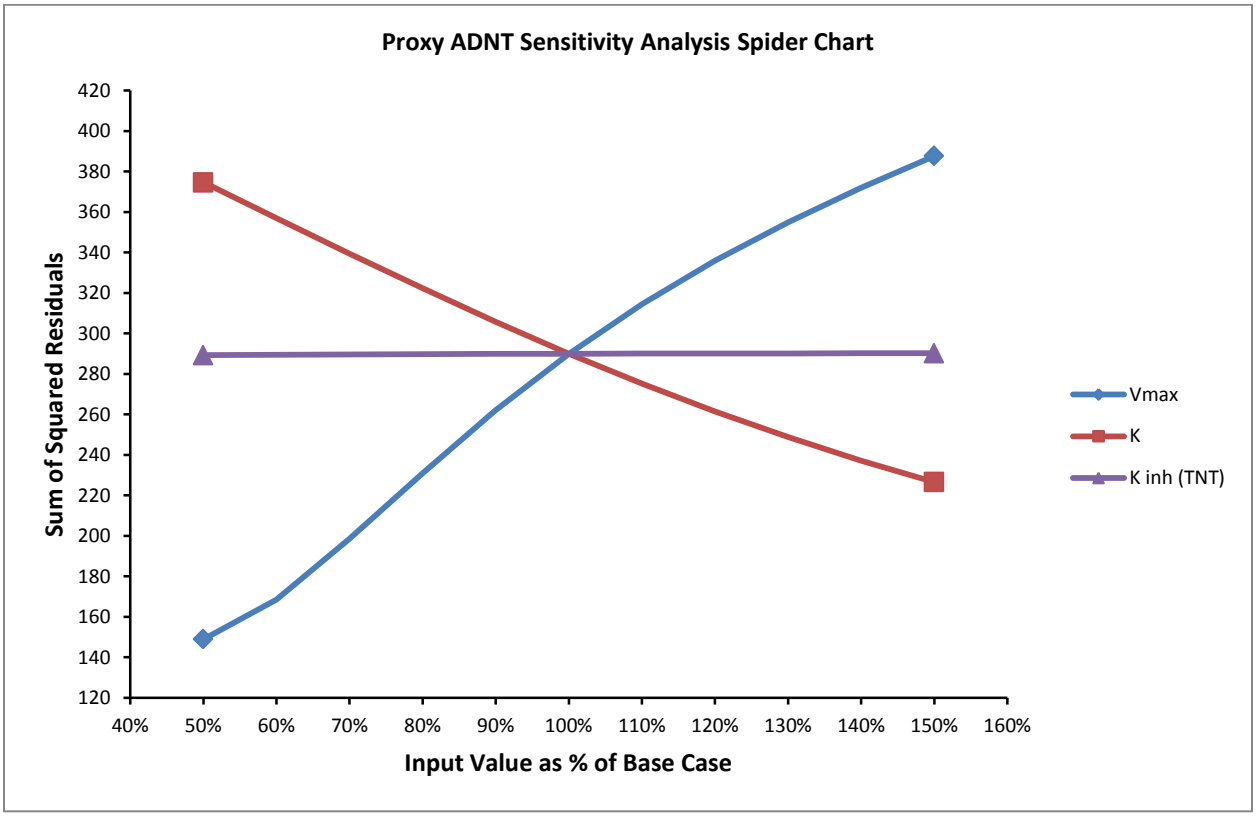

Figure A.31. Proxy ADNT Model Parameters Sensitivity Analysis Results (Case Study III)

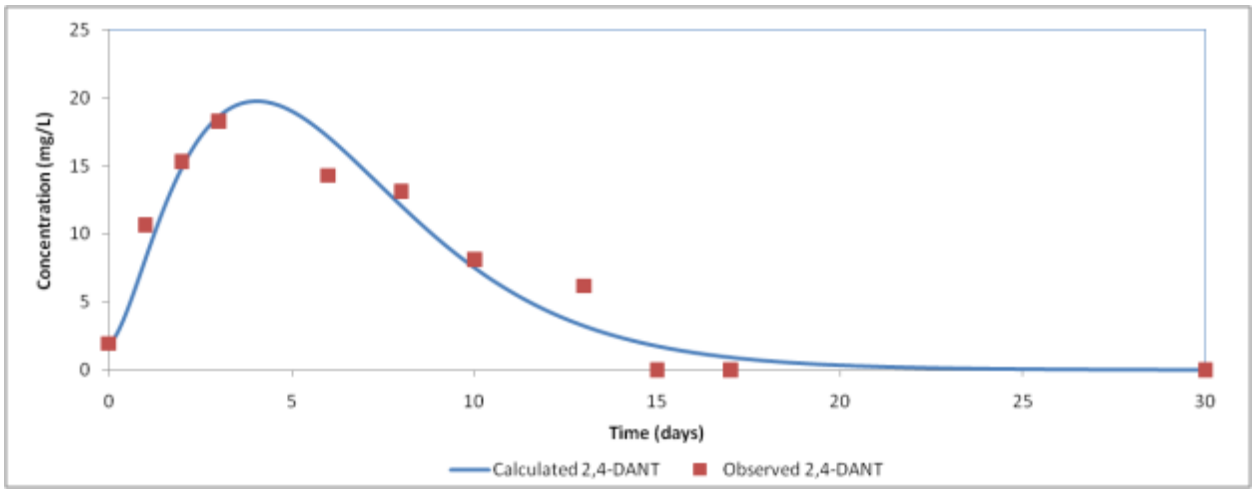

Figure A.32. Experimental and Model Predicted 2,4-DANT Concentrations with Time (Case Study III)

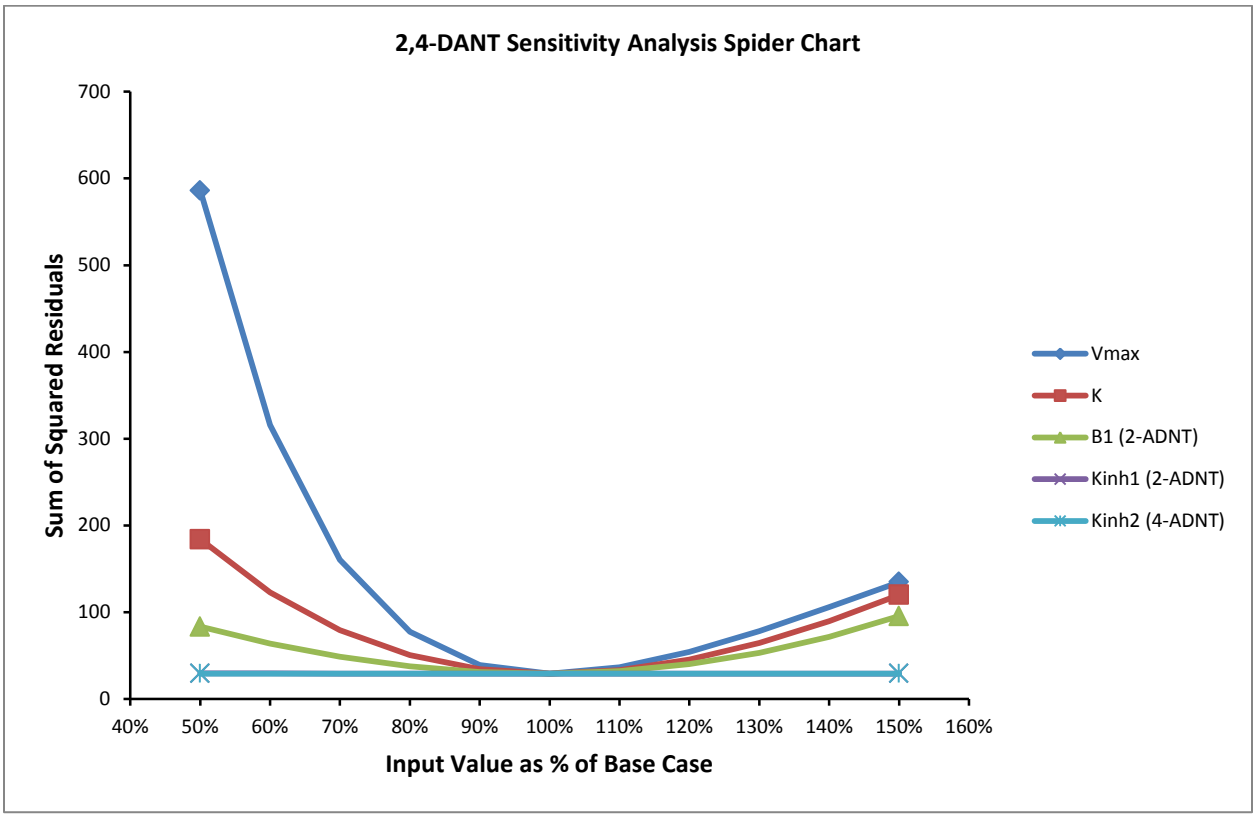

Figure A.33. 2,4-DANT Model Parameters Sensitivity Analysis Results (Case Study III)

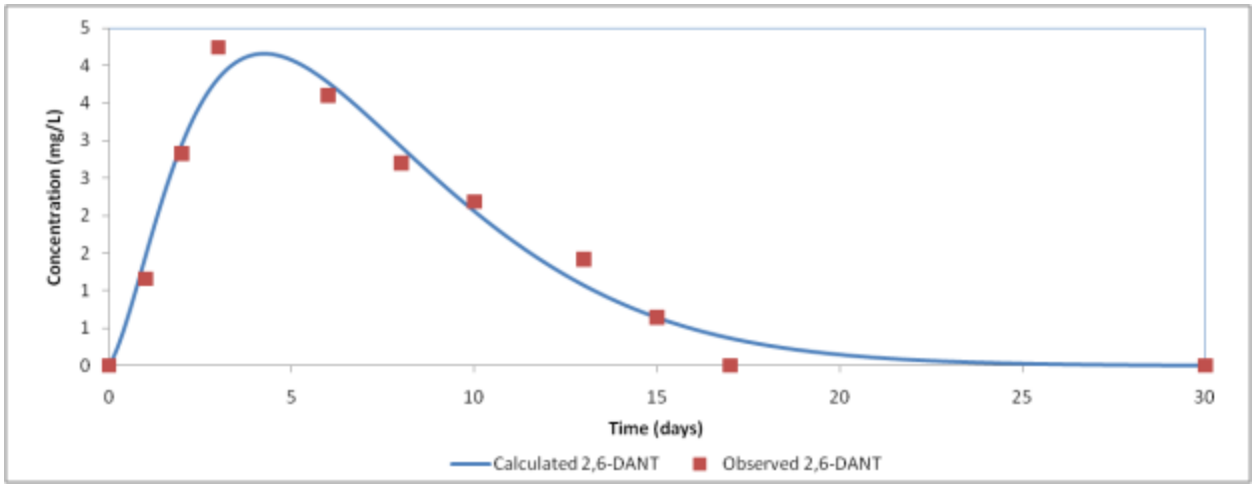

Figure A.34. Experimental and Model Predicted 2,6-DANT Concentrations with Time (Case Study III)

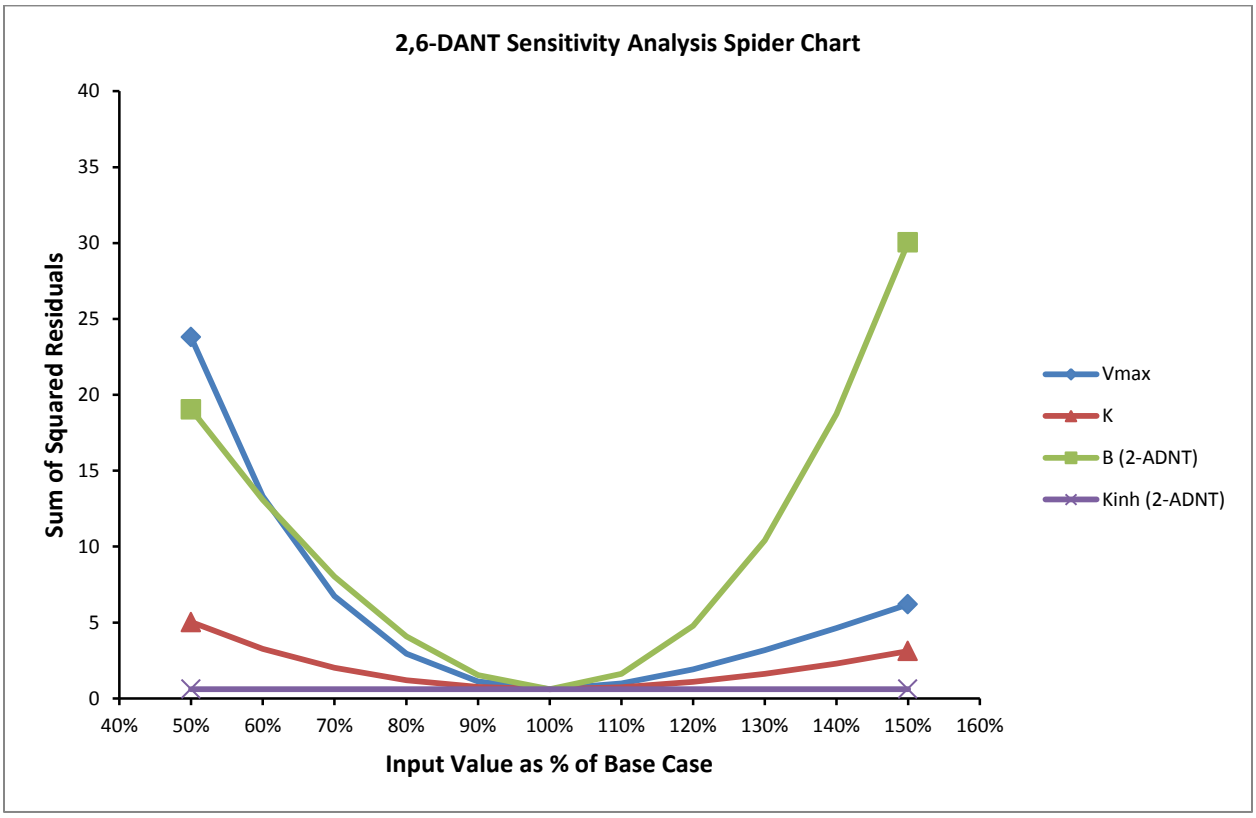

Figure A.35. 2,6-DANT Model Parameters Sensitivity Analysis Results (Case Study III)

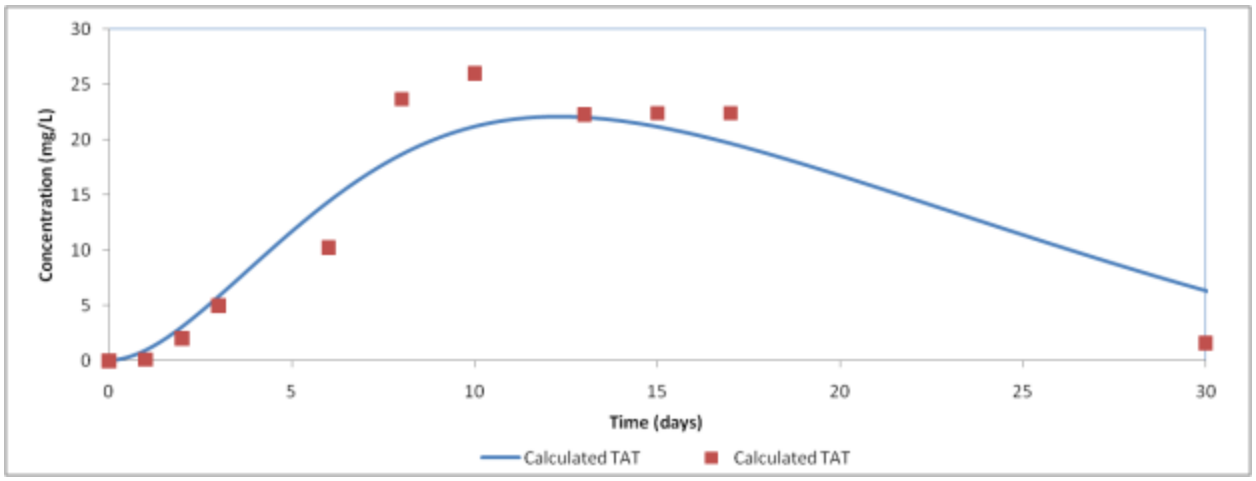

Figure A.36. Experimental and Model Predicted TAT Concentrations with Time (Case Study III)

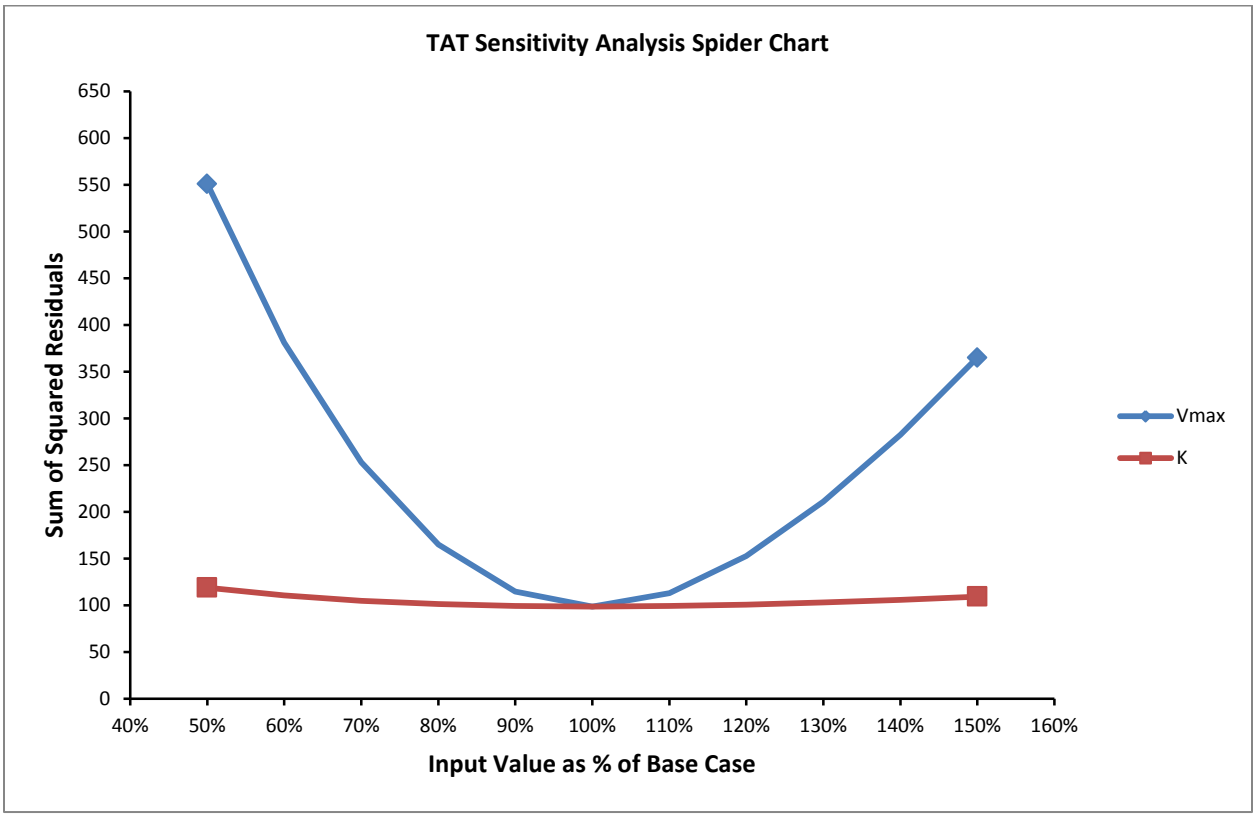

Figure A.37. TAT Model Parameters Sensitivity Analysis Results (Case Study III)